INTERNATIONAL COUNCIL FOR THE EXPLORATION OF THE SEA

C.M. 1980/C : 3

Hydrography Committee
(Réf. Biol. Oceanogr. Cttee)

Proceedings of the final ICES/JONSIS Workshop on JONSDAP '76

(Liège, Belgium, 29 April - 2 May, 1980)

é. t. a. b. é. t. y. p.
1980

Proceedings of the final ICES/JONSIS Workshop on JONSDAP '76

(Liège, Belgium, 29 April - 2 May, 1980)

INTERNATIONAL COUNCIL FOR THE EXPLORATION OF THE SEA

C.M. 1980/C : 3

Hydrography Committee
(Réf. Biol. Oceanogr. Cttee)

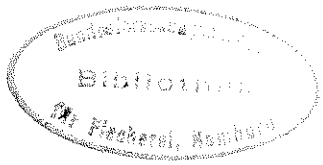

Proceedings of the final ICES/JONSIS Workshop on JONSDAP '76

(Liège, Belgium, 29 April - 2 May, 1980)

edited by

Georges PICHOT

Table of contents

Foreword

In spring of 1976, oceanographers from Belgium, Canada, Denmark, France, the Federal Republic of Germany, the Netherlands, Norway, Sweden, the United Kingdom and the United States of America took part in the Joint North Sea Data Acquisition Programme 1976 (JONSDAP '76).

Patronized by the International Council for the Exploration of the Sea and the Joint North Sea Information System (JONSIS) group, the programme consisted of two components. The first one (FLEX) related plankton dynamics in the area of the Fladen Ground to the various physical, chemical and biological interactions which control its evolution. The other one (INOUT) dealt with the distribution of currents in the North Sea area.

The present report collects most of the contributions which were presented at the final ICES/JONSIS workshop on JONSDAP '76 in Liège, Belgium (April 29th - May 2nd, 1980).

A very large number of data have been shown on the horizontal and vertical distribution and the seasonal evolution of phytoplankton, of zooplankton and its excretion products of different constituents of the organic matter, ... One has put forward a certain number of hypotheses to quantitatively explain the ecological interaction mechanisms between these different variables and the exact role played by the marine currents and the deepening of the thermocline on their distribution in time and space.

If it is true that this workshop formally concludes the JONSDAP '76 experiment, it is also evident that the quality and the quantity of the data which

have been collected on this occasion and the fundamental questions that their interpretation did not fail to raise will continue, in the near future, to be the subject of many interdisciplinary works and publications.

In behalf of all participants to the final ICES/JONSIS workshop on JONSDAP '76, the editor hereby wishes to thank the Belgian Ministry for Science Policy for sponsoring the organization of the meeting and the publication of the proceedings.

Georges PICHOT

Unité de Gestion du Modèle mathématique
de la mer du Nord,
C.A.E. Vésale 2/3

B-1010 Bruxelles (Belgium)

The chlorophyll development at the Central Station during FLEX '76

Two data sets*

G. RADACH**, J. TRAHMS*** and A. WEBER***

Abstract

During the Fladen Ground Experiment (FLEX '76) in the Northern North Sea two data sets of chlorophyll measurements were obtained at the Central Station (58° 55' N, 0° 32' E) over about three months, one by measuring *in vivo* fluorescence using a submersible EOS-fluorometer *in situ* (Trahms) and the other by analysing water samples by a spectral photometer (Weber). The two data sets are put in relation to each other. Using chlorophyll as an indicator, the development of the spring phytoplankton bloom is discussed.

1.- Introduction

The Fladen Ground Experiment (FLEX '76) aims at a better understanding of the flow of matter through the lower trophic levels of the marine ecosystem in the northern North Sea. The key problem is the relationship between phytoplankton dynamics and the physical dynamics of the upper layer of the ocean, the latter being the formation of the seasonal thermocline during this experiment (March 25th - June 6th).

---

* This is JONSDAP '76 contribution n° 67.

** Institut für Meereskunde, Universität Hamburg, Hamburg, F.R.G.

*** Institut für Allgemeine Botanik, Universität Hamburg, Hamburg, F.R.G.

Within the Fladen Ground Experiment several data sets were gathered for the description of phytoplankton: the FLEX box was covered 6 times by surveys of British and German ships which monitored chlorophyll in 3 m depth (R.V. Explorer, R.V. Cirolana) or with an undulator ("Delphin") going down to 30 m (R.V. Anton Dohrn). These data sets were mainly used for the determination of the horizontal scales of phytoplankton patchiness (Horwood, 1978, Steele and Henderson, 1979). Another data set which will give synoptic maps of the whole FLEX region was obtained by measurements from an aircraft and is being evaluated by Doerffer (See this volume).

Stationary work within the FLEX box was carried out by the British, Dutch and German groups, part of which has been published (e.g. Gieskes and Kraay, 1980).

The most extensive stationary work was performed at the Central Station (58° 55'N, 0° 32'E, R.V. Meteor and R.V. Anton Dohrn). Among a great number of parameters, chlorophyll was monitored. This was done by two different methods, namely by analysing water samples using a spectral photometer and by using a submersible fluorometer *in situ*.

In this paper these two data sets are described and related to each other by regression analysis. The spring phytoplankton bloom is described by the development of chlorophyll concentration.

A third data set at the Central Station, the phytoplankton cell counts, will be presented in a separate paper (Gillbricht and Radach, 1980).

2.- Methods

2.1.- *IN VIVO* FLUOROMETRIC DETERMINATIONS OF CHLOROPHYLL *IN SITU*

In vivo chlorophyll was measured *in situ* in vertical profiles down to about 80 to 100 m depth using a submersible EOS-fluorometer. A pulsing gas discharger flash lamp (Bhaumik and Telk, 1964; Goncz and Newell, 1966) with a Balzers DT cyan blue filter is used as light source (5 flashes/sec) in this instrument. The sensor is a silicon photodiode with a Schott filter (685 nm). The sensitivity is independent of temperature between -2° and 50° C because of an interior heating. Further properties of the equipment are: coherent detection, sample/hold synchronized to emitter, solid optics collimator for emitter and receiver, optical aperture 1:1;

the light beam is vertically incident to the interference filter; the distance between collimator front and sampling volume is very small (15 mm). The time constant is about 0.35 sec/decade.

The armoured instrument was lowered and raised on the hydrographic wire at about 0.33 m/sec. Power was supplied by a 24 V ± 20% battery with a (5 strand) rubber armoured cable. The current consumption was 260 mA.

Depth registration was done with a piezoresistive pressure transducer (Kistler, Type 4041 A 50). Signals were recorded in mV on a Rikadenki multi-pen recorder Type B 381.

During the entire experiment 153 profiles were taken. The recorded values were read from the graph produced by the multi-pen recorder in depth intervals of 5 m.

Measurements by the fluorometer will be denoted by c_f in the following.

2.2.- CONVENTIONAL METHOD OF DETERMINING CHLOROPHYLL

2.2.1.- *Sampling*

To obtain a phytoplankton sample for the determination of chlorophyll *a*, 2 ℓ of sea water were filtered through a glass fibre filter (Whatman GFC). Subsequently, the filter was frozen in a closed glass tubule (at least $-20^{\circ}C$). To neutralize cell fluid, which might be exudated, the filters were moistened with $MgCO_3$ solution before the filtration procedure.

2.2.2.- *Sample processing*

For extraction of chlorophyll 5 ml Acetone (85%) was added to the deep-frozen samples, which were then submitted to ultrasonic treatment at maximum intensity twice for 10 sec (ultrasonic generator from Branson). The sample was centrifuged after 20 minutes of extraction in the dark, and the clear extract was filled into a 1 cm quartz cuvette. The measurement itself consists of determining the extinction in the wave range of 300 to 750 nm using a spectral photometer (Unicam SP 1800, Philips). The whole spectrum was plotted, permitting a subsequent calculation of chlorophyll values according to the methods of several authors. We used the formulae of Strickland and Parsons (1968) and of Lorenzen (1967). While the calculation according to Strickland and Parsons results in the determination of total chlorophyll a, Lorenzen's method allows a certain differentiation. By subtracting phaeophytine a from total chlorophyll a, a quantity is calculated which

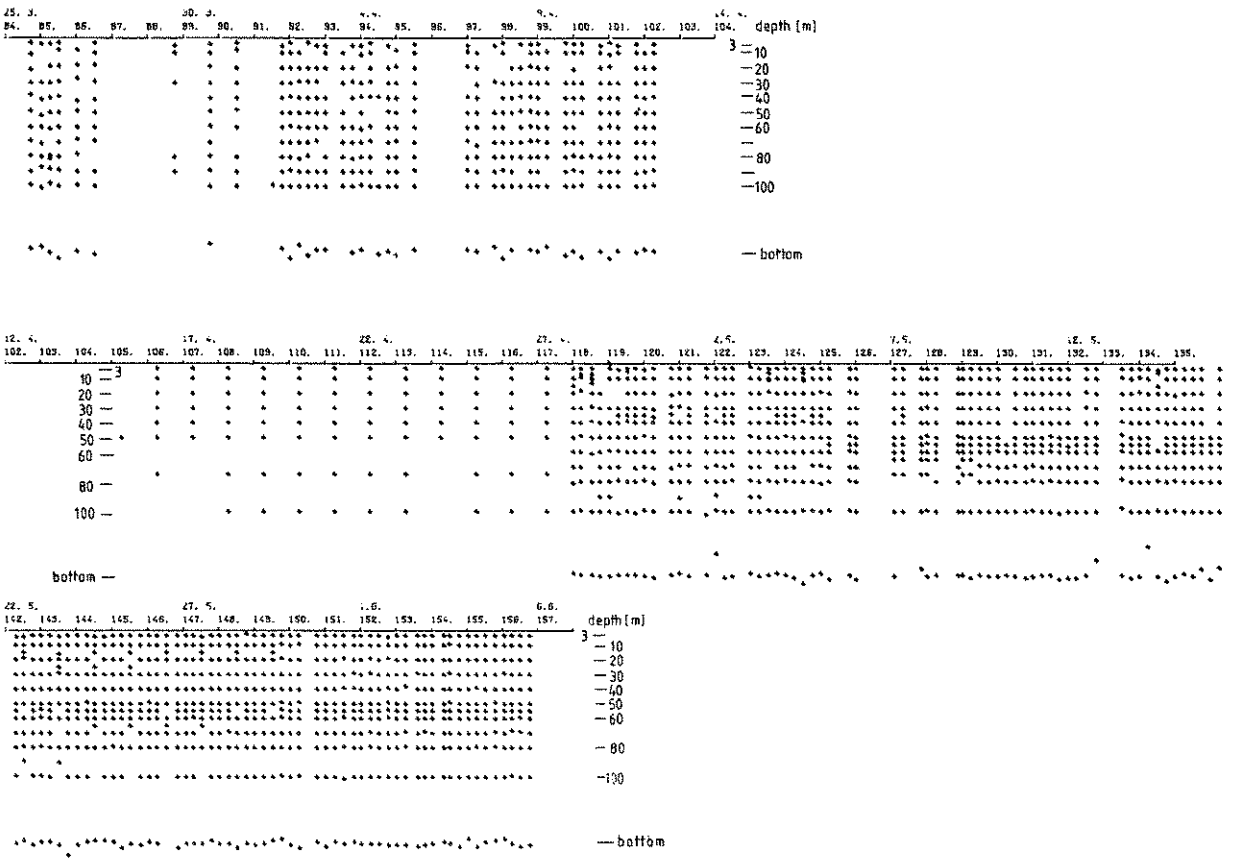

fig. 1.

Sampling grid over depth and time at the Central Station (58° 55' N, 0° 32' E) for water samples analysed by spectral photometry.

corresponds largely to 'active chlorophyll a'. This latter chlorophyll a is able to photosynthesize and does not include 'dead chlorophyll'.

The chlorophyll determinations were finished 5 months after the Fladen Ground Experiment. The reduction of chlorophyll content due to storage was not determined.

In total, more than 2000 samples were treated in the described way. Fig. 1 shows their distribution in time and over depth. During the R.V. Anton Dohrn cruise only one series was collected daily. During the other cruises, generally 4 series were obtained daily. The values of pigments obtained by extinction measurements will be denoted by c_e, with a second index t, a or p for total chlorophyll a, active chlorophyll a or phaeophytine a ($c_{e,t}$; $c_{e,a}$; $c_{e,p}$).

3.- Chlorophyll data set from extinction measurements

Total chlorophyll a and active chlorophyll a determined by the photometric method are shown in Figs. 2 and 3 for the whole of FLEX in the form of isopleths over time and depth at the Central Station.

The phytoplankton bloom is characterized by a maximum chlorophyll a concentration close to the surface of more than 10 mg Chl/m^3 around April 30th. Between April 24th and may 6th chlorophyll a concentrations are greater than 3 mg Chl/m^3 in the mixed layer. The values for active chlorophyll are slightly less, but the structure in time and space is identical.

There are indications of a second chlorophyll maximum around May 23th, which is much less pronounced than the first, showing values around 3 mg Chl/m^3.

Phaeophytine a (Fig. 4) shows a distribution pattern in which the maximum occurs 2 to 3 days after that of chlorophyll. This maximum is not situated at the surface but in the lower half of the mixed layer (about 30 - 60 m). The local maximum in the water column sinks down from May 7th on, and it sinks below the thermocline on May 12th. Phaeophytine, as an indicator of detrital material, illustrates how the declining phytoplankton bloom changes into detritus and sinks out of the mixed layer into deeper layers and down to the bottom.

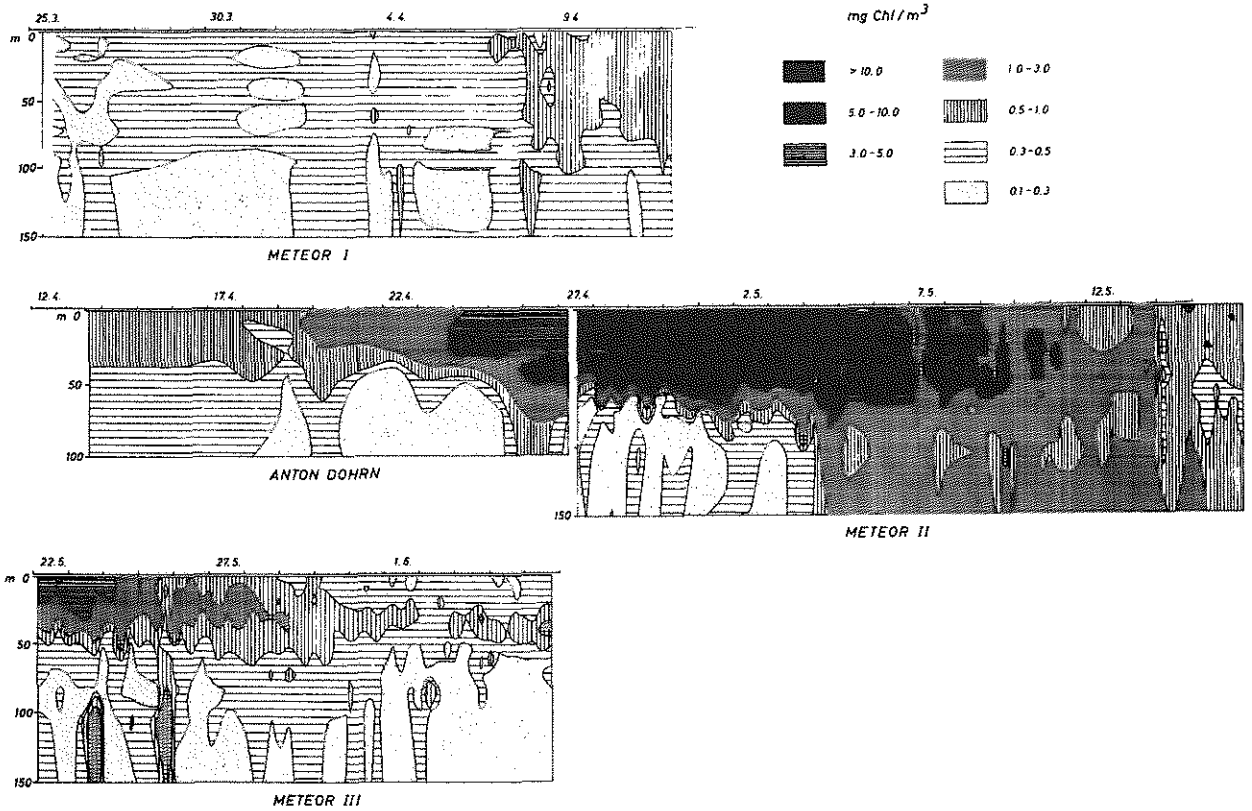

fig. 2.

Total chlorophyll a, $c_{a,t}$: distribution over depth and time at the Central Station

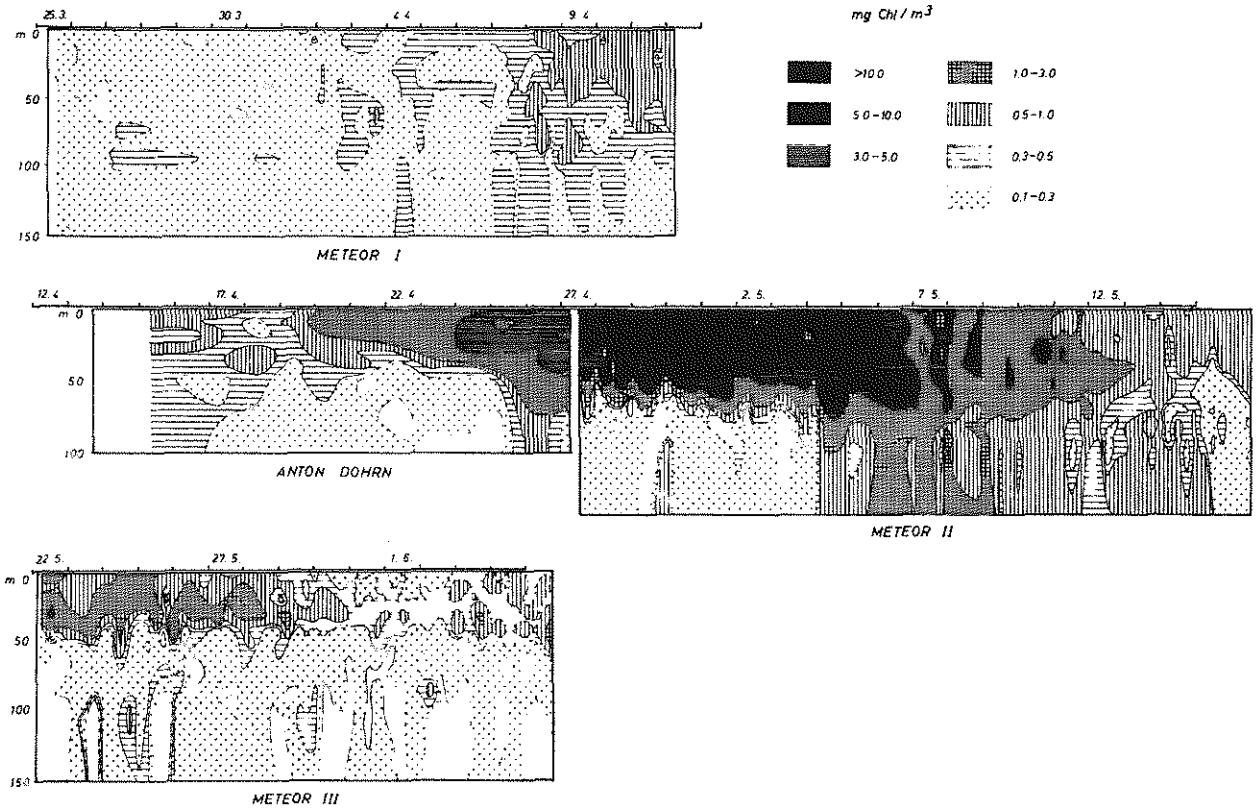

fig. 3.

Active chlorophyll a, $c_{e,a}$: distribution over depth and time at the Central Station

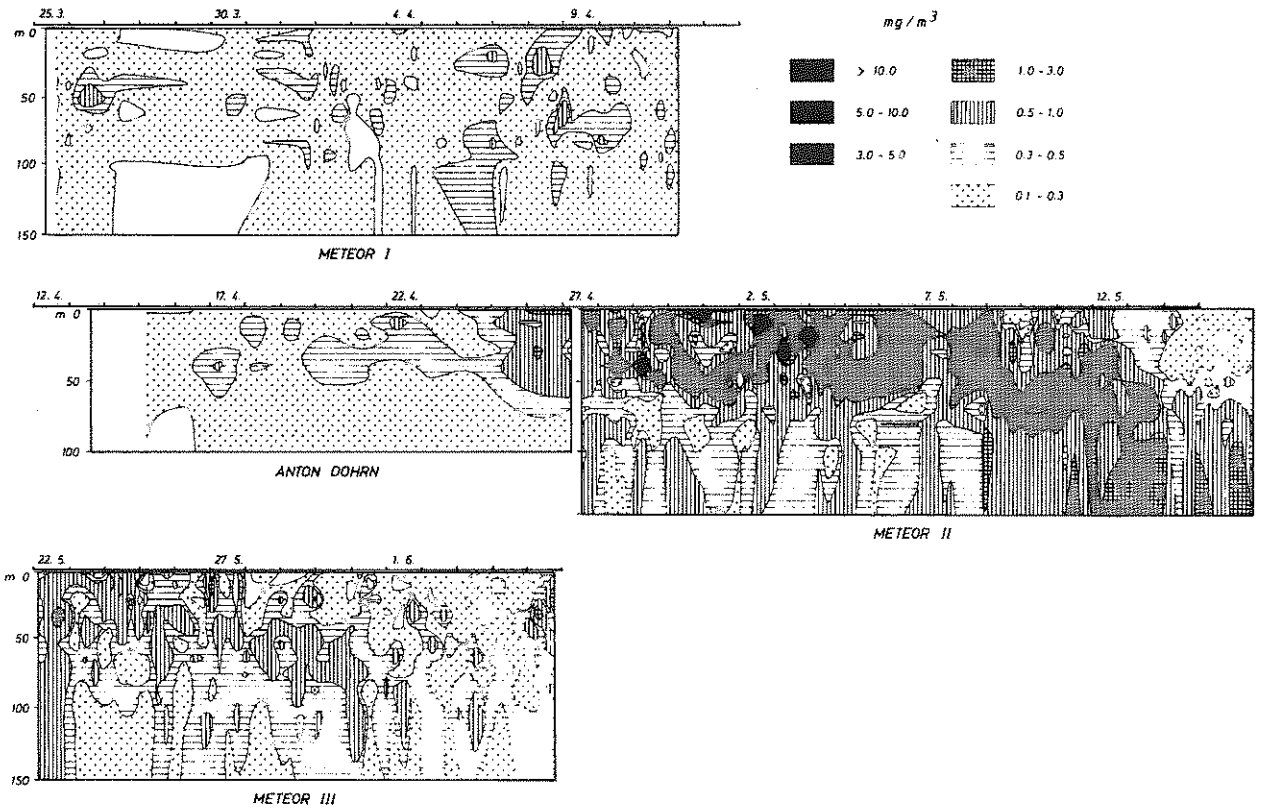

fig. 4.

Phaeophytine a, $c_{e,p}$: distribution over depth and time at the Central Station

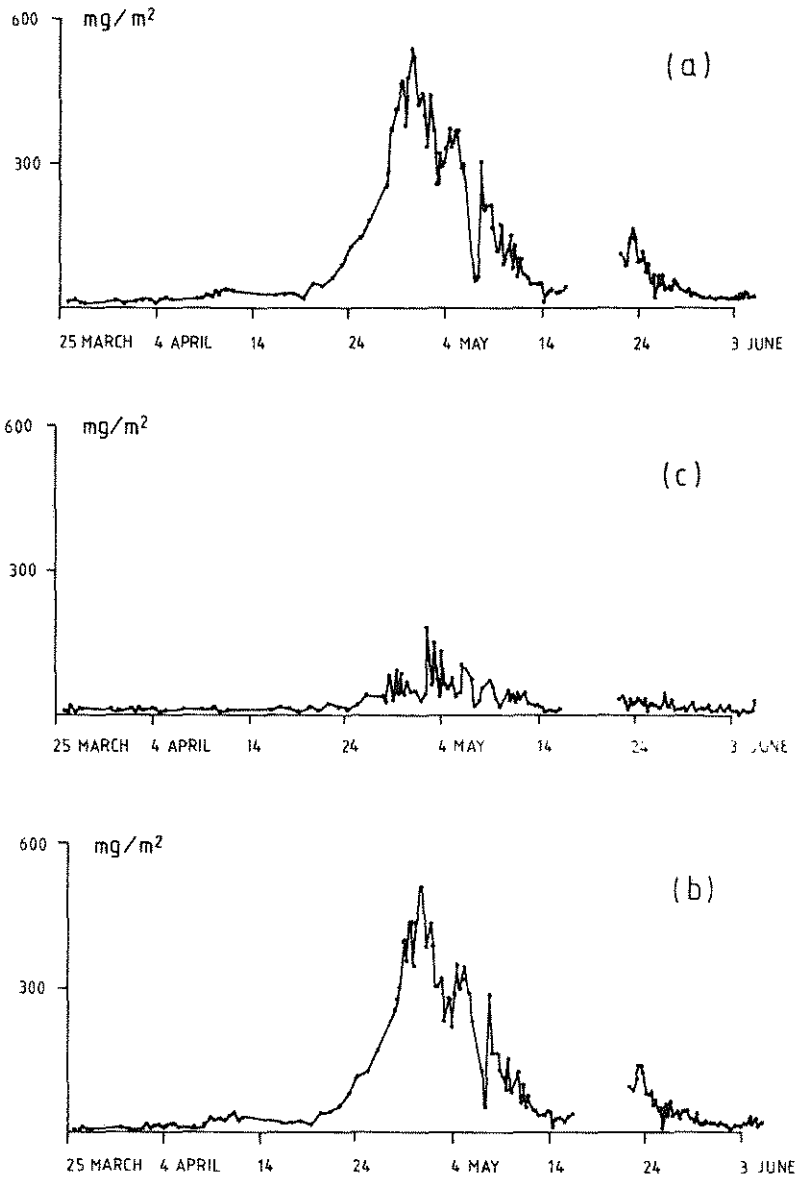

fig. 5.

Cortent of (a) total chlorophyll a, (b) active chlorophyll a and (c) phaeophytine a in the upper 50 m of the water column, in mg/m^2, at the Central station.

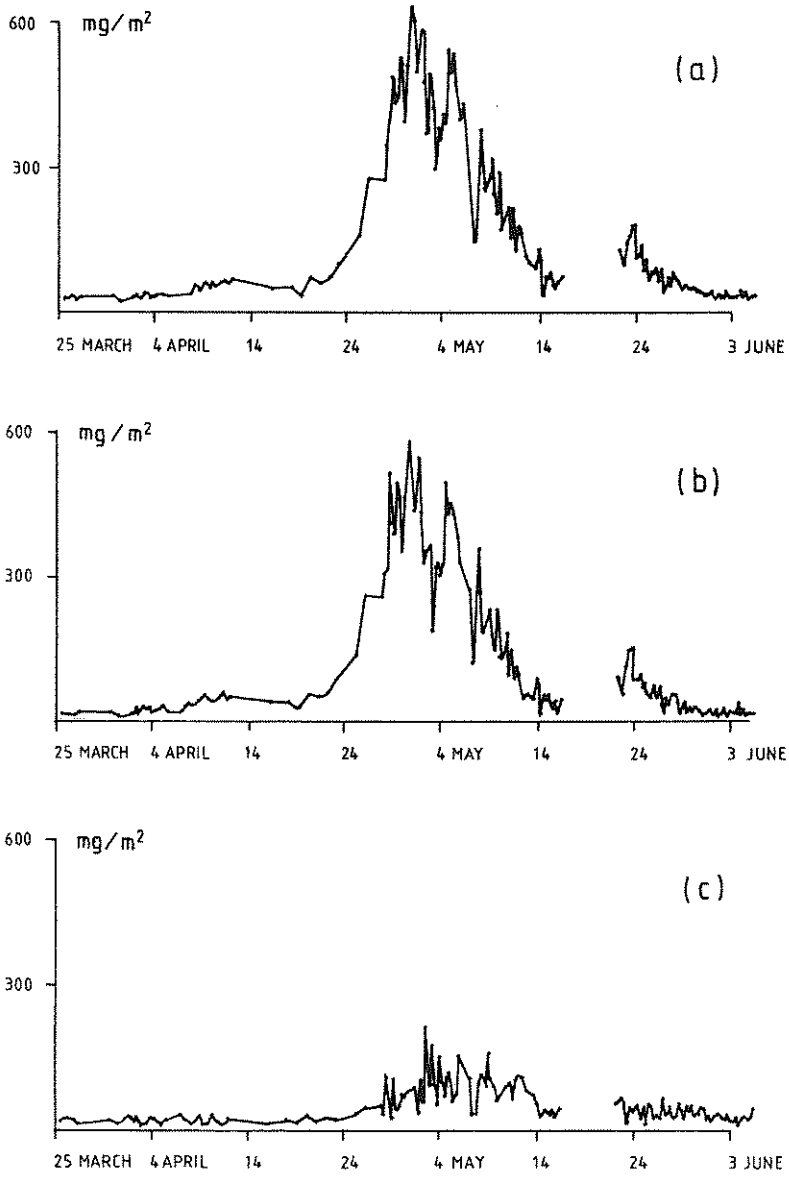

fig. 6.

Content of (a) total chlorophyll a, (b) active chlorophyll a and (c) phaeophytine a in the upper 100 m of the water column, in mg/m^2, at the Central Station.

The amounts of total chlorophyll a, active chlorophyll a and phaeophytine a per m^2 within the upper 50 m and 100 m respectively, are presented as time series in Figs. 5 and 6. The maximum total chlorophyll a content in the upper 50 m lies around April 30th and is about 500 mg Chl/m^2. The same is true for active chlorophyll a.

During the exponential growth phase (until April 30th) only small amounts of phaeophytine a are found. Later on the concentration of phaeophytine a increases to a fourth or a third of the weight of the total chlorophyll a content.

4.- Chlorophyll data set from fluorometer profiles

The second chlorophyll data set from the Central Station of FLEX stems from profiles taken by a fluorometer. From the continuous registrations values were read at every 5 m depth. There are no measurements from the cruise of R.V. Anton Dohrn. The values are given in the unit mV. The fluorometer was launched directly before the collection times for the water samples. Thus, to calibrate this data set both data sets had to be interpolated on a fixed grid (depths: 3, 10, 20, 30, 40, 50, 60, 70, 80, 100 m; times: 0, 6, 12, 18 h). As the composition of the phytoplankton population changes with time it would theoretically be appropriate to calibrate the data sets for time intervals which correspond to the bloom of a single species. From the practical point of view this procedure does not seem to be necessary because a few Chaetoceros species make up the diatom bloom to a large degree until the end of the second cruise of R.V. Meteor (Gillbricht and Radach, 1980). Therefore, we restricted ourselves to calibrating the data sets for each of the three Meteor cruises.

Within the range of chlorophyll values occurring during FLEX the fluorometer did not work along a linear relationship between chlorophyll and the observed voltage but along an exponential relation

$$c_e = A\, e^{B \cdot c_f} \quad . \tag{1}$$

The two data sets were related to each other by linear regression analysis applied to

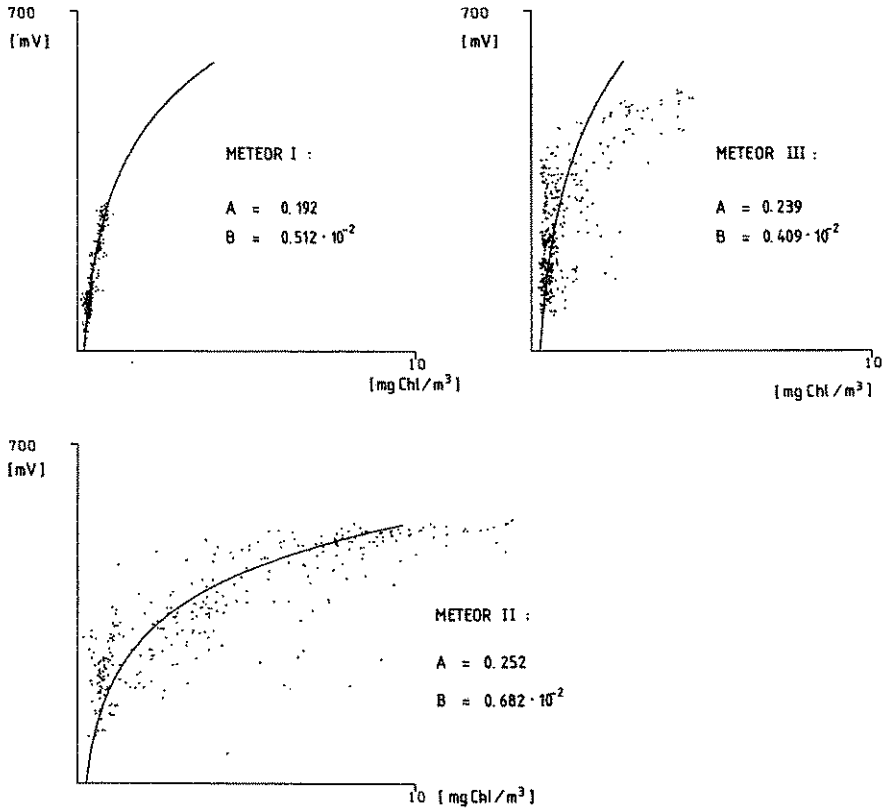

fig. 7.

Correlation between spectral photometric chlorophyll c_e and fluorometric chlorophyll cf and the regression lines

$$c_e = A\, e^{B\, cf}$$

for the three cruises of R.V. Meteor at the Central Station, using data from the upper 50 m only.

$$y = A' + Bx,$$

where

$$y = \ln c_e, \quad x = c_f, \quad A' = \ln A,$$

and the constants A', B are to be determined. The correlations and the resulting exponentials (1) are shown for the 3 cruises of R.V. Meteor in Fig. 7

using the data in the upper 50 m . The exponentials look different for the three cruises. It is obvious that these relations are of value only for calibrating the fluorometer measurement during *this* experiment. While the exponential works perfectly for the first cruise it does not for the third cruise. Perhaps the data from the last cruise should have been divided up once more, because there are mainly two clouds of dots. During the second cruise the peak of the bloom is attained and the highest chlorophyll values occur. From the correlation it is clear that the fluorometer measurements are less sensitive than the photometric method for the highest chlorophyll values. The fitted exponential is a little more sensitive for high mV-values than the dots in the correlation figure show.

There is no significant difference in the correlations if the upper 100 m are used instead of the upper 50 m. The constants A and B in relation (1) are given in Table 1.

Table 1

Constants A and B in relation (1)
for the three cruises of *R.V. Meteor*.

	A	B
Meteor I	0.192	$0.512\ 10^{-2}$
Meteor II	0.252	$0.632\ 10^{-2}$
Meteor III	0.239	$0.409\ 10^{-2}$

Using these constants for the three cruises, the fluorometer measurements in mV/m^3 were converted to mg Chl/m^3.

Fig. 8 shows the chlorophyll distribution derived from the fluorometric measurements over depth and time at the Central Station. The vertical structure is very similar to that of the photometric chlorophyll values (Fig. 2). The same can be seen from the vertically integrated chlorophyll content (0 - 50 m) presented in Fig. 9.

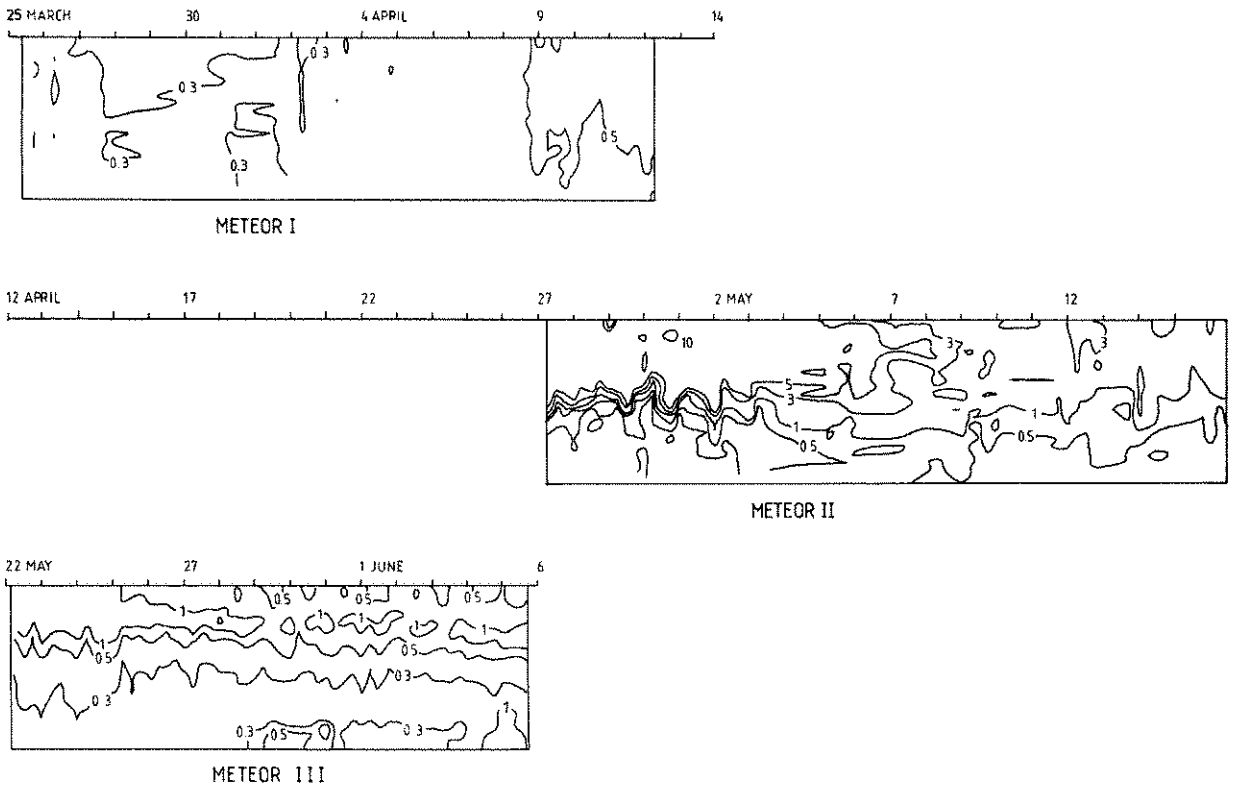

fig. 8.

Total chlorophyll from fluorometric measurements, converting the data from mV to mg Chl by the regression functions (1) shown in fig. 7.

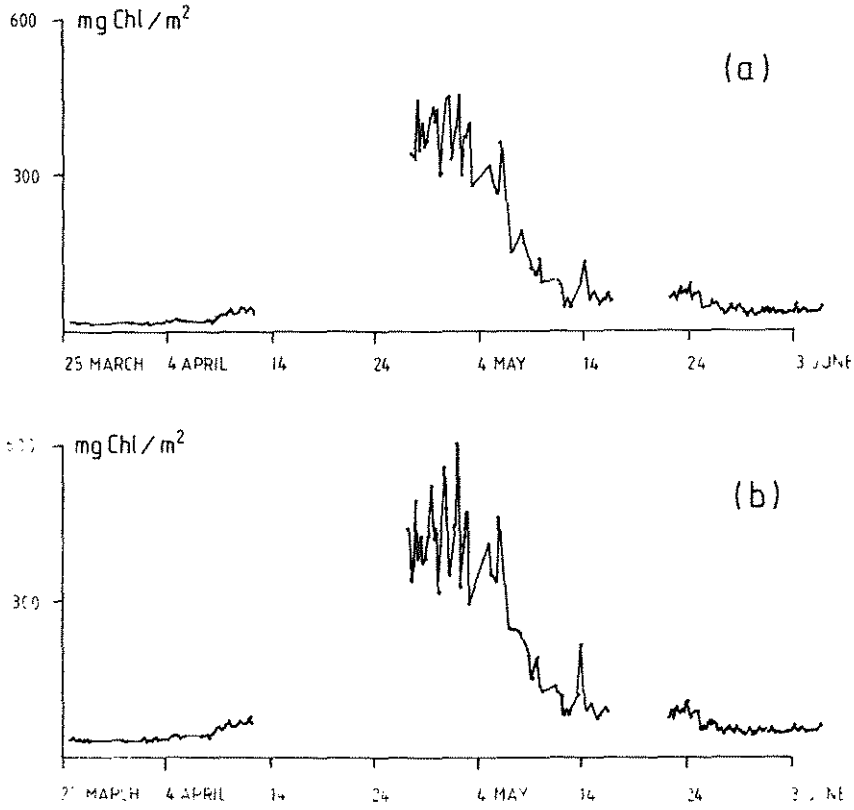

fig. 9.

Content of total chlorophyll in the upper 50 m and 100 m resp. from fluorometer measurements, converting mV into mg Chl by the regression functions (1) shown in fig. 7.

5.- Discussion

For the discussion of the chlorophyll data - as for all other data from the Central Station - it is of great interest whether the time series obtained represent local dynamics or whether strong advectional disturbances have to be dealt with. Important information about advection can be obtained from the investigation of the development of the thermal structure. This leads to the conclusion that the local heat budget is fulfilled up to 10% of the heat content of the water column. The difference could be due to errors in the

computational procedure or a long term advectional influence (Soetje and Huber, 1980). Thus, we may assume that the first order dynamics are determined locally for the physical parameters. Biological parameters have a patchy distribution (e.g. Steele and Henderson, 1979) as the FLEX box surveys show. According to Gillbricht's studies (pers. comm.), however, the biological dynamics can be treated as local dynamics, at least until the end of the 2nd Meteor cruise (May 16th). Accepting this point of view the data may be interpreted as follows.

First of all, the development of chlorophyll is described equally well by both data sets. The fluorometric method has the advantage of high vertical resolution, which is especially valuable within the thermocline where strong chlorophyll gradients occur, and the data are immediately available. The disadvantage lies, of course, in the fact that absolute chlorophyll values can be obtained only after calibrating the data with chlorophyll values determined from simultaneous water samples.

The magnitude of the chlorophyll values is in good agreement with the values determined by Gieskes and Kraay (1980).

Fortunately, the whole spring phytoplankton bloom was covered by the measurements. The development of phytoplankton proceeds parallelly to the warming of the upper layers of the sea, both being strongly coupled to incident radiation. The start of the bloom occurred when the temperature in the surface water increased to 6.25°C. The increase continued gradually. On April 19th the temperature at the surface reached 6.5°C and chlorophyll passed 1 mg Chl/m^3. From this date on the heat content of the water began to increase; the daily input surpassed the output at night (Soetje and Huber, 1980). The chlorophyll concentration increased exponentially and reached its maximum of about 550 mg Chl/m^2 on April 30th. The sea surface temperature had reached only about 6.7°C by then. The bloom had a half-width of 10 to 12 days. The logarithmic curve of chlorophyll in the water column (Fig. 10) shows two different growth phases devided by April 19th. Before this date the growth rate is much smaller than thereafter. We may hypothesize that this results from the fact that peridineans dominated in the phytoplankton until diatoms took over at about April 19th (Gillbricht and Radach, 1980), and that peridineans have smaller growth rates than the main diatom species (*Chaetoceros sp.*).

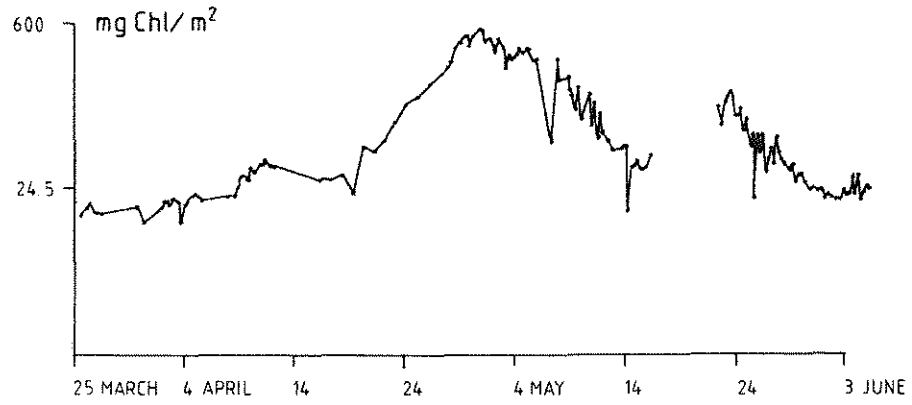

fig. 10.

Total chlorophyll a in the upper 50 m , as in fig. 5a but on a logarithmic scale

In general, the stratification structure determines the vertical distribution of chlorophyll during FLEX '76: During the first cruise the water column is fully mixed until April 9th, when the surface warms up slightly. The 6.25°C - isopleth corresponds nicely to the 0.5 mg Chl/m^3 isopleth, and from April 19th on the same is true for the 6.5°C- and the 1 mg Chl/m^3-isopleths until April 29th. From then on the thermocline limits the chlorophyll to the upper mixed layer; below this layer only very small chlorophyll concentrations are found until May 4th.

During the second half of the breakdown of the bloom (4th to 15th of May) chlorophyll is distributed over the whole water column, also below the thermocline (1 - 3 mg Chl/m^3). This is not the case for phytoplankton carbon, in which much larger differences were observed during that period between the upper and lower layers (Gillbricht and Radach, 1980).

The distributions of phaeophytine a and active chlorophyll a during the second cruise of R.V. Meteor (Figs. 3 and 4) support the assumption that strong sinking of phytoplankton occurred between May 4th and 13th. From May 6th to 8th there is more active chlorophyll in the lower layer than later on, and from May 9th to 13th there is more phaeophytine than before. This indicates a continuing degradation of active chlorophyll into phaeophytine while the material is decaying in the upper layer and sinking down through the water column. If all the sinking material falls within the

10 day period from 60 m to the bottom, a maximum sinking speed of 9 m/d would result for the detrital material.

During the third cruise of R.V. Meteor new shallow warm layers form, creating new thermoclines. The chlorophyll concentration is largest below these layers and the seasonal main thermocline. At the beginning of the third cruise a second maximum is observed, which has concentrations of 3 to 5 mg Chl/m^3. An interesting feature is that this bloom - different from the first diatom bloom - is situated in the middle of the upper layer.

A more detailed analysis of the chlorophyll dynamics during the 1st and 2nd Meteor cruise would have to include nutrients (Weichart, 1980; Eberlein et al., 1980) as well as zooplankton (Krause and Radach, 1980a, b). Analysis of the third cruise will necessitate the introduction of remineralisation and thus draw on the results for zooplankton excretion and bacterial activity. Phaeophytine, for example, is correlated with fecal pellets (Krause, 1980).

The overall dynamics regulating the distribution of chlorophyll before, during and directly after the bloom seem to be determined primarily by algal growth, turbulent diffusion and sinking (probably depending on the physiological state of the algae). Under these assumptions simulations should be performed similar to those for the reproduction of the phytoplankton carbon dynamics (Radach, 1980) for comparison with the latter. This could indicate which parameter, chlorophyll or phytoplankton carbon, is more appropriate for use in model simulations.

Acknowledgements

Special thanks are due to Sabine Grimme for her help in programming and plotting the figures. Thanks are also due to Rotraut Maison and Renate Krautwald for drawing figures.

We are particularly grateful for the assistance on board and in the laboratory of Thomas Christlieb, Erika Heuer, Rüdiger Kopp, Michael Krause and Alex Sanchez.

This research was supported by the Deutsche Forschungsgemeinschaft through the Sonderforschungsbereich 94 — Meeresforschung Hamburg.

References

BHAUMIK, M.L. and TELK, C.L. (1964). Fluorescence quantum efficiency of rare-earth chelates, *J. opt. Soc. Amer.*, 54 (10), 1211-1214.

DOERFFER, R. (1980). The determination of the horizontal phytoplankton distribution by remote sensing during FLEX '76, in this volume.

EBERLEIN, K., KATTNER, G., BROCKMANN, U. and HAMMER, K.D. (1980). Nitrogen and phosphorus in different water layers at the central station during FLEX '76, *Meteor Forsch. Ergebn. A*, 22, 87-98.

GIESKES, W.W.C. and KRAAY, G.W. (1980). Primary production and pigment measurements in the northern North Sea during FLEX '76, *Meteor Forsch. Ergebn. A*, 22, 105-112.

GILLBRICHT, M. and RADACH, G. (1980). Phytoplankton cell counts at the Central Position during FLEX '76, in prep.

GONCZ, J.H. and NEWELL, P.B. (1966). Spectra of pulsed and continuous Xenon discharges, *J. opt. Soc. Amer.*, 56 (1), 87-92.

HORWOOD, J.W. (1978). Observations on spatial heterogeneity of surface chlorophyll in one and two dimensions, *J. Mar. Biol. Ass. U.K.*, 58, 487-502.

KRAUSE, M. (1980). Vertical distribution of fecal pellets during FLEX '76, in this volume.

KRAUSE, M. and RADACH, G. (1980). On the succession of developmental stages of herbivorous zooplankton in the northern North Sea during FLEX '76, *Meteor Forsch. Ergebn. A*, 22, 133-149.

KRAUSE, M. and RADACH, G. (1980). On the vertical distribution and migration of herbivorous zooplankton in the northern North Sea during FLEX '76, in prep.

LORENZEN, C.J. (1967). Determination of chlorophyll and phaeo-pigments : spectrometric equations, *Limn. Oceanogr.*, 12, 343-346.

RADACH, G. (1980). Preliminary simulations of the phytoplankton and phosphate dynamics during FLEX '76 with a simple two-component model, *Meteor Forsch. Ergebn. A*, 22, 151-163.

SOETJE, K.C. and HUBER, K. (1980). A compilation of data on the thermal stratification at the Central Station in the northern North Sea during FLEX '76, *Meteor Forsch. Ergebn. A*, 22, 69-77.

STEELE, J.H. and HENDERSON, E.W. (1979). Spatial pattern in North Sea plankton, *Deep Sea Res.*, 26, 955-963.

STRICKLAND, J.D.H. and PARSONS, T.R. (1968). A practical handbook of seawater analyses, Fish. Res. Bd. Can., Bulletin n° 167, Ottawa.

WEICHART, G. (1980). Chemical changes and primary production in the Fladen Ground area (North Sea) during the first phase of a spring phytoplankton bloom, *Meteor Forsch. Ergebn. A*, 22, 79-86.

The determination of the horizontal phytoplankton distribution by remote sensing during FLEX '76 *

Roland DOERFFER**

1.- Introduction

The aircraft remote sensing experiment of FLEX'76 was carried out with two main objectives:

- to study techniques for the remote measurement of the phytoplankton distribution under different environmental conditions of the northern North Sea,
- to supply the Fladenground-experiment with information about the horizontal distribution of different water masses including plankton patches by using the backscattered solar radiation and the sea surface temperature under the assumption of proven techniques.

The demand for a horizontal survey was given because the knowledge of the horizontal variability has been considered as an important prerequisite for the interpretation of time series of the biological parameters during the FLEX plankton bloom.

This paper describes the application of a method, which has been developed for the FLEX data set to retrieve the significant information about the horizontal varibility from the spectra of the backscattered radiance.

---

* This is JONSDAP '76 contribution n° 65.

** GKSS Forschungszentrum, 2054 Geesthacht, F.R.G.

2.- Measurements

The aircraft program was carried out by the DFVLR (principle investigator V. Amann) in cooperation with the University of Hamburg (SFB94) and the University of Lille in the period 4th of April - 5th of May.

Corresponding to the objectives two different pattern were flown alternatively during the campaign:

- for only experimental work a rosette pattern in the vicinity of the central ship ("Meteor", "Anton Dohrn") should allow to study the influence of different solar angles, wave directions and flight altitudes on the optical and IR signal,
- for the horizontal survey a pattern of 6 profiles (s. fig. 1) was flown according to the ship tracks recommended for the British research vessels.

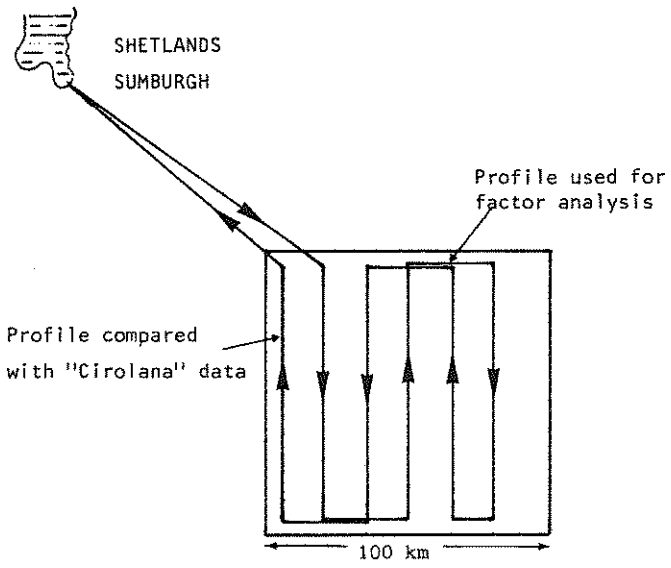

fig. 1.
Flight pattern of the FLEX-BOX aerial survey

The data used for this study are from the FLEX-Box survey of the 5th of May. At this time the British RV "Cirolana" started a horizontal

survey which was completed at the 9th of May. This was a good opportunity to compare the results of both surveys.

For the following calculations the data of a multichannel radiometer (manufactured by Suarez) has been used. This instrument measures the upward directed radiance from the sea as well as the downward directed irradiance in the spectral range 425-725 nm in 16 channels.

The instrument was directed 20° off the the nadir to avoid any sunglint. The weather of the 5th of may showed a clear sky with a horizontal visibility of 30 km and little wind, the flight altitude was 600 m.

The chlorophyll values used for calibration are from *R.V. Cirolana* (Horwood, 1977), the sample were taken from 3 m depths.

3.- The interpretation of the backscattered radiance

Before applying any algorithms to calculate concentrations of substances in the water from the backscattered radiance, it is necessary to analyze how many independent components are effecting the variability of the spectra along the flight track and if all or part of these components can be interpreted as concentrations of different substances in the water. For the first analysis of the FLEX data a 30 km flight profile with a strong variability was selected (fig. 1).

The first step in the extraction of the useful information out of the spectra is the eigenvalue analysis (Mueller, 1973; Doerffer, 1980) : the 16 wavelengths can be considered as variables, so that 16 eigenvectors can be calculated. Fig. 2 shows the eigen values in order of their significance. It is clearly to be seen that two significant components can be seperated, while all others are representing the noise.

The separation is supported by the following criteria :

- the first two eigenvalues are above 1 ,
- the discontinuance in the eigenvalue diagram,
- a low-pass filtering of the data enhances the eigenvalues of the first two components and reduces the eigenvalues of those components interpreted as noise.

The interpretation of the significant two components can be done by the factor analysis. The method used here is described in Überla (1971).

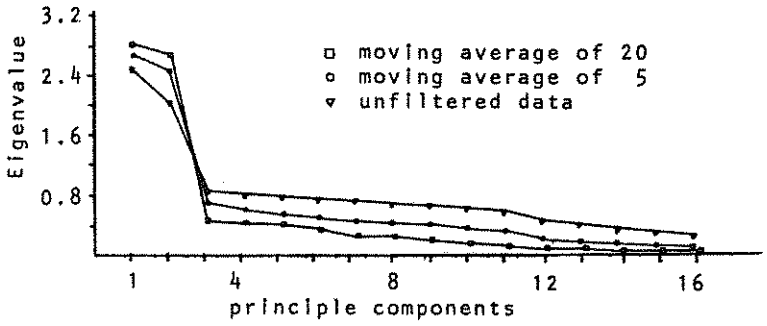

fig. 2.

Eigenvalues of the principle components in order of their variance

Fig. 3 shows the two extracted factors after orthogonal rotation and their correlation (factor loadings) with the 16 spectral channels.

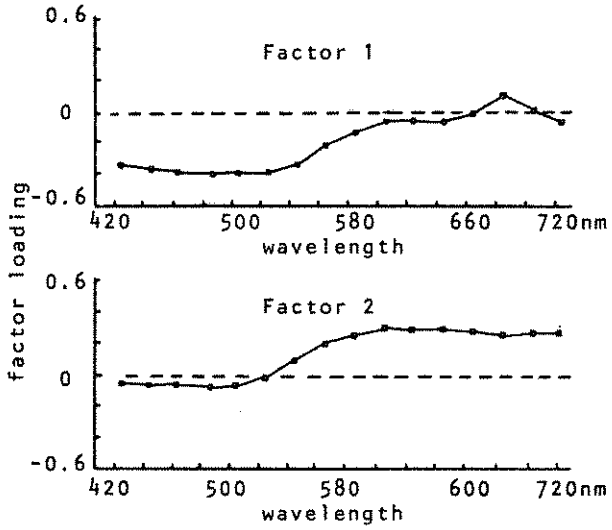

fig. 3.

Correlation between the two factors and the spectral channels

The dominant factor 1 shows a high negative correlation in the blue part of the spectrum (around 470 nm) and a positive correlation at 685 nm. Due to these properties this factor can be interpreted as phytoplankton.

Factor 2 can be related to suspended matter because of the increasing factor loadings towards the red part of the spectrum, however this was not verified by sea truth.

Because of the peak at 685 nm of factor 1, which is supposed to be due to the chlorophyll fluorescence, an algorithm was performed like this of Neville and Gower (1977). It uses the peak hight above the base line calculated from the radiometer channels at 645 nm and 724 nm :

$$I(685) - [I(724) - I(645)]/2 \ .$$

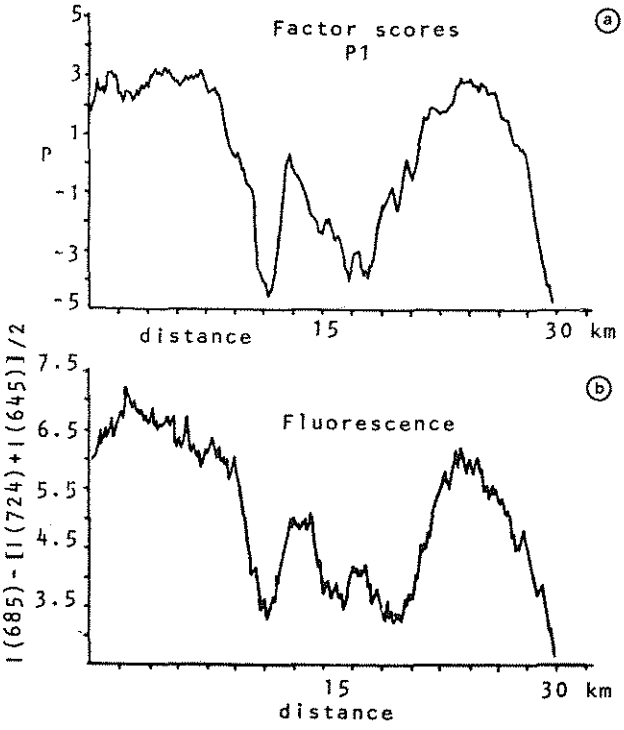

fig. 4.

Comparison of the factor values with the fluorescence algorithm

The fluorescence calculated with this algorithm was compared with the values of factor 1 estimated for each spectrum of the flight profile (factor scores). Fig. 4 shows the good agreement between both curves.

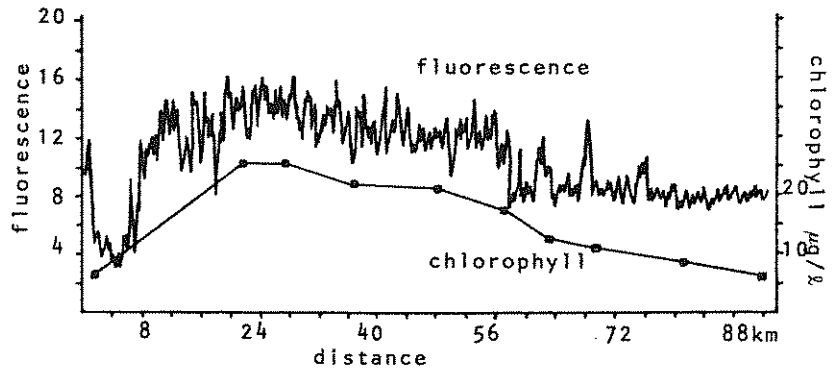

fig. 5.

Fluorescence measured from 500 m altitude and chlorophyll samples from 3 m depth

By using the *in situ* data from the ship the fluorescence algorithm could now be calibrated in terms of absolute chlorophyll concentrations. The comparison between the ship and aircraft measurements was done only from the western profile, because only here the time difference was not greater than 1 day. Fig. 5 shows the fluorescence measured from the aircraft in arbitrary units and the chlorophyll concentration measured from the ship from that profile. The good agreement is manifested by the high linear correlation given in Fig. 6.

This calibration was now used to calculate the concentration along all 6 profiles and for contouring the horizontal distribution in the whole FLEX box for that day (Fig. 7).

When comparing this map with the result of the "Cirolana" survey (Horwood, 1977) it can be seen that the agreement is high in the western part of the FLEX box where the time difference is small and becomes lower towards the east where the time shift was 4 days.

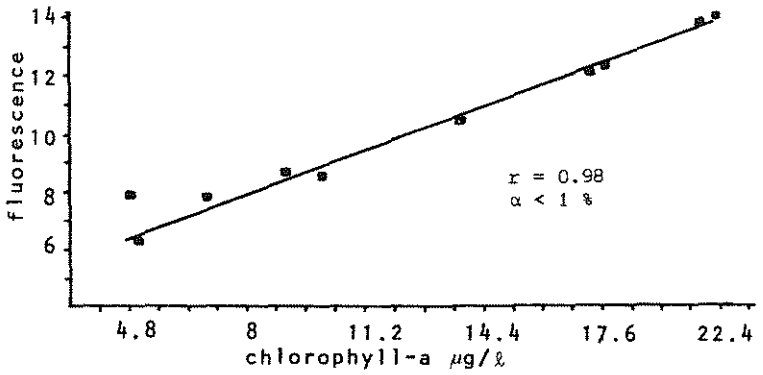

fig. 6.

Calibration of the fluorescence measurements with sea truth chlorophyll values

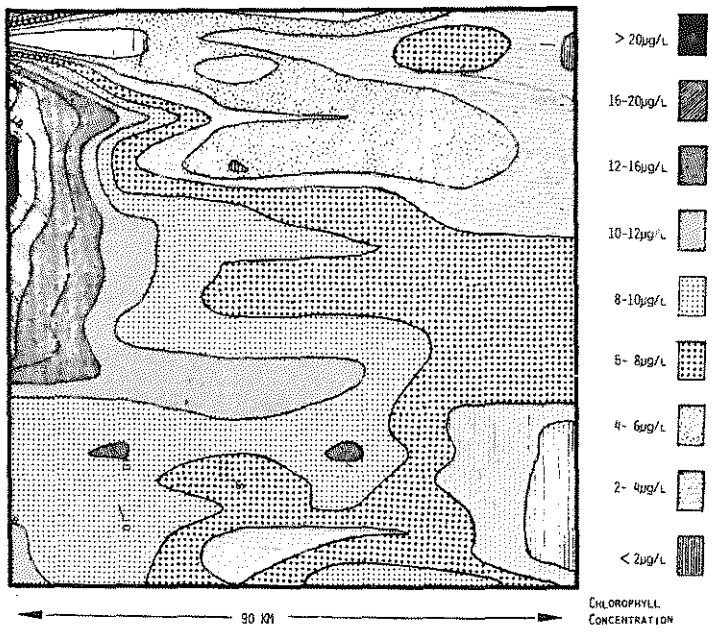

fig. 7.

Chlorophyll distribution in the FLEX-BOX (5-5-76) calculated from aircraft measurements of the fluorescence.

4.- Conclusions

The analysis of the backscattered radiance has shown that two significant components can be retrieved from which the first represent the variability in the phytoplankton chlorophyll concentration.
The factor loading diagram proves that the fluorescence of the chlorophyll stimulated by the sunlight can be used for remote detection and the calculation of its concentration. The comparison with sea truth data shows a high linear correlation between the chlorophyll concentration and the fluorescence detected from the aircraft.

References

DOERFFER, R. (1980). Factor analysis in ocean color interpretation, *Proc. of the IUCRM/SCOR/COSPAR Symposium "Oceanography from Space"*, Venice (in press).

HORWOOD (1977). Chlorophyll data of *RV Cirolana* cruise 5th May - 9th May, FLEX DATA CENTRE, HAMBURG and FLEX-ATLAS.

MUELLER, J.L. (1973). *The influence of phytoplankton on ocean color spectra*, Ph. D. Thesis, Oregon State University N., Corvallis.

NEVILLE, R.A. and GOWER, I.F.R. (1977). Passive remote sensing of phytoplankton via chlorophyll *a* fluorescence, *J. Geophys. Res.*, 82, 3487-3493.

ÜBERLA, K. (1971). *Faktorenanalyse*, Springer Verlag, Berlin.

Seasonal variations of the parameters of the photosynthesis-light relationship during the Fladen Ground Experiment 1976*

J.P. MOMMAERTS**

1.- Introduction

Photosynthesis measurements were performed from March to June 1976 at the central station of the Fladen Ground sampling grid or in the immediate vicinity (fig. 1).

The results referred to in this paper relate to $^{14}CO_2$ fixation rates in particulate matter of samples incubated under a range of daylight intensities (either *in situ* or in a deck incubator). Four teams*** have cooperated to these measurements, using fairly similar experimental procedures, in accordance with the standardisation Workshops held at Texel, 26-27 November 1975 and Brussels, 10-11 February 1976.

An extensive data set has thus become available for the calculation of phytoplanktonic productions. However, the conversion of these raw data into daily integrated figures of primary production is not simple and the various approaches used — for which no total agreement had been found — could lead to poorly intercomparable results.

---

* This is JONSDAP '76 contribution n° 64.

** Management Unit of the Model of the North Sea and the Scheldt Estuary, Ministry of Public Health and Environment, Vesaliusgebouw 2/3, B-1010 Brussels, Belgium.

*** Data originators :
E. Hagmeier and P. Weigel (Biologische Anstalt Helgoland) : R.V. Meteor.
I. Baird (Dept. of Agriculture and Fisheries of Scotland, Aberdeen) : R.V. Explorer.
W. Gieskes and G. Kraay (Netherlands Institute for Sea Research, Texel) : R.V. Aurelia.
J.P. Mommaerts and J. Nijs (Free University of Brussels, Lab. of Ecology & Systematics) : R.V. Mechelen.

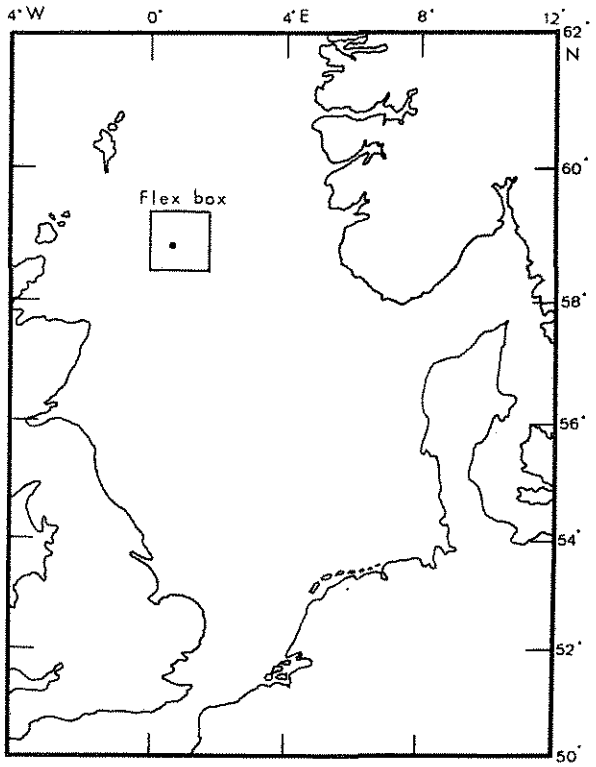

fig. 1.
The North Sea, the Fladen Ground sampling grid ("Flex Box") and its central station

Therefore, the author was given permission by the data originators to handle the entire data set with a single method he had already been using extensively for other areas of the North Sea (Mommaerts, 1978). The method uses a simulation model where the photosynthesis-light (PL) relationship occupies a central position (Mommaerts, submitted) :

$$k = \frac{\alpha I}{\left[1 + \left(\frac{\alpha I}{b\ k_{max}}\right)^2\right]^{\frac{1}{2}} \left[1 + \left(\frac{\gamma \alpha I}{b\ k_{max}}\right)^2\right]^{n/2}} \qquad (1)$$

where k is the rate of carbon fixation in phytoplankton per unit chlorophyll a (in mg C $m^{-3}.h^{-1}$/mg chlor.a m^{-3}), I is the photosynthetic available light energy (400 - 700 nm) [in μeinsteins.$cm^{-2}.s^{-1}$]; k_{max}, α, γ, b and

n are parameters discussed in this paper. Production figures are normalised to active chlorophyll (*sensu* Lorenzen) values*, thus having the dimensions of the ratio rate/biomass *i.e.* a kinetic constant.

This paper aims at the analysis of the seasonal variations of the parameters of the PL curves and their relation to environmental or experimental factors.

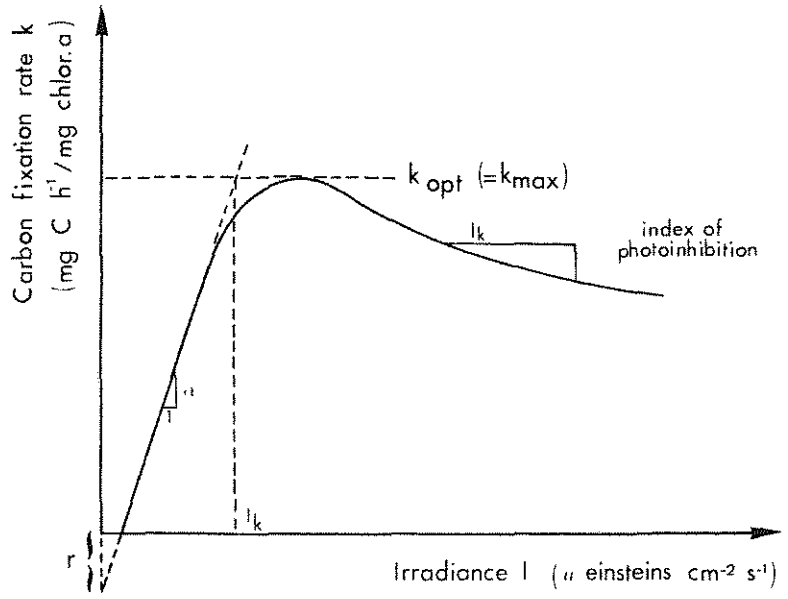

fig. 2.

The photosynthesis-light (PL) relationship and the parameters used for its characterization

Two parameters — presumably mutually independant and biologically significant (Jassby and Platt, 1976) — suffice to characterize most of a PL curve (fig. 2). They are :

• k_{max} measures theoretically the maximum rate of enzymatic processes related to the "dark" reaction of photosynthesis. This rate is also sometimes referred to as "assimilation number";

* Originator for the Meteor data set : A. Weber (Institut für Allgemeine Botanik, Hamburg).

• α is the rate per unit irradiance in the non-photoinhibited range *i.e.* a measure of the photochemical processes. This parameter is similar to the "productivity index" defined by Strickland (1960).

The ratio

$$I_K = \frac{k_{max}}{\alpha}$$

has often been used as a saturation constant in the literature (*e.g.* Smith, 1936; Talling, 1957; Vollenweider, 1965) but contains obviously less information about the environmental control factors or the physiology of the populations concerned.

Photoinhibition — a possible artefact — has been expressed by an index measuring the fraction of k_{max} inhibited per I_K-unit, since this can easily be read from the PL curves. It is related to the photoinhibition parameters of the model by an empirical curve (fig. 3) and :

• for $b < 2.6$: $\gamma = b - 1$ and $n = 1$

• for $b = 2.6$: $\gamma = 1$ and $n = 2$.

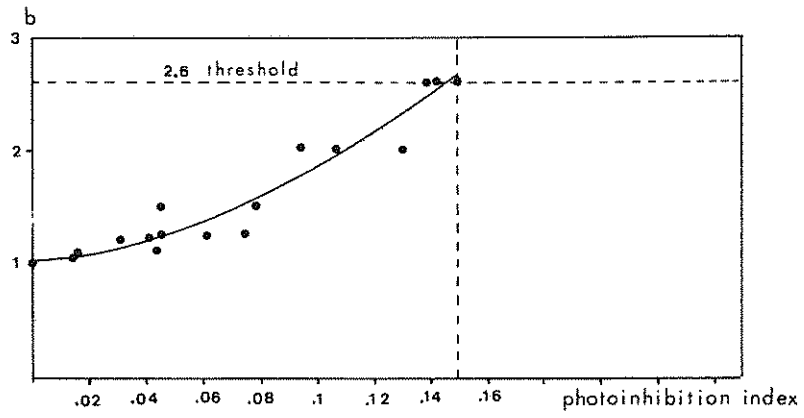

fig. 3.

Empirically determined relationship between the fitted model parameter (b) and the photoinhibition index measured on the curves. Curves with inhibition indices higher than 0.15 cannot be adequately simulated in their photoinhibited range.

r is measured at the intersect of the extrapolated curve with the y-axis. No interpretation is given here for r : apparent loss identified as respiration by several authors (*e.g.* Steemann-Nielsen and Hansen, 1959) but controversed by others (*e.g.* Bunt, 1965).

Measuring these parameters could be considered as a mere necessity of the approach as far as the calculation of primary production with the author's model is concerned. This is however of paramount importance with respect to the study of regulation mechanisms and the design of ecological models.

Thus, k appears in the simplified evolution equation for phytoplanktonic biomass B :

$$\frac{dB}{dt} = k\,B - \text{grazing} - \text{sinking} + \text{exchanges at the boundaries} \qquad (2)$$

where k possibly depends on several factors :

$$k = K_{max} \cdot [f(I)\ ,\ f(N)\ ,\ f(T)\ ,\ f(t)\ ,\ \ldots] \qquad (3)$$

where f(I) is a function of photosynthetically available irradiance, *e.g.* the PL curve; f(N) is a function of limiting nutrient concentration, *e.g.* Michaëlis-Menten kinetics; F(T) is a function of water temperature, *e.g.* the Arrhenius law; f(t) is a function of time, *e.g.* the diel fluctuations described by Mc Caull and Platt (1977).

α — a parameter of f(I) — is believed to depend largely on the nature and/or the degree of light adaptation of the phytoplankton populations. With respect to this, the fractionation into size-classes (*e.g.* nanno- and netplankton) could improve the interpretation of the data markedly. Indeed, a globally measured k ($= k_{tot}$) can be strongly misleading especially if it is intended to be used in a simulation model, since :

$$k_{tot} = \frac{1}{B_{tot}} [B_i k_i + B_j k_j + \ldots + B_n k_n] \qquad (4)$$

Moreover, these time-series of PL curve parameters can also be used for a quality check or looked at with respect to experimental conditions (*e.g. in situ* versus deck incubations) so that choices or corrections can be decided upon before feeding the data into the production model.

2.- Results

Fig. 4 gives a sample of PL curves measured during the Fladen Ground Experiment. Altogether, the results from the four teams are fairly consistent for all PL curve parameters : no data set departs significantly from the

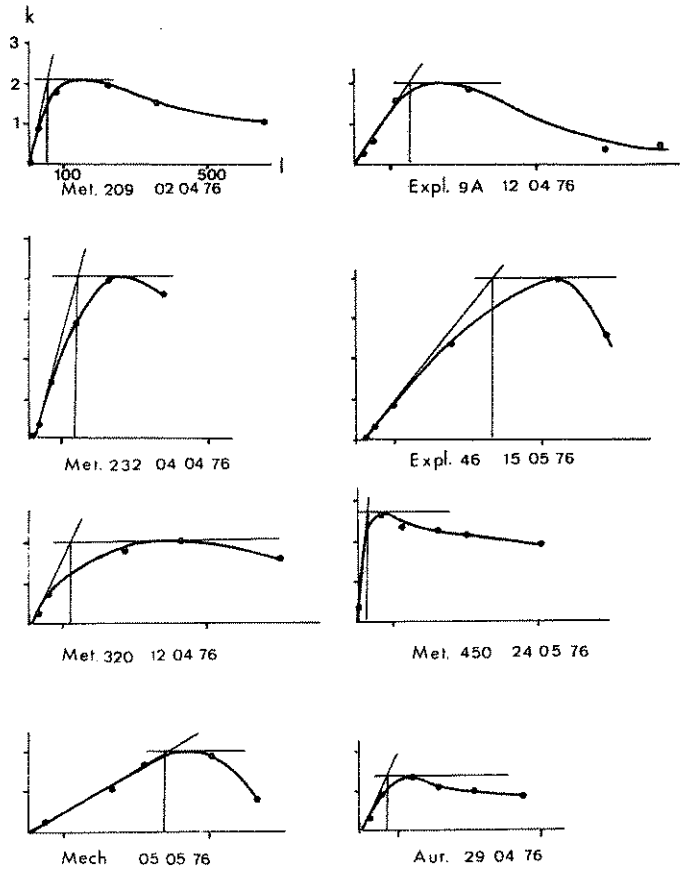

fig. 4.

Representative phosynthesis-light curves measured during the Fladen Ground Experiment. (Units as in fig. 2.)

others. On the other hand, the results are rather scattered (fig. 5). The reasons for this can be multiple : spatial heterogeneity, diel variation, natural variability, cumulated errors on the estimations of the numerous parameters involved in the calculations (irradiance, reflexion, transparency, active chlorophyll *a*, photosynthesis), etc.

Nevertheless, trends can be recognized. A moving average technique, including weighting, has been used to smoothe these variations.

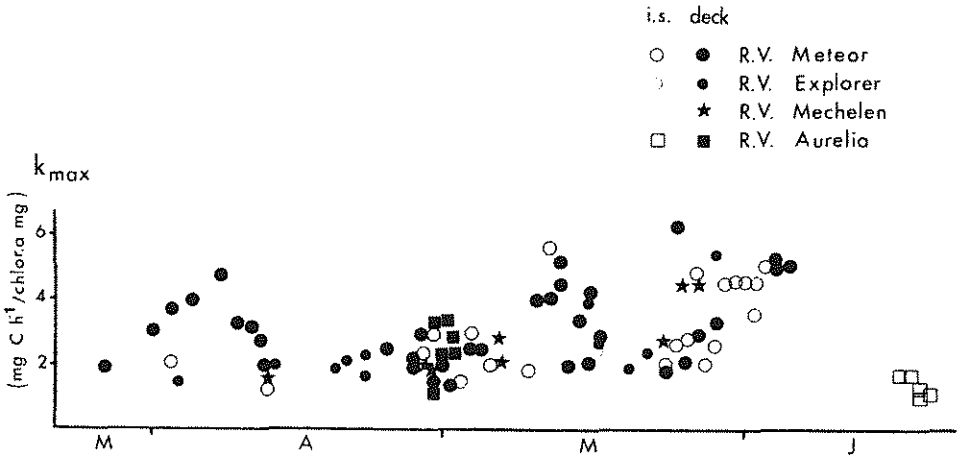

fig. 5.

Actual values of k_{max} measured in situ or in deck incubator by the four teams during the Fladen Ground Experiment.

2.1.- THE SEASONAL VARIATION OF k_{max}

The average value of k_{max} during these three months is 3 mg C h^{-1} mg chlor^{-1}, with numbers comprised between 1 and 6. Tentative corrections for r and for the effect of diel variation, using a variant of the Mc Caull and Platt (1977) equation did not lessen the scatter neither could a possible systematic difference between *in situ* and deck incubation results account for it in any appreciable way.

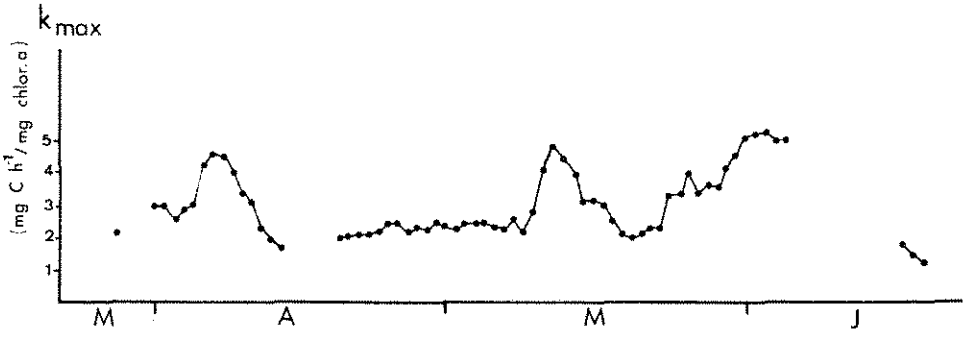

fig. 6.

Seasonal variation of k_{max} (smoothed curve) during the Fladen Ground Experiment

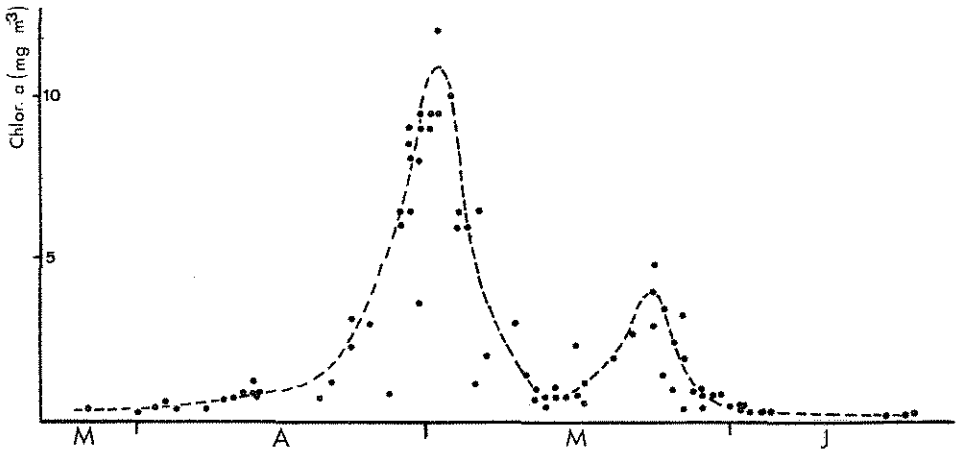

fig. 7.

Seasonal variation of mean chlorophyll a concentration in the euphotic zone during the Fladen Ground Experiment (actual numbers and hand-fitted curve).

The smoothed seasonal curve of k_{max} (fig. 6) shows a trend opposite to that of phytoplankton chlorophyll (fig. 7) since lower values of k are observed during the two consecutive blooms. There is no obvious interpretation for this apparent negative feedback of population density on biological activity : it is at least clear that the major nutrients do not control this evolution in a Michaëlis-Menten mode (fig. 8).

Moreover, the next paragraph casts some doubt on any straighforward interpretation of k_{max} values.

The ratio of net- to nannoplankton production (fig. 9) varies in the same way as biomass, thus revealing that the first bloom was mainly due to an outgrow of netplankton whereas the second one was due to nannoplankton. This was confirmed by the observations of Gieskes and Kraay (1980), Gillbricht (pers. comm.) and Wandschneider (pers. comm.) who ascertained that the netplankton bloom was mainly due to diatoms (especially *Chaetoceros spp.*) and the nannoplankton bloom to microflagellates (especially *Haptophyceae, Chrysophyceae* and *Cryptophyceae*).

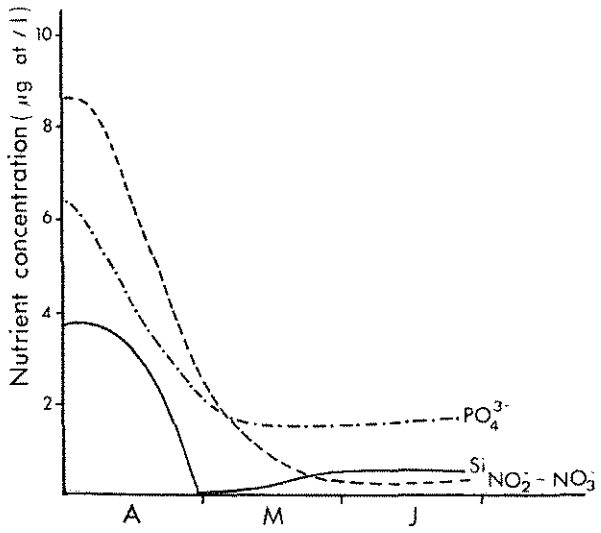

fig. 9.

Evolution of the concentrations of the major nutrients in the euphotic zone during the Fladen Ground Experiment (trends as figured out from the time-depth concentration patterns published in the Draft Flex Atlas by Hannen, Kattner and Eberlein, SFB 94, Hamburg).
Units : $NO_2^- + NO_3^-$: x 1
PO_4^{---} : x 10^{-1}
Si : x 10^{-1}

The ratio of net- to nannoplankton chlorophyll *a* has also been measured on three occasions, thus allowing separate estimations for $k_{max\text{-}nanno}$ and $k_{max\text{-}netpl}$. These measurements covered the period comprised between the two blooms. Table 1 shows that the photosynthesis rate of nannoplankton is quickly increasing during this time, whereas that of netplankton is rather diminishing : the coming population change is clearly announced.

This also demonstrates that, in some circumstances at least, globally measured rates only give a poor reflexion of the processes at work.

Whether this is the reason why no visible relationship exists between k_{max} and the concentrations of the major nutrients is only one of the possibilities. A microscale nutrient distribution ("marine snow") might account as well for the results obtained (*cf.* Shanks and Trent, 1979). It must also be remembered that these results are pertinent to the carbon cycle only and that there is no direct coupling between the nutrient uptake kinetics and photosynthetic carbon assimilation.

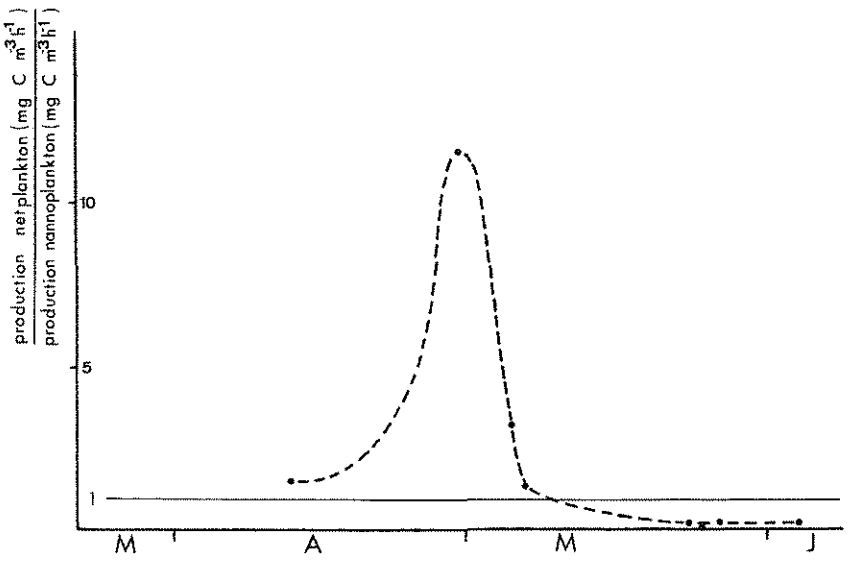

fig. 9.

Ratio of net- to nannoplankton production during the Fladen Ground Experiment, showing the dominance of nannoplankton from early May on.

Table 1

Comparison of the production and chlorophyll *a* ratios and the rates of carbon fixation by netplankton and nannoplankton in the beginning of May 1976

Date	Prod. netpl. / Prod. nanno.	Chlor. netpl. / Chlor. nanno.	k_{tot}	$k_{netpl.}$	$k_{nanno.}$
29-04-76	11.50	2.00	2.06	2.85	0.49
05-05-76	3.20	4.30	1.92	1.80	2.42
06-05-76	1.25	2.30	2.74	2.18	4.01

The sole relationship with an environmental factor that could be ascertained is temperature dependency. Indeed, the general trend towards an increase of k_{max} is linearly correlated with the logarithm of water temperature ($r = 0.983$). The computed Q_{10} value was 2.29 .

2.2.- THE SEASONAL VARIATION OF α AND PHOTOINHIBITION INDEX

From the second bloom onwards, the results for *in situ* and deck incubations depart clearly from each other as far as α and photoinhibition (fig. 10 and 11) are concerned. As these results associate a particular type of phytoplankton (microflagellates) with a given experimental condition (the incubators), one may conclude that this could be an artefact (*e.g.* ill effects due to an excess of UV radiation, *cf.* Steemann-Nielsen, 1975) detrimentary to more delicate organisms.

Therefore, only *in situ* results will be considered in the next paragraphs from mid-May onwards.

2.2.1.- *The parameter* α (fig. 10)

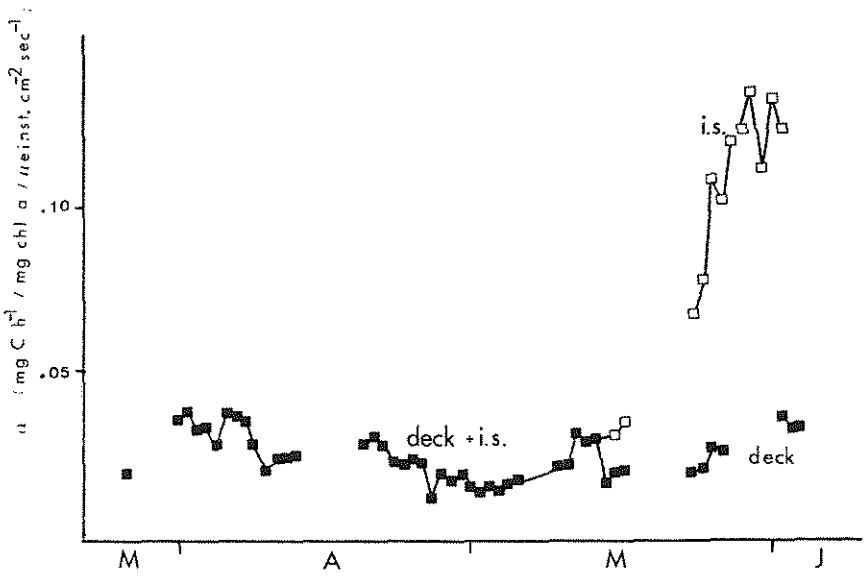

fig. 10.

Evolution of the parameter α (smoothed curve) during the Fladen Ground Experiment. From mid-May on, the results from in situ (i.s.) and deck incubations are given separately.

The average value of α is 0.25 mg C h^{-1}/mg Chl. a/μeinst.$cm^{-2}s^{-1}$ in the period preceding the microflagellates bloom. During the microflagellates

bloom it reaches a peak value of 3, demonstrating a photosynthetic efficiency six times as high as during the first bloom.

This different behaviour of nannoplanktonic algae might be related to a better light harvesting ability in those organisms, depending on cellular architecture and pigment composition (see discussion in Platt and Jassby, 1976). To our knowledge, the higher efficiency of nannoplankton had until now mostly been ascribed to higher assimilation numbers *i.e.* k_{max} (*e.g.* Malone, 1971).

There is no statistical relation between α and k_{max}. This confirms the assumptions made in the introduction about the independence of these parameters.

2.2.2.- *The photoinhibition index* (fig. 11)

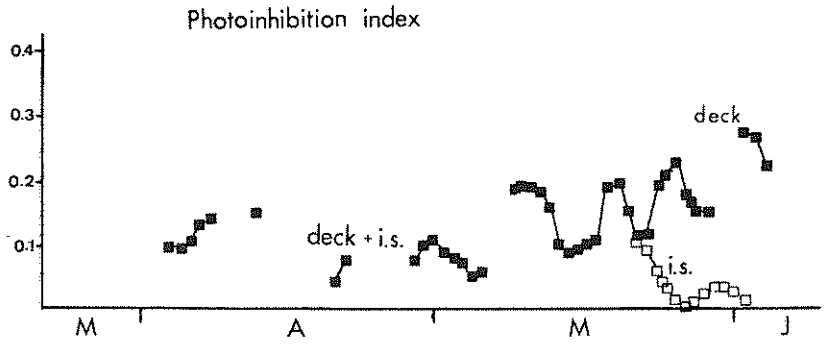

fig. 11.

Variation of the photoinhibition index (smoothed curve) during the Fladen Ground Experiment. From mid-May on, the results from in situ (i.s.) and deck incubations are given separately.

Generally comprised between 0 and .2 I_K - units this parameter shows no identifiable seasonal pattern of variation. The little oscillations observed in May-June are not believed to have a particular significance either since the smoothing technique used could produce such artefacts. The photoinhibition effect is believed to be an artefact altogether. Indeed, phytoplankton cells in nature circulate whereas the incubation system locks them into position so that there is an exposure problem next to the instantaneous response to light intensity.

2.3.- THE PARAMETER r (fig. 12)

Unlike α and the photoinhibition index, the extrapolated parameter r is depending on the experimental conditions of incubation since the beginning of the sampling period : 19 on 23 (*i.e.* 83 %) *in situ* experiments show null or low r values whereas 44 on 54 (*i.e.* 81 %) deck incubation results show a r value averaging about 10 % of k_{max} . The latter percentage is consistent with the observations of Steemann-Nielsen and Hansen (1959) who assumed this was related to respiration (or more exactly to 60 % of it, if there is such a reassimilation of respiratory CO_2 that k_{max} is comprised between gross and net rates). Since then, this 10 % figure has been used extensively in primary production research and ecosystem modelling for correcting for algal respiratory losses.

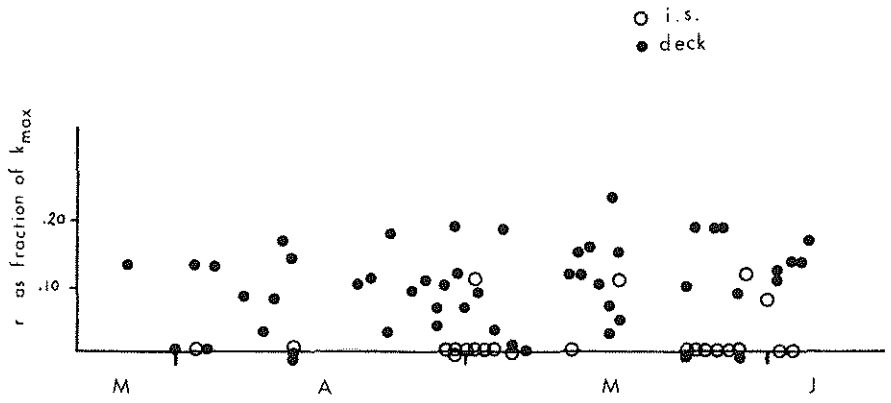

fig. 12.

Values of r measured during the Fladen Ground Experiment and given separately for in situ and deck incubations.

However, the fact that this kind of result strongly depends on the experimental set up casts doubt on the validity of such a practice. Moreover, the assumption that r measures respiration is neither supported by other primary production studies (Bunt, 1965) nor by recent ecosystem budget evaluations (Joiris *et al.*, 1979) or by direct determinations of phytoplanktonic respiration (Hoch *et al.*, 1963; Radmer and Kok, 1976; Nijs and Nihoul, pers. comm.).

It seems therefore that the recurrent discussions on the interpretation of PL curves in terms of net, gross or in-between production should be founded on more recent findings.

3.- Synthesis : the seasonal evolution of the $f(I_0)$ function

As discussed in the introduction, photosynthesis varies with light intensity according to a relationship for which a model has been suggested (eq. 1). Integrated over depth, this equation has the form :

$$\int_{d=0}^{d=\infty} k_z \cdot d_z = \frac{k_{max}}{\eta} f(I_0)$$

where I_0 is the surface irradiance and η the vertical attenuation coefficient (in m^{-1}).

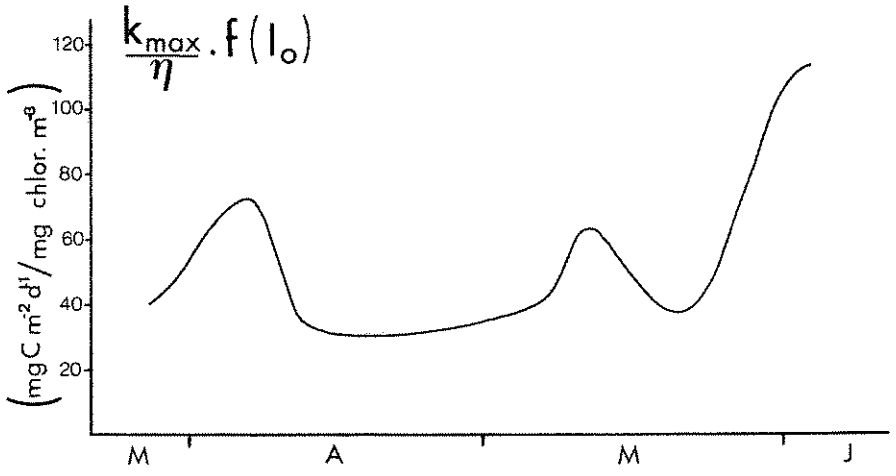

fig. 13.

Variation of the depth-integrated photosynthesis-light profile at 12 h (with average values for irradiance and light attenuation in water) during the Fladen Ground Experiment (based on the smoothed curves of the PL parameters).

At constant water penetration and surface irradiance levels, the seasonal evolution of this integral pictures the evolution of the production potential per m^2 of the phytoplankton during the Fladen Ground Experiment (fig. 13). It is clear that this pattern is greatly determined by the evolution of k_{max} (fig. 6). An amplification is however observed for the second bloom. It is accounted for by the seasonal evolution of $f(I_0)$ (fig. 14) which reflects the changes of adaptative properties of the phytoplankton as well as taxonomic

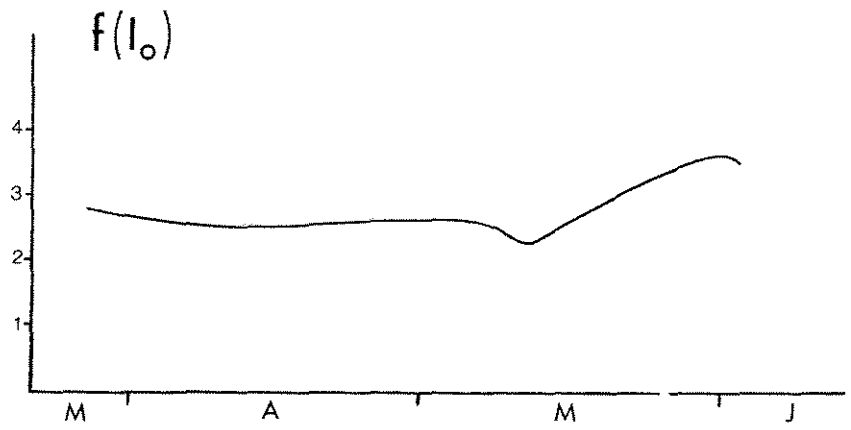

fig. 14.

Variation of the depth-integrated light-dependent function $f(I_0)$ during the Fladen Ground Experiment (based on the smoothed curves of the PL parameters).

composition. In this case, an increase of 50 % of the production potential of biomass was relevant to that term *i.e.* essentially to the increase of α at the end of May 1976.

4.- Conclusion

The analysis of the seasonal fluctuations of the parameters of the photosynthesis-light relationship during the Fladen Ground Experiment has been conceived as a means of studying the regulation of photosynthesis in the environment without having to depend on laboratory experiments and monospecific cultures. Our interest was particularly focused on the control possibly exercised by limiting nutrients.

With respect to the latter point, this approach has not proven successful. Yet, this work has thrown some light on several sapects both methodological or fundamental.

The methodological aspects concern the artefacts caused by the deck incubator with respect to the efficiency of light energy conversion and to photoinhibition : both effects might be related to overexposure to UV radiation. "Respiration" as measured by the extrapolated photosynthesis-light curve might be an artefact as well, perhaps with similar causes.

The fundamental aspects relate mostly to the implications of community changes (*i.e.* nannoplankton versus netplankton) in this study. These are important with respect to the two major parameters of the photosynthesis-light relationship. The photosynthetic yield at undersaturating light intensity (slope α) is markedly higher (by a factor 6) when nannoplankton predominates. In addition, the light-saturated rate of photosynthesis (k_{max}), however fluctuating in a quite different way, also depends on the populations assemblage. Yet, this will appear only when the specific rates are uncoupled.

The environmental control on the photosynthesis-light curve parameters or, indirectly, on the succession pattern is much less evident. There are several hypotheses which could explain why nutrients seem not to control the maximal rate of carbon intake (*e.g.* in a Michaëlis-Menten way). An obvious one is that nutrient assimilation and carbon uptake are only loosely coupled. Hence, far better results could be expected from nutrient uptake (*e.g.* ^{15}N) measurements.

On the other hand, the control exercised by temperature on k_{max} could be observed on the long term. The observed short-time fluctuations can however not be explained by temperature changes.

This important data set and the present study have provided an opportunity to look more directly at parameters and relations that are usually hypothetised in ecosystem models. One of the lessons that can be drawn from these results is that existing models could fail to simulate the evolution of phytoplanktonic biomass adequately because they totally ignore such problems as have been discussed above, and possible others just as significant which have thus far escaped identification. Without making a case for the development of mammoth models, the author believes however that the reductionist approach that has been chosen by a majority of modellers is meaningless if it is not driven to the complexity level that will satisfy minimal requirements. Whether there is such a compromise between complexity and tractability is a question as yet unsolved.

References

BUNT, J. (1965). Measurements of photosynthesis and respiration in a marine diatom with the mass spectrometer and with carbon-14, *Nature*, 5004, 1373-1374.

GIESKES, W. and KRAAY, G. (1980). Primary production and phytoplankton pigments measurements in the Northern North Sea during FLEX 76, *Meteor Forschungssergebnisse* (in press).

HOCH, G., OWENS, O. and KOK, B. (1963). Photosynthesis and respiration. *Arch. Biochem. Biophys.*, 101, 171-180.

JASSBY, A.D. and PLATT, T. (1976). Mathematical formulation of the relationship between photosynthesis and light for phytoplankton, *Limnol. Oceanogr.*, 21, 540-547.

JOIRIS, C., BILLEN, G., LANCELOT, C., MOMMAERTS, J.P., DARO, M.H., BOSSICART, M., GILLAIN, G., BERTELS, A., HECQ, J.H. and WIJNANTS, J. (1979). Dynamics of organic matter in three planktonic ecosystems of the Southern North Sea, in *Actions de recherche concertées, Océanologie, Rapports des journées d'études (1979)*, Programmation de la Politique scientifique, Bruxelles.

Mac CAULL, W.A. and PLATT, T. (1977). Diel variations in the photosynthetic parameters of coastal marine phytoplankton, *Limnol. Oceanogr.*, 22, 723-731.

MALONE, T.C. (1971). The relative importance of nannoplankton and netplankton as primary producers in the California Current system, *Fishery Bull.*, vol. 69 (4), 799-820.

MOMMAERTS, J.P. (1978). *Systeembenadering van een gesloten marien milieu, met de nadruk op de rol van het fytoplankton*, Ph. D., Vrije Universiteit Brussel.

MOMMAERTS, J.P. (198.). The calculation of particulate primary production in a stratified body of water, using a modification of the Vollenweider formula (submitted to *Meteor Forschungssergebnisse*).

PLATT, T. and JASSBY, A.D. (1976). The relationship between photosynthesis and light for natural assemblages of coastal marine phytoplankton, *J. of Phycol.*, 12 (4), 421-430.

RADMER, R.J. and KOK, B. (1976). Photoreduction of O_2 primes and replaces CO_2 assimilation, *Plant Physiol.*, 58, 336-340.

SHANKS, A.L. and TRENT, J.D. (1979). Marine snow : microscale nutrient patches, *Limnol. Oceanogr.*, 24, 850-854.

SMITH, E.L. (1936). Photosynthesis in relation to light and carbon dioxide, *Proc. Nat. Acad. Science*, Wash., 22, 504-511.

STEEMANN-NIELSEN, E. and HANSEN, V.K. (1959). Measurements with the carbon-14 technique of rates of respiration in natural populations of phytoplankton, *Deep-Sea Res.*, 5, 222-233.

STEEMANN-NIELSEN, E. (1975). *Marine Photosynthesis*, Elsevier Oceanography Series, Amsterdam.

STRICKLAND, J.D.H. (1960). Measuring the production of marine phytoplankton, *Fish. Res. Bd. Canada*, Bull. 122, Ottawa, 172 pp.

TALLING, J.F. (1957). The phytoplankton population as a compound photosynthetic system, *The New Phytologist*, 56, 133-149.

VOLLENWEIDER, R.A. (1965). Calculation models of photosynthesis-depth curves and some implications regarding day rate estimates in primary production measurements, in C.R. Goldman (ed.), *Primary productivity in aquatic environments*, Univ. Calif. Press, Berkeley, pp. 425-457.

Population growth parameters and production of *Calanus finmarchicus* in the Fladen Ground as calculated with a simulation model*

M. BOSSICART**

Abstract

A mathematical model taking the life history of copepods into account has been developed. Thus, parameters that are difficult to measure *in situ* can be calculated. These are growth and mortality rates, development times, reproductive efficiency for the several stages, as well as net production and mortality for the total population.

This model has been applied to the situation observed in the Fladen Ground with the experimental data of Dr. Krause (Universität Hamburg, F.R.G.).

1.- Introduction

Copepods are a prominent fraction in the zooplankton. They are small swimming crustacea generally not exceeding a length of 2 mm. Being herbivorous and/or omnivorous, they play an essential role in the cycle of organic matter since they make a link between the first trophic level (synthesis of organic matter by the phytoplanktonic micro-algae) and the higher trophic levels (carnivorous zooplankton, fish ...) .The life history of the copepods is rather complex as there are many development stages (nauplii I to VI and copepodites I to V) from the egg to the fertile adult.

---

* This is JONSDAP '76 contribution n° 58.

** Laboratorium voor Ekologie en Systematiek, V.U.B.

Each of these stages can be fully considered as a population with its specific functional characteristics (Fig. 1). Since hatching is spread in time , the populations of the different stages occur together in the natural samples. The resulting seasonal curves can possibly show a succession of maxima for the various development stages. The correct interpretation of the observable data in terms of population dynamics is much more complex and requires the development of an adequate mathematical model (Mommaerts and Bossicart, 1975; Mommaerts, 1978).

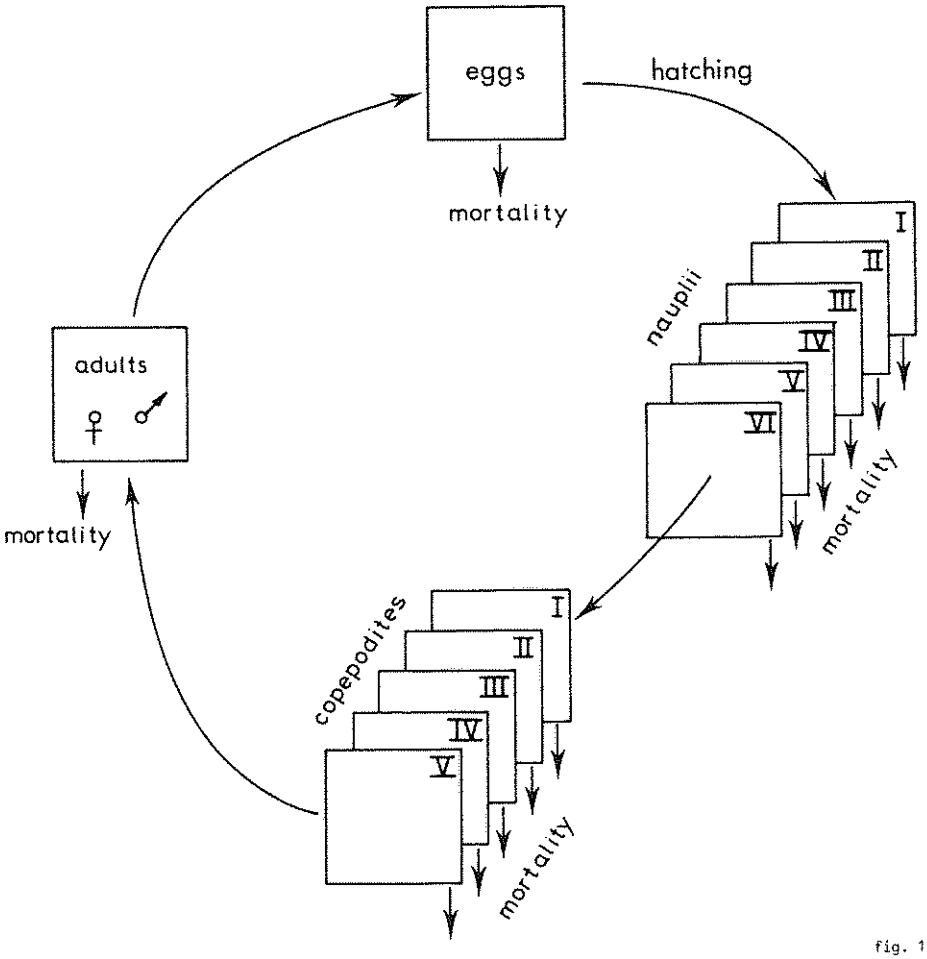

fig. 1.

Parameters that are particularly relevant to the population dynamics of marine copepods (*i.e.* growth, mortality rate) and their production can be calculated.

2.- General description of the model

At the present stage of development, the model is able to describe the dynamics of a full generation in the case of a homogeneous waterbody. For the needs of the model, the occurence of nauplii has been discretized in time, considering there are as much cohorts generated as there are days in the hatching period. The hatching curve is parametrized. The six naupliar stages are globalized but the next five copepodite stages are described. One has considered that growth is exponential. At the adult stage, the model makes a distinction between males and females, using a sex-ratio as observed in nature.

One is also considering that just before dying, each female will have produced a given average number of eggs that will be the input to the next generation.

3.- Biological functions and evolution equations*

3.1.- THE HATCHING CURVE

At the present time this curve is still parametrized. A normal law describes the phenomenon in a acceptable way :

$$N^j = b\, e^{-\alpha(t-\beta)^2} \qquad (1)$$

3.2.- EQUATIONS FOR THE NAUPLIAR STAGES

Mortality causes an exponential decrease of the number of individuals in a cohort.

Living population observable at a time t for the globalized naupliar stages :

---

* For the explanation of the symbols see table 1.

$$N_t^T = \int_{i_1=0}^{i_1=p_1} b\, e^{-\alpha(t-\beta-i_1)^2 - m_1 i_1}\, di_1 \qquad (2)$$

Table 1

Legends of the symbols

Nauplii	Copepodites	Adults	
			Populations parameters :
N_t^T	$C_{It}^T \cdots C_{Vt}^T$	A_t^T	Numbers (all cohorts) still alive on day t
i_1	$i_I \cdots i_V$	i_3	Age of a given individual (days)
p_1	$p_I \cdots p_V$	p_3	Maximum age of a given individual (days)
m_1	$m_I \cdots m_V$	m_3	Specific mortality rate
			Stocks and production parameters :
B_o^N			Initial biomass of an individual
$B_{i_1}^N$			Actual biomass of an individual of age $i_{(1)}$
k_1			Specific exponential growth rate
P_t^N			Net production (all cohorts) on day t
			Spawning and hatching :
E			Numbers (all cohorts) of eggs observable during the whole generation.
Y			Average number of eggs/female.
δ			Proportion of females in the totale population.
α			Coefficient giving the dispersion of the normal curve.
β			Day with the highest hatched number.
b			Number of nauplii hatched on day β

3.3.- EQUATIONS FOR THE COPEPODITE STAGES

Similar considerations as those developed for the nauplii lead to the various equations.

Living population observable at a time t for each copepodite stage :

$$C^T_{It} = \int_{i_I=0}^{i_I=p_I} b\, e^{-\alpha(t-\beta-p_1-i_I)^2-m_1p_1-m_Ii_I}\, di_I \qquad (3)$$

$$C^T_{IIt} = \int_{i_{II}=0}^{i_{II}=p_{II}} b\, e^{-\alpha(t-\beta-p_1-p_I-i_{II})^2-m_1p_1-m_Ip_I-m_{II}i_{II}}\, di_{II} \qquad (4)$$

.
.
.

$$C^T_{Vt} = \int_{i_V=0}^{i_V=p_V} be^{-\alpha(t-\beta-p_1-p_I-\cdots-p_{IV}-i_V)^2-m_1p_1-m_Ip_I-\cdots-m_{IV}p_{IV}-m_Vi_V}\, di_V \qquad (5)$$

3.4.- EQUATIONS FOR THE ADULT STAGES

$$A^T_t = \int_{i_3=0}^{i_3=p_3} be^{-\alpha(t-\beta-p_1-p_I-\cdots-p_V-i_3)^2-m_1p_1-m_Ip_I-\cdots-m_Vp_V-m_3i_3}\, di_3 \qquad (6)$$

3.5.- PRODUCTION OF THE EGGS FOR THE NEXT GENERATION

The total number of individuals (all cohorts) that will have reached the adult stage within a generation cycle is :

$$A = \int_{t=t_o}^{t=t_f} b\, e^{-\alpha(t-\beta)^2-m_1p_1-m_Ip_I-\cdots-m_Vp_V}\, dt \qquad (7)$$

and hence the number E of produced eggs is :

$$E = \int_{t=t_o}^{t=t_f} \gamma\delta\, b\, e^{-\alpha(t-\beta)^2 - m_1 p_1 - m_I p_I - \ldots m_V p_V}\, dt \qquad (8)$$

4.- Calculation of net production*

4.1.- NAUPLII

4.1.1.- *Growth*

The growth equation for a given individual can be written :

$$B^N_{i_1} = B^N_0\ e^{k_1 i_1} \qquad (9)$$

4.1.2.- *Net production*

Furthermore, the net production of a given individual during the day i_1 being :

$$B^N_{i_1+1} - B^N_{i_1} = B^N_o e^{k_1 i_1}(e^{k_1} - 1) \qquad (10)$$

and combinating with eq. (2), it follows that the global net production at time t is :

$$P^N_t = \int_{i_1=o}^{i_1=p_1} b\, e^{-\alpha(t-\beta-i_1)^2 - m_1 i_1} N_{B_o} e^{k_1 i_1}(e^{k_1} - 1)\, di_1 \qquad (11)$$

4.2.- COPEPODITES

In a similar way, equations are written for the growth and the production of the copepodites.

---

* The loss of exuviae during the transformations has not been taken into account.

4.3.- ADULTS

There is no significant weight increase at that stage but a production of eggs.

5.- Application to the Fladen Ground data

We have attempted to apply this model to the experimental data from the Fladenground acquired by Dr. Krause(Universität Hamburg, F.R.G.) Samples were taken from the research vessel "Meteor" at the central station 4 times a day and from 9 sampling depths. At this time, only adults and copepodites had been sorted. The information concerning the nauplii is presently available so that the same simulation work will also be possible for the naupliar stage in the future.

Fig.2 gives the time series of numbers for each of the 5 copepodite stages and the female and male adult stages.

A moving average technique (5 points) has been used for the smoothing of the curves. This data set is limited in time, however we were able to fit our model to the experimental curves and thus evolve the values of the various rates implied (table 2).

Table 2

	Developing time (days)	Growth rate (day^{-1})	Mortality rate (day^{-1})
Copepodites I	5	0.15	0.04
II	5	0.25	0.04
III	6	0.12	0.05
IV	7	0.18	0.05
V	7	0.04	0.05
Total (C_I - C_V)	37		
Adults			0.06

α = 0.0015

β = 145 day

b = 45 individuals

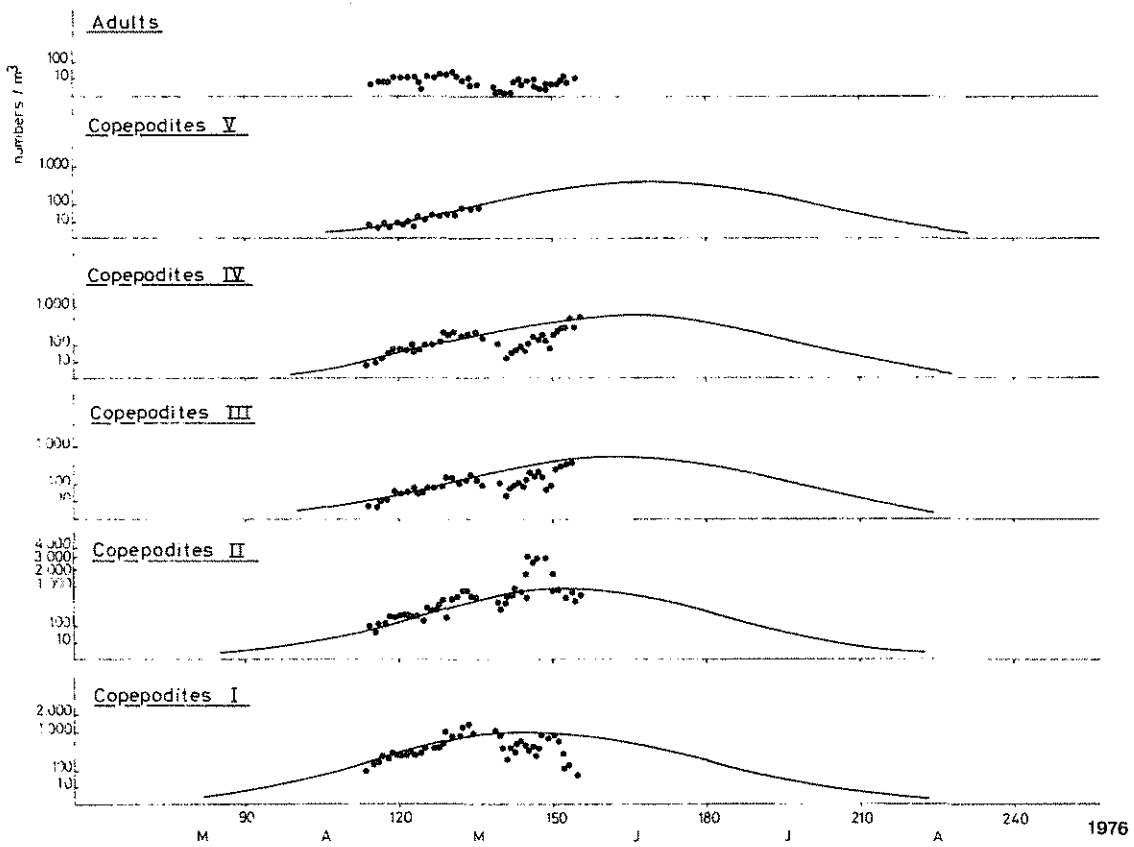

fig. 2.

FLEX : Season evolution of the numbers of Calanus finmarchicus (copepodites and adults)
Experimental values of M. Krauze.

5.1.- DEVELOPING TIME

The developing times for the copepodite stages are 5 , 5 , 6 , 7 and 7 days. The life span for a copepodite from stages I to VI is consequently of 37 days.

Marshall and Orr (1972) find in laboratory culture a life span of 60 - 70 days. It amounts to 3 months in Norwegian coastal water (Ruud, 1929), 71 - 79 days in the Gulf of Maine (Fish, 1936), 70 - 80 days in the North Sea (Rees, 1949) (in Marshall and Orr, 1972).

5.2.- GROWTH RATE

The individual weights at the beginning of each development stage have been measured by B. Williams (Plymouth; personal communication) and are respectively for C_I to C_{VI} 2.7, 5.2, 20.1, 145.2, 191.6 µg dry weight.

Knowing the development time for each stage and the weights, the exponential growth rates can be calculated.

They are respectively for C_I to C_V 0.15, 0.25, 0.12, 0.18, 0.04 per day.

Mullin and Brooks (1970) find a coefficient of exponential growth of 0.17 per day for C_I to C_{IV} for Calanus feeding on Thalassiosira at 10° C and 0.08 per day for C_{IV} to Adult.

At 15°C this coefficient is higher: 0.27 per day for C_I to C_{IV} and 0.22 per day for C_{IV} to Adult.

5.3.- MORTALITY

The mortality rates calculated for the 5 copepodites stages are respectively 0.04 , 0.04 , 0.05 , 0.05 , 0.05 per day and 0.06 per day for the adults.

5.4.- OTHERS PARAMETERS.

45 individuals (b in the model) are the highest hatched number on day 145 (β in the model). The constant α giving the dispersion of the normal curve is 0.0015 .

References

MARSHALL, S.M. and ORR, A.P. (1972). *The Biology of a Marine Copepod*, Springer-Verlag, Berlin - Heidelberg - New York, 195 pp.

MOMMAERTS, J.P. and BOSSICART, M. (1975). Towards a simulation model for the copepods zooplankton spring growth in the Sluice Dock at Ostend, Techn. Report 1975/Biol./04.

MOMMAERTS, J.P. (1978). *Systeembenadering van een gesloten marien milieu, met de nadruk op de rol van het fytoplankton*, Ph. D., Vrije Universiteit Brussel, 335 pp.

MULLIN, M.M. and BROOKS, E.R. (1970). Growth and metabolism of two planktonic, marine copepods as influenced by temperature and type of food, in *Marine food chains*, J.H. Steele (ed.), 74-95.

Development of organic substances at the Central Station during FLEX '76

I.- Particulate and dissolved fatty acids*

G. KATTNER, K.D. HAMMER and U.H. BROCKMANN**

Abstract

During FLEX '76 a component of organic matter in sea water, the lipids containing fatty acids, were investigated. After filtration, the fatty acid composition of the chlororoform soluble part was analysed in the particulate and dissolved fractions, respectively. During both phytoplankton blooms main increases of particulate fatty acids occurred in the stationary phase, with maximum values of 20 µgat $C.\ell^{-1}$ and 9 µgat $C.\ell^{-1}$ in the uppermost meters of the water column and mean values of 10 µgat $C.\ell^{-1}$ and 5 µgat $C.\ell^{-1}$ in the upper layer. Maxima of dissolved fatty acids were found in the lower layer in conjunction with the phytoplankton blooms and having mean values of 4 µgat $C.\ell^{-1}$ and 2.6 µgat $C.\ell^{-1}$. This indicates that the main release of fatty acids is caused by decomposition processes of phytoplankton and detritus during sedimentation. Hypothesized release processes during the exponential growth of phytoplankton are discussed.

Introduction

The interpretation of data of the Fladen Ground Experiment (FLEX '76) has shown that biological and chemical developments are not strongly influenced by hydrodynamic processes during various periods, in particular during the phytoplankton spring

---

* This is JONSDAP '76 contribution n° 61.

** Institut für Organische Chemie und Biochemie der Universität Hamburg, Martin-Luther-King-Platz, 6, D-2000 Hamburg 13, F.R.G.

bloom (see Meteor Forsch.-Ergebnisse, Reihe A, No. 22, JONSDAP 76). The FLEX data set offers the opportunity to combine results from a multitude of individual research projects with a great number of ecological basis data. At the central station we determined the amount of certain components of dissolved and particulate organic matter in some vertical profiles.

Dissolved organic matter (DOM) is the main component in the organic carbon budget of sea water. It is subject to a succession of biological and abiotic changes and plays an important role in the marine ecosystem. At present quantification of DOM is still very unreliable, reported concentrations differing widely from each other. Even more difficult is the chemical characterisation of the individual components. Only a part of the DOM has been identified as yet.

A fraction of the dissolved organic carbon (DOC) which includes carbohydrates, amino acids and fatty acids, is chemically unstable and is subject to a rapid biological and chemical transformation (Fogg, 1975; Bada and Lee, 1977; Brockmann et al., 1979). These substances play an essential role in marine ecosystems for obligate heterotrophic organisms and in the case of anorganic nutrient deficiency. One part of the DOC, the lipids, has hardly been studied until now. Because of their amphipatic properties, they have been studied as part of surface films (Garrett, 1967; Jarvis et al., 1967; Larsen et al., 1974; Kattner and Brockmann, 1978). The principal components of lipids are fatty acids, both as free molecules and in the form of ester compounds. In cells, they are incorporated in different chemical forms as reserve material or membrane elements. Some investigations of lipids have already been carried out in sea water considering different depth zones (Slowey et al., 1962; Jeffrey, 1970; Treguer et al., 1972; Kayama and Yamada, 1975; Marty and Courtot, 1976, 1979-80).

During FLEX '76 in connection with numerous analysises of biological and chemical parameters from the same sample lipid determinations were carried out for selected depth profiles. The particulate and dissolved fraction of the fatty acid-

containing compounds were measured. Trends in the development of concentration and composition of fatty acids will be presented and discussed here for the entire FLEX period.

Methods

1 ℓ of sea water samples was filtered through glass fibre filters (Whatman GF/C, 1.2 µm retention ability). The residue, together with the filter, was fixed in chloroform, and the filtrate was fixed with 10 mℓ of chloroform per liter.

1000 mℓ of filtrate was extracted three times, each with 100 mℓ of chloroform. The residue was extracted with chloroform/methanol (2:1, v/v) mixture according to the method of Folch et al. (1957). The densitometric and gas chromatographic methods are described by Brockmann et al. (1976) and Kattner and Brockmann (1978).

All concentration data are expressed in terms of carbon. The following profiles were chosen for lipid analysis.

No.	Date	Time	Conditions
1	26. 3.	12.15	Mixed water column
2	3. 4.	12.00	" " "
3	10. 4.	12.08	" " "
4	24. 4.	14.32	Formation of thermocline, first phytoplankton bloom
5	30. 4.	6.16	Stable thermocline
6	3. 5.	18.00	Particulate carbon maximum
7	10. 5.	12.08	End of first phytoplankton bloom
8	22. 5.	1.47	Second phytoplankton bloom
9	24. 5.	12.09	Formation of further thermoclines
10	29. 5.	12.13	End of second phytoplankton bloom
11	5. 6.	12.06	" " " " "

Results and Discussion

Particulate matter is the main source of DOC within the marine environment. It is mostly formed by phytoplankton. In

order to determine the origin and distribution of fatty acids (FA), it is necessary to determine the FA content of particulate matter. The sum of all individual FA present in the particulate matter was determined. The individual measurements within each depth profile were integrated over the depth so that the value represented the concentration in the whole water column beneath one square meter of the surface (method described by Eberlein et al., 1980).

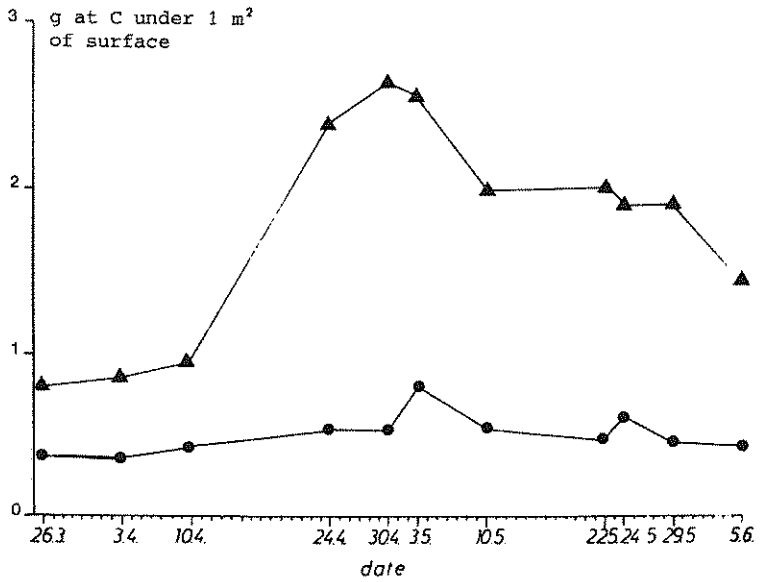

fig. 1.

Concentrations of particulate organic carbon (Weigel et al., unpubl.) ▲——▲ and particulate fatty acids ●——● in the total water column.

Fig. 1 shows the fatty acid concentration in particulate matter in comparison with total particulate carbon (POC). Before the beginning of the spring phytoplankton bloom, the percentage of FA in the POC was about 40 %. During the exponential growth phase, the absolute amount of fatty acids increased slightly, but decreased in relation to the POC to about 10 %.

An increased build-up of FA-containing substances was first observed on May 3rd, during the stationary growth phase of the phytoplankton bloom. A second small maximum occurred during the second phytoplankton bloom.

To clarify the direct correlation between the phytoplankton blooms and the appearance of particle-bound FA, mean concentrations above the thermocline ("upper layer") and below the thermocline ("lower layer") was calculated separately (Fig. 2).

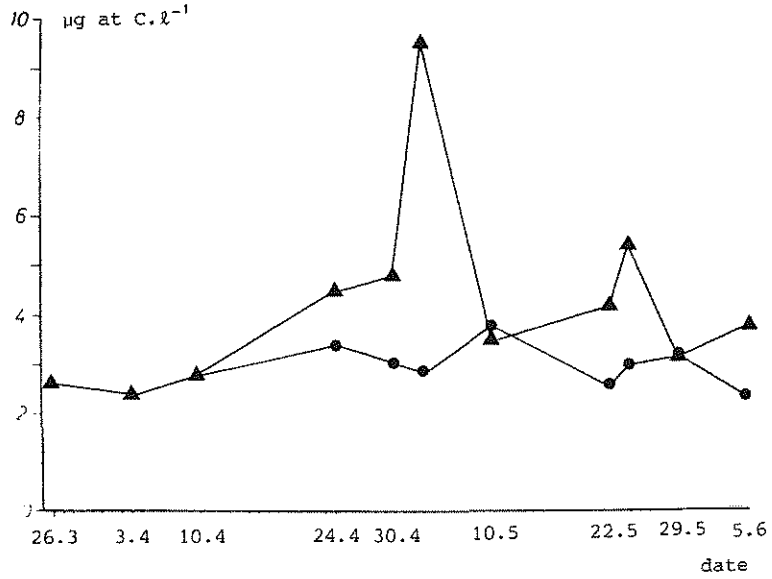

fig. 2.

Concentrations of particulate fatty acids in different water layers, ▲——▲ upper layer, ●——● lower layer.

The depths of main thermocline were taken from Soetje and Huber (1980). The increase of FA during both phytoplankton blooms is confined to the upper layer of the water column, the amount in the lower layer remaining relatively constant. The amount of total FA at the beginning of the experiment was about 2 µgat $C \cdot \ell^{-1}$, rising on May 3rd to a maximum value of 20 µgat $\cdot C\ \ell^{-1}$ in the uppermost meters of the water column with mean

values of 10 µgat $C \cdot \ell^{-1}$ in the upper layer. During the second phytoplankton bloom, the value increased to a maximum of 5 µgat $C \cdot \ell^{-1}$ in the upper layer. At the end of the experiment, after the end of both phytoplankton blooms, there was a decrease to the initial value. Considering the total FA it can be deduced that at the end of the experiment, the FA produced by phytoplankton have been katabolized already. The main components of the fatty acids were oleic acid (18:1 n-9)* and palmitic acid (16:0), followed by myristic acid (14:0), palmitoleic acid (16:1 n-7) and stearic acid (18:0).

The displacement of the POC and particulate FA maxima seems to indicate that, during the exponential growth phase, the phytoplankton first synthetized other substances such as nitrogenous compounds. These are, for example, amino acids and proteins, which form the main component of the phytoplankton cells during the exponential growth phase (Myklestad, 1974, 1977). The slight increase of FA during the exponential growth phase shows that there was only small biosynthesis of FA compounds. There will be built no storage lipids during this time, only membrane compounds.

Not until the limitation of nutrients in the euphotic zone (Eberlein et al., 1980) are nitrogen-free compounds such as carbohydrates and lipids built up to a greater extent. These findings were confirmed through experiments in enclosures (Antia et al., 1963; Brockmann et al., 1977).

Fig. 3 shows the distribution of the dissolved lipids integrated over the depth. Distinct maxima occur during both the phytoplankton blooms. The bulk of the lipids is in the form of free fatty acids. The free fatty acids show the same distribution as the total FA, only with less distinct maxima. They constitute more than half of the total FA. The triglycerides (TG) remain relatively constant. Significant correlations exist between these components. During the first phytoplankton

---

* x:y n-z means : x = number of carbon atoms in the FA
y = number of double bonds
z = terminal C atom of the first double bond.

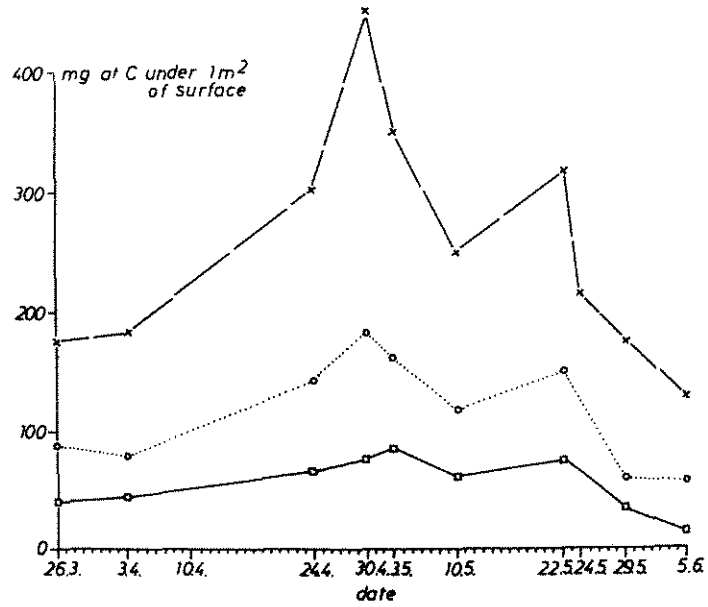

fig. 3.

Concentrations of dissolved lipids containing fatty acids in the total water column.
x—— —x total fatty acids
o·····o free fatty acids
o——o triglycerides

bloom, the maxima of the TG is displaced in contrast to the total FA. A small percentage occurs in the form of less-polar lipids, with some analyses showing maximal concentrations, which may be an indication of decomposition processes.

Fig. 4 gives a more detailed view of the distribution of the dissolved lipids as calculated in the upper and lower layer using the main thermocline as a boundary. The examination of the individual values of the depth profile shows that the extreme maxima, especially during phytoplankton blooms, are near the thermocline. Other maxima can be observed close to the bottom. The thermocline seems to be a barrier for dissolved substances. The concentrations of dissolved FA before the bloom are around 1 - 2 µgat $C \cdot \ell^{-1}$ and increase to maximal values of 5 µgat $C \cdot \ell^{-1}$ during the phytoplankton bloom. The

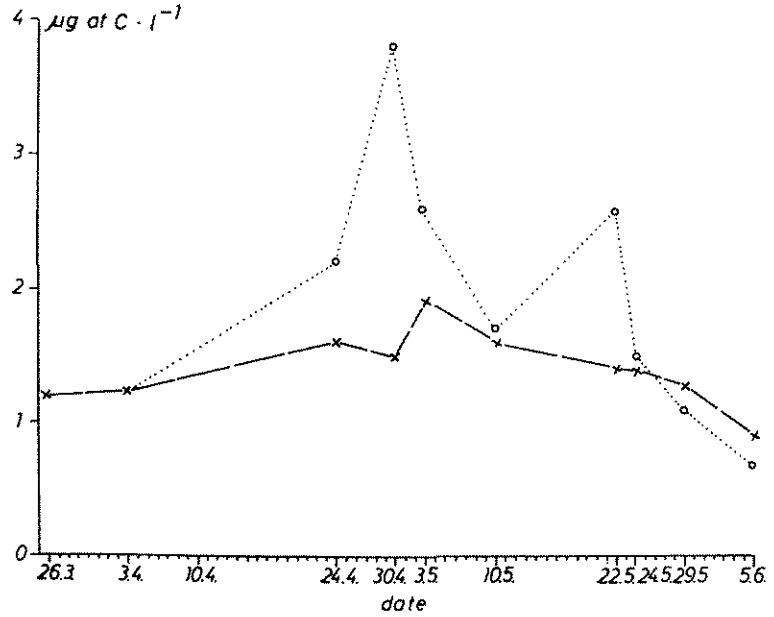

fig. 4.

Concentrations of total dissolved fatty acids in different water layers.
x—— ——x upper layer o·····o lower layer

main component of the dissolved FA is palmitic acid (16:0), followed by myristic acid (14:0), oleic acid (18:1 n-9) and stearic acid (18:0).

Another indicator for the relationship between the phytoplankton bloom and dissolved FA is given by the poly-unsaturated FA. During periods with reduced biological activities the proportion of poly-unsaturated FA amounts to approximately 5 %, but rises to about 10 % during the phytoplankton bloom. Poly-unsaturated FA are characteristic of marine plankton (Kates and Volcani, 1966; Ackman et al., 1968; Chuecas and Riley, 1969; Harrington et al., 1970). Before and after the phytoplankton bloom the saturated FA constitute the main part of FA, because the chemical, biological and photolytic degradation of poly-unsaturated FA proceeds much quicker than that of saturated FA.

Since the main decomposition processes occur primarily below the thermocline, this demonstrates that the main release of FA is a function of decomposition of phytoplankton cells and detritus during the sedimentation. Another part is released in a similar way as amino acids and carbohydrates during "grazing" by zooplankton. Also, faecal pellets and bacteria can be sources of FA in sea water. The decrease of dissolved FA may be caused by chemical degradation, heterotrophic uptake and adsorption to particulate matter.

For the first and second phytoplankton bloom the maximum values of dissolved FA in the lower layer occur simultaneously to the maximum values of particulate carbon, but before the part of FA in the particulate matter has reached maximum values in the upper layer. In the lower layer the particulate FA increase slightly between the maxima of dissolved FA.

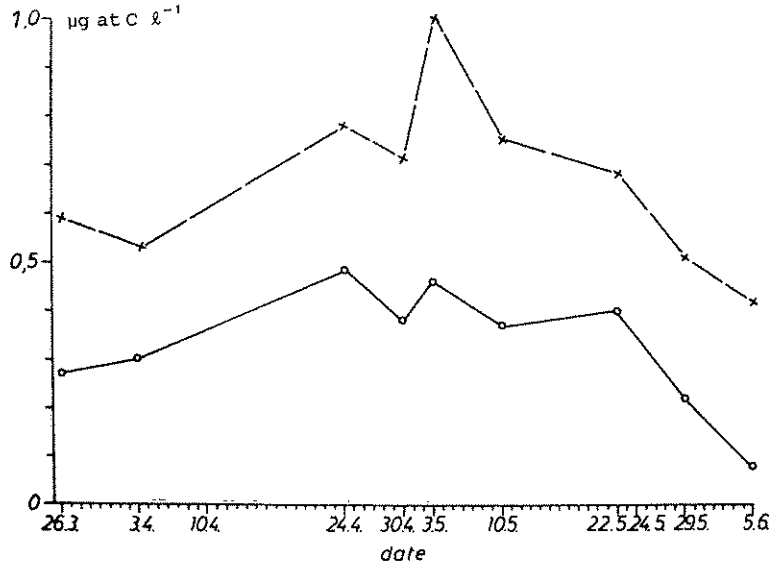

fig. 5.

Concentrations of dissolved lipids in the upper layer.
x—x free fatty acids
o—o triglycerides

These might be due to first sedimentation processes during phytoplankton growth and subsequent decomposition.

A small increase of dissolved FA in the upper layer is parallel to the increase of particulate FA. This supports the assumption that release processes also play a role in the upper layer. Fig. 5 shows the calculation of mean concentrations of free FA and TG in the upper layer. In this more detailed calculation the TG already have reached a slight maximum during the exponential growth phase and in the stationary growth phase in contrast to the free FA concentrations, which increase more in the stationary growth phase. During this time TG will be released in greater values relatively to free FA. Explanations of these trends will be hypothetic. It is possible that free FA are decomposition products of TG.

A detailed analysis of FA pattern and individual FA will be done in future in order to gain more informations on the origin and fate of fatty acid-containing lipids in sea water.

Acknowledgements

This work was supported by the Deutsche Forschungsgemeinschaft through the Sonderforschungsbereich 94 — Meeresforschung — Hamburg.

References

ACKMAN, R.G., TOCHER, C.S. and MACHLAN, J. (1968). Marine phytoplankter fatty acids. *J. Fish. Res. Board Can.*, 25, 1603-1620

ANTIA, N.J., MCALLISTER, C.D., PARSONS, T.R., STEPHENS, K. and STRICKLAND, J.D.H. (1963). Further measurements of primary production using a large-volume plastic sphere. *Limnol. Oceanogr.*, 8, 166-183.

BADA, J.L. and LEE, C. (1977). Decomposition and alteration of organic compounds dissolved in seawater. *Mar. Chem.*, 5, 523-534.

BROCKMANN, U.H., KATTNER, G., HENTZSCHEL, G., WANDSCHNEIDER, K., JUNGE, H.D. and HÜHNERFUSS, H. (1976). Natürliche Oberflächenfilme im Seegebiet vor Sylt. *Mar. Biol.*, 36, 135-146.

BROCKMANN, U.H., EBERLEIN, K., HENTZSCHEL, G., SCHÖNE, H.K., SIEBERS, D., WANDSCHNEIDER, K. and WEBER, A. (1977). Parallel plastic tank experiments with cultures of marine diatoms. *Helgol. wiss. Meeresunters.*, 30, 201-216.

BROCKMANN, U.H., EBERLEIN, K., JUNGE, H.D., MAIER-REIMER, E. and SIEBERS, D. (1979). The development of a natural plankton population in an outdoor tank with nutrient-poor sea water. II. Changes in dissolved carbohydrates and amino acids. *J. Mar. Ecol. Prog. Ser.*, 1, 283-291.

CHUECAS, L. and RILEY, J.P. (1969). Component fatty acids of the total lipids of some marine phytoplankton. *J. mar. biol. Ass. U.K.*, 49, 97-116.

EBERLEIN, K., KATTNER, G., BROCKMANN, U. and HAMMER, K.D. (1980). Nitrogen and phosphorus in different water layers at the central station during FLEX '76. "Meteor" Forsch.-Ergebn. A, No. 22, 87-98.

FOLCH, J., LEES, M., SLOANE STANLEY, G.H. (1957). A simple method for the isolation and purification of total lipids from animal tissues. *J. Biol. Chem.*, 226, 497-509.

FOGG, G.E. (1975). Primary Productivity. In: J. Riley and G. Skirrow (Eds). *Chemical Oceanography*, Vol. II (2nd ed.) Academic Press, New York, pp. 385-453.

GARRETT, W.D. (1967). The organic chemical composition of the ocean surface. *Deep-Sea Res.*, 14, 221-227.

HARRINGTON, G.W., BEACH, D.H., DUNHAM, J.E. and HOLZ, JR., G.G. (1970). The polyunsaturated fatty acids of marine dino-flagellates. *J. Protozool.*, 17, 213-219.

JARVIS, N.L., GARRETT, W.D., SCHEIMAN, M.A. and TIMMONS, C.O. (1967). Surface chemical characterization of surface-active material in seawater. *Limnol. Oceanogr.*, 12, 88-96.

JEFFREY, L.M. (1970). Lipids of marine waters. In: D.W. Hood (Ed.), *Organic matter in natural waters*. Institute of Marine Science, University of Alaska, pp. 55-76.

KATTNER, G.G. and BROCKMANN, U.H. (1978). Fatty-acid composition of dissolved and particulate matter in surface films. *Mar. Chem.*, 6, 233-241.

KATES, K. and VOLCANI, B.E. (1966). Lipid components of diatoms. *Biochem. Biophys. Acta*, 116, 264-278.

KAYAMA, M. and YAMADA, H. (1975). Studies on the lipids of coastal waters. I. General composition of lipids in sea water, sediments and suspensoids. *J. Fac. Fish. Anim. Husb.*, Hiroshima Univ., 14, 23-35.

LARSSON, K., ODHAM, G. and SÖDERGREN, A. (1974). On lipid surface films on the sea. I. A simple method for sampling and studies of composition. *Mar. Chem.*, 2, 49-57.

MARTY, Y. and COURTOT, P. (1976). Variations de la concentration des acides gras libres dissous en rade de Brest. In: *Les substances organiques naturelles dissoutes dans l'eau de mer*. Actualités de Biochimie Marine, pp. 101-119.

MARTY, Y. and COURTOT, P. (1979-80). Les acides gras dans la rade de Brest: variation saisonnières. *Océanis*, Vol. 5, Fasc. Hors-Série, 621-625.

MYKLESTAD, S. (1974). Production of carbohydrates by marine diatom. I. Comparison of nine different species in culture. *J. exp. mar. Biol. Ecol.*, 15, 261-274.

MYKLESTAD, S. (1977). Production of carbohydrates by marine planktonic diatoms. II. Influence of N/P ratio in the growth medium on the assimilation ratio, growth rate, and production of cellular and extracellular carbohydrates by Chaetoceros affinis var. willei (Gran) Hustedt and Skeletonema costatum (Grev.) Cleve. *J. exp. mar. Biol. Ecol.*, 29, 161-179.

SLOWEY, J.F., JEFFREY, L.M. and HOOD, D.W. (1962). The fatty-acid content of ocean water. *Geochim. et Cosmochim. Acta*, 26, 607-616.

SOETJE, K.C. and HUBER, K. (1980). A compilation of data on the thermal stratification at the central station in the northern North Sea during FLEX '76. "Meteor" Forsch.-Ergebn. A, No. 22, 69-77.

TREGUER, P., LE CORRE, P. and COURTOT, P. (1972). A method for determination of the total dissolved free fatty-acid content of sea water. *J. mar. biol. Ass. U.K.*, 52, 1045-1055.

WANGERSKY, P.J. (1978). Production of dissolved organic matter. In: O. Kinne (Ed.), *Marine Ecology*, Vol. IV. Wiley, Chichester. pp. 115-220.

Development of organic substances at the Central Station during FLEX '76

II.- Dissolved free amino acids*

K.D. HAMMER, S. KATTNER and K. EBERLEIN **

Abstract

During FLEX '76 the development of dissolved free amino acids (DFAA) was investigated from March 26th to May 15th. Samples were taken from different depths at the Central Station. The filtered samples were analyzed by a highly sensitive fluorometric detection method. 16 different amino acids could be identified and quantified from the Fladen Ground area. During the experiment strong concentration changes occurred in the layer above the thermocline. In this layer the amount of DFAA varied from 40 n moles.ℓ^{-1} to 350 n moles.ℓ^{-1}. In the early exponential phytoplankton growth phase the DFAA increased very suddenly to the highest value. Related to DFAA nitrogen, the release amounted to 91 ng at N.ℓ^{-1}.d^{-1}. During the bloom the C:N ratio of DFAA increased from 3.0 to 3.4 above the thermocline and decreased again to lower values during the decomposition phase.

Introduction

Because of the complicated interactions with marine biomass little is known about the origin and fate of individual compounds of the dissolved organic substances. During the Fladen Ground Experiment (FLEX '76) the first phytoplankton bloom does not seem to be affected by hydrodynamic influences.

---

* This is JONSDAP '76 contribution n° 62.

** Institut für Organische Chemie und Biochemie der Universität Hamburg, Martin-Luther-King-Platz, 6, D-2000 Hamburg 13, F.R.G.

The great number of biological, chemical and physical data which were collected present a good background for the investigation of these complicated interactions.

The bulk of dissolved organic matter is quite inert with respect to biological and chemical degradation processes. A smaller proportion is subject to a great variability in concentration. It mainly consists of amino acids, proteins, carbohydrates and lipids (Bada and Lee, 1977). These substances appear as exudation (Fogg, 1977; Larsson and Hagström, 1979) or decomposition (Smith et al., 1977; Sorokin, 1977) products of marine plankton and seem to have an important position in marine ecosystems.

During FLEX vertical profiles were sampled every day at 12 h GMT at the Central Station ($58^{o}55'N$, $0^{o}32'E$) for analyzing amino acids. The development of dissolved free amino acids (DFAA) during the first phytoplankton bloom is elaborated in this study.

Methods

During the "Meteor" and "Anton Dohrn" cruises samples were taken at the Central Station ($58^{o}55'N$, $0^{o}32'E$), 12 h GMT and filtered immediately through glass fiber filters (Whatman GF/C 1.2 µm retention ability). Then the filtrate was fixed with 386 µ moles$\cdot\ell^{-1}$ mercury-(II)-chloride and kept at 4^{o} C until analysis was carried out. The sea water samples were not desalted in order to avoid falsification by adsorption and contamination.

Amino acid separation was done by means of a column (6 × 400 mm, cation resin Durrum DC 6, 12 mµ). For detection the highly sensitive fluorometric method with o-phtaldialdehyd was used (Roth and Hampai, 1973). The detection limit amounted to 1 p mole. The average analysis error was estimated to be about ± 10 % (for analytical details see Hammer and Eberlein, in press). Mean values of concentrations were com-

puted above the thermocline ("upper layer") and below the thermocline ("lower layer") and for the total water column (method see Eberlein et al., 1980). The thermocline is defined as the maximum temperature gradient. Data on thermoclines were obtained from Soetje and Huber (1980).

Results and discussion

At present seven vertical profiles of dissolved free amino acids (DFAA) taken at the Central Station have been measured and evaluted. There is a high temporal resolution during the period of April 22nd to 26th to substantiate the strong dynamics of DFAA fluxes during this time period. On the other hand, there is still a lack of analytical data between April 26th and May 15th. Therefore interpretations including this time period must be taken with some care.

Compared with other measurements from the North Sea (Dawson and Pritchard, 1978) the concentration of total DFAA in the Fladen Ground area was very low. The lowest concentration amounted to 40 n moles$\cdot \ell^{-1}$ and maximum was about 350 n moles$\cdot \ell^{-1}$.

Figure 1 shows the development of some nitrogen compounds as mean concentration values in the upper and lower layer and in the total water column. Up to April 12th all compounds remained relatively constant, with small increases in particulate nitrogen and DFAA, and small decreases in nitrate/nitrite. Up to April 20th DFAA as well as nitrate/nitrite concentrations decreased to lower values, while other parameters did not show any significant changes.

The formation of the first thermocline occurred on the 19th of April (Soetje and Huber, 1980). Around this time the phytoplankton bloom had started, and the particulate material increased up to May 1st, as represented by the concentration of particulate nitrogen in the upper layer (data from Weigel et al., unpublished).

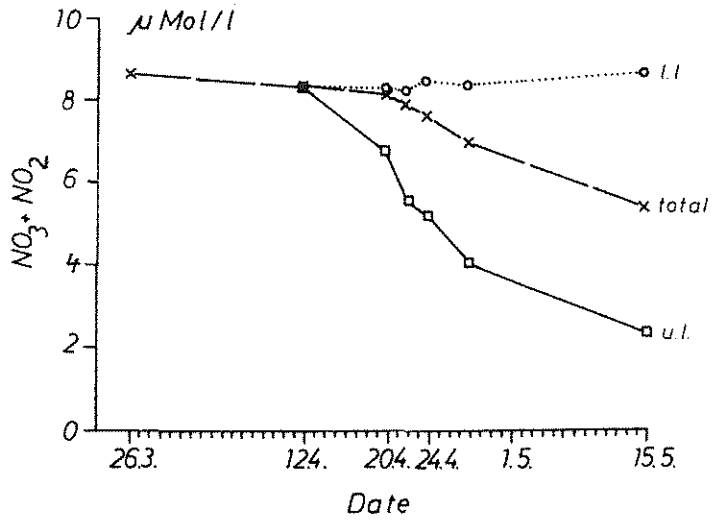

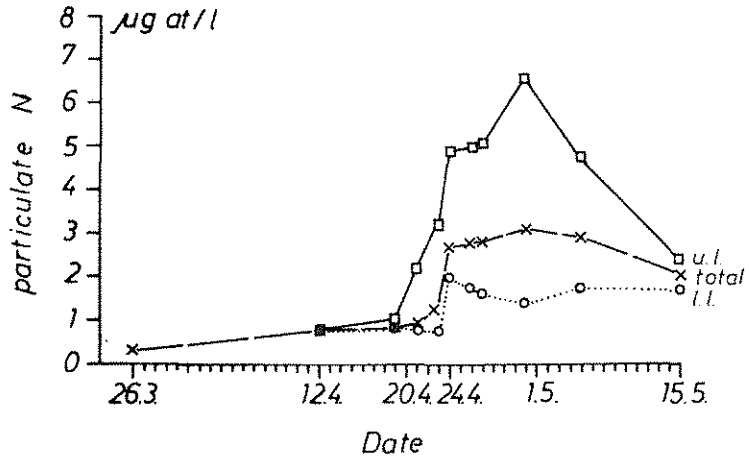

fig. 1a et 1b.

Mean concentrations of nitrate/nitrite and particulate nitrogen in the upper layer (u.l.), lower layer (l.l.) and the total water column during March 26th - 15th.

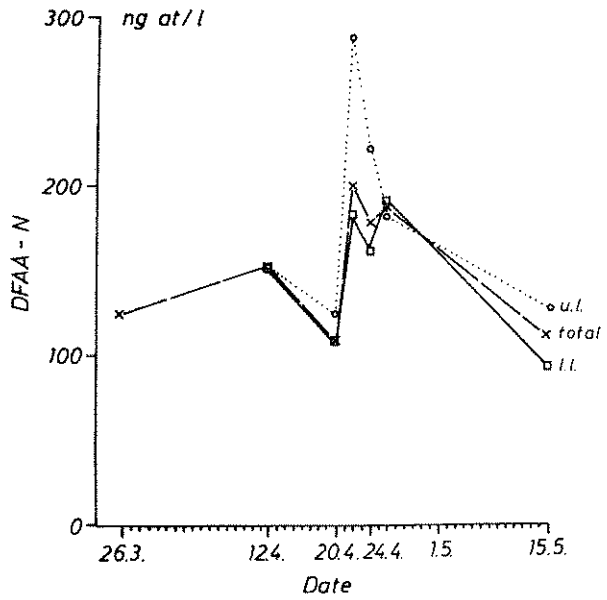

fig. 1c.

Mean concentrations of dissolved free amino acids (DFAA) in the upper layer (u.l.), lower layer (l.l.) and the total water column during March 26th - May 15 th.

During the time period from the 19th to 27th of April the highest fluxes of nitrogen occurred: In the upper layer the production of particulate nitrogen increased by 490 ng at$\cdot\ell^{-1}\cdot d^{-1}$, while nitrate/nitrite decreased by the same amount (Kattner et al., 1980). In this layer these strong dynamical processes were accompanied by a considerable increase of DFAA (expressed in DFAA nitrogen, Fig. 1) from the 20th to the 22nd. The flux rate amounted to about 91 ng at$\cdot\ell^{-1}\cdot d^{-1}$, which was 15 % of the nitrate/nitrite uptake (595 ng at$\cdot\ell^{-1}\cdot d^{-1}$, Table 1).

In this time interval the highest changes in nutrient concentrations converged with the strongest production phase of DFAA. This fact seems to be another evidence for the release of amino acids by "healthy" phytoplankton cells, a phenomenon, which is still in discussion (Sharp, 1977; Fogg, 1977; Larsson

Table 1

Increase and decrease (-) rates of DFAA nitrogen (DFAA-N), nitrate/nitrite and particulate nitrogen (N_p) above the thermocline during special time periods. DFAA-N : NO_3/NO_2 ratio

Time period	20.4.-26.4.	20.4.-22.4.	22.4.-24.4.	24.4.-26.4.
	(ng at·litre^{-1}·day^{-1})			
DFAA-N	1.3	91	-67	-20
NO_3/NO_2	-443.3	-595	-185	-550
DFAA-N :NO_3/NO_2 ratio	0.00	-0.15	0.36	0.04
N_p	512.7	585	903	50
Time period	19.4.-26.4.	19.4.-21.4.	21.4.-24.4.	24.4.-26.4.

and Hagström, 1979; Brockmann et al., 1979; Hammer and Eberlein, in press). In large plastic enclosures under nearly natural conditions Hammer and Eberlein observed high excretion and uptake rates of DFAA during the exponential growth phase of a marine diatom. The maximum excretion rate amounted to about 300 ng at·ℓ^{-1}·d^{-1}. The short excretion periods were always followed very rapidly by heterotrophic uptake periods. Taking into account that during FLEX the DFAA maximum concentrations as well as the excretion rates were three times less, there is a good agreement between both the experiments.

From the 22nd to the 24th of April the main part of biomass consisted of phytoplankton. During this time period the mean uptake rate of nitrate/nitrite was reduced from 595 to 185 ng at·ℓ^{-1}·d^{-1} (Tab. 1) and the amount of DFAA decreased to a concentration of 67 ng at·ℓ^{-1}·d^{-1}. The development of heterotrophic bacteria started in May (Hentzschel, unpublished data). Supposing that physical and chemical processes could not cause such a strong decrease, a substitution of reduced nitrate uptake by heterotrophic uptake of organic nitrogen compounds could be assumed for this time interval. The part which DFAA play during a spring phytoplankton bloom is not clear, though it seems that there is a significant uptake of these sub-

stances by phytoplankton (Wheeler, 1977). Nevertheless, DFAA played a role in nitrogen uptake to an extent of 36 % related to nitrate/nitrite (Tab. 1).

In spite of the high DFAA fluxes, the overall budget came to zero in the upper layer: Throughout the later plankton development the DFAA continued to decrease, and on May 15th it reached the original values (Fig. 1, 2).

At the beginning of the bloom a small increase of particulate material could be observed in the lower layer, but there were no significant changes of nitrate/nitrite (Fig. 1). Also a slight increase of DFAA occurred from April 22nd to 26th in this layer. These increases may have been caused by first sedimentation processes, in the course of which some parts of the plankton already might have been decomposed. In the stationary phase of the phytoplankton bloom, Kattner et al. pointed out an increase in the concentration of dissolved fatty acids in the lower layer, also caused by sedimentation.

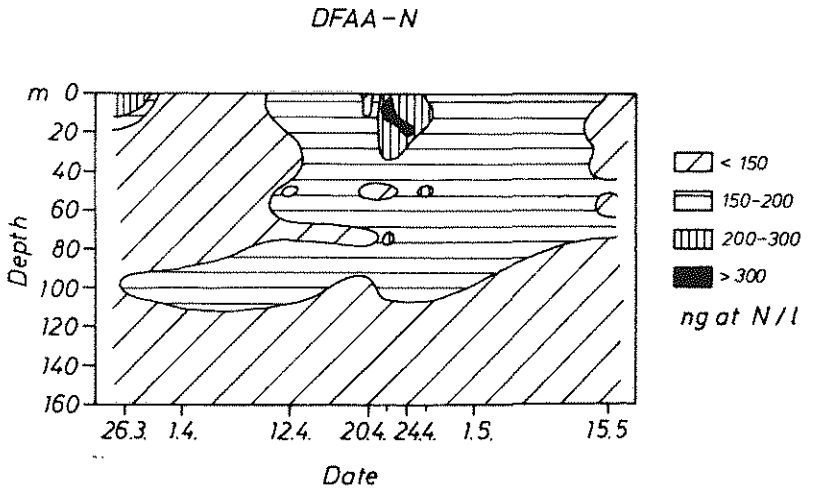

fig. 2.
Concentration of DFAA nitrogen (DFAA-N)

During the experimental period concentrations of total DFAA changed from 40 to 350 n moles·ℓ^{-1}. Figure 2 shows an isoline plot of DFAA nitrogen at the Central Station. Striking is the location of the maximum concentration during the exponential phytoplankton growth in the upper layer and a constant value in the very deep layers. In the upper layer DFAA increased up to April 24th. The maximum (> 300 ng at N·ℓ^{-1}) shifted from 3 m depth to 20 m during the development. On May 15th original values were found again for the whole water column.

The following 16 individual amino acids were detected in significant amounts: 1) maximum concentrations greater than 10 n moles·ℓ^{-1}: aspartic acid, glutamic acid, threonine, serine, ornithine, lysine, glycine, alanine and leucine. 2) maximum concentrations lower than 10 n moles·ℓ^{-1}: arginine, histidine, phenylalanine, tyrosine, isoleucine, valine and β-alanine.

The main part of DFAA consisted of the four amino acids serine, glycine, alanine and glutamic acid. Most of the individual amino acids showed a parallel development, as observed by Andrews and Williams (1971) and Bohling (1972).

Nearly all DFAA had very low concentrations in the bottom zone. As an example for the development of the main part of the DFAA the values of glycine are plotted in Figure 3.

The course of development of serine is strictly parallel to that of glycine. Both substances are related directly to each other in metabolism by the enzyme hydroxymethyl-transferase. Their metabolic pathways of synthesis are short and proceed directly during photosynthesis over 3-phosphoglyceric acid or during photo-respiration over glycolate. In tank experiments Hammer and Eberlein (in press) also found that these two amino acids are dominating during the main production activity of phytoplankton. With the exception of glutamic acid and ornithine all other amino acids had a nearly parallel development to glycine.

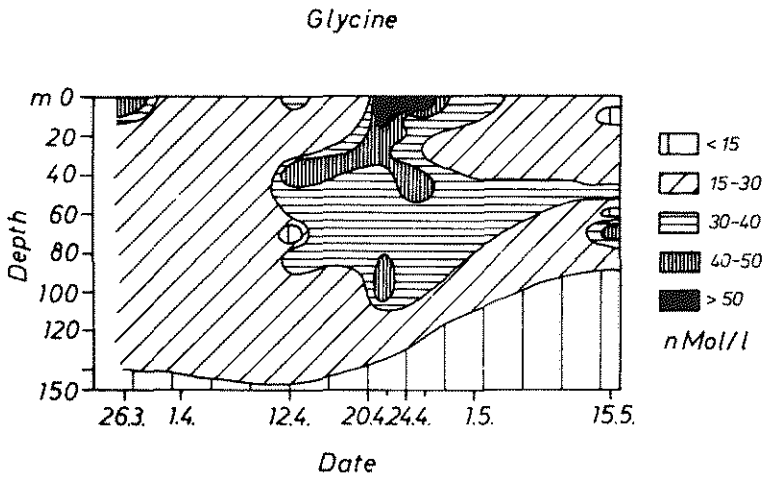

fig. 3.
Concentration of glycine

Glutamic acid can be encountered in the combined amino acid fraction in 10-times greater values than in the free one, as shown by Bohling (1972). The later occurrence of this

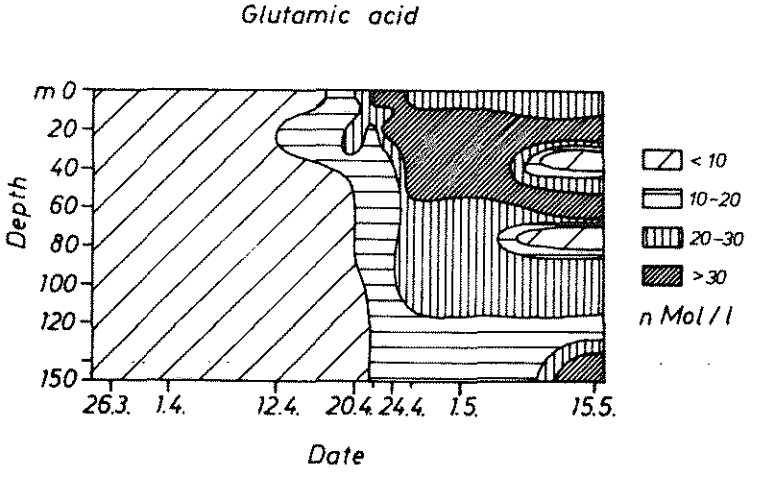

fig. 4.
Concentration of glutamic acid

amino acid (Fig. 4) could be explained by enhanced proteolytic activity of these combined amino acids and decomposition of particulate material.

Ornithine also had a development which was different from that of glycine (Fig. 5). It almost gave an inverse picture of glutamic acid with high concentrations before and low concentrations during the plankton bloom. An interpretation of this phenomenon would only be speculative.

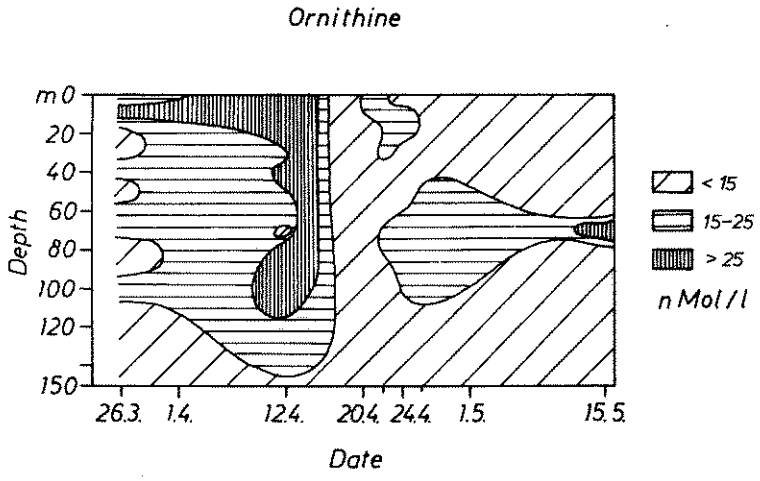

fig. 5.
Concentration of ornithine

In Figure 6 the C:N ratio of DFAA is presented. Prior to the phytoplankton bloom the ratio was kept constant at about 3.0. During the bloom it increased up to 3.4 in the upper layer and 3.2 in the lower layer. An increase of the C:N ratio might have been caused by an adaptation to lowered nitrate/ nitrite concentrations in the upper layer. In the stationary growth phase the DFAA had a high carbon content and were accompanied by an increasing production of nitrogen-free organic compounds, such as carbohydrates and lipids (Brockmann et al.,

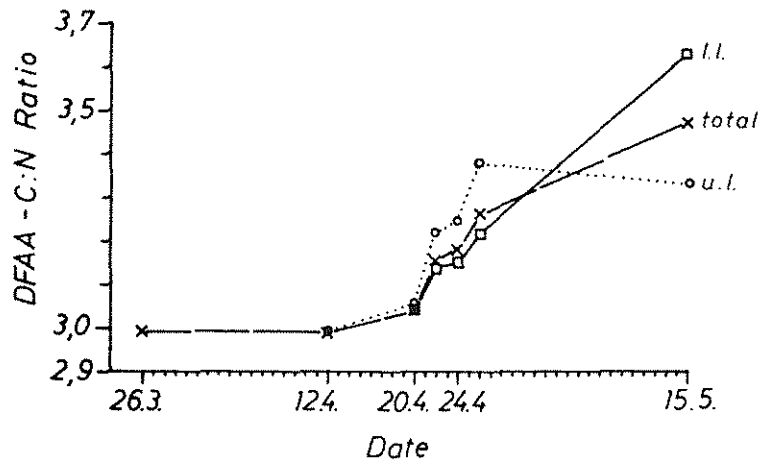

fig. 6.

DFAA carbon to nitrogen (C:N) ratio in the upper layer (u.l.), lower layer (l.l.) and the total water column.

1979; Kattner et al., in this volume). During the decomposition phase of phytoplankton in the upper layer the C:N ratio was reduced again, the source of DFAA was then mainly based on proteolytic activities.

During FLEX the development of total DFAA showed a positive correlation with the exponential growth rate of phytoplankton. This fact is another indication of the release of DFAA by "healthy" phytoplankton cells. Since excretion and heterotrophic uptake are related in a steady state, the real rates should be much higher than presented in Table 1. By this means, organic bound nitrogen was synthesized in large amounts via primary production, and in this way these compounds were available for heterotrophs at this early period of phytoplankton bloom.

Acknowledgements

Thanks are due to all who contributed data, in particular to W. Hickel, G. Weichart and P. Weigel. This work was supported by the Deutsche Forschungsgemeinschaft through the Sonderforschungsbereich 94 — Meeresforschung — Hamburg.

References

ANDREWS, P. and WILLIAMS, P.J. LEB. (1971). Heterotrophic utilisation of dissolved organic compounds in the sea. III. Measurement of the oxidation rates and concentrations of glucose and amino acids in sea water. *J. Mar. Biol. Ass. U.K.*, 51, 11-125.

BADA, J.L. and LEE, C. (1977). Decomposition and alternation of organic compounds dissolved in seawater. *Mar. Chem.*, 5, 523-539.

BOHLING, H. (1972). Gelöste Aminosäuren im Oberflächenwasser der Nordsee bei Helgoland: Konzentrationsveränderungen im Sommer 1970. *Mar. Biol.*, 6, 281-289.

BROCKMANN, U.H., EBERLEIN, K., JUNGE, H.D., MAIER-REIMER, E., and SIEBERS, D. (1979). The development of a natural plankton population in an outdoor tank with nutrient-poor sea water. II. Changes in dissolved carbohydrates and amino acids. *Mar. Ecol. Prog. Ser.*, 1, 283-291.

DAWSON, R. and PRITCHARD, R.G. (1978). The determination of -amino acids in sea water using a fluorimetric analyser. *Mar. Chem.*, 6, 27-40.

EBERLEIN, K., KATTNER, G., BROCKMANN, U. and HAMMER, K.D. (1980). Nitrogen and phosphorus in different water layers at the central station during FLEX '76. "Meteor" Forsch.Ergebn. A, 22, 87-98.

FOGG, G.E. (1977). Excretion of organic matter by phytoplankton. *Limnol. Oceanogr.*, 22, 576-577.

HAMMER, K.D. and EBERLEIN, K. (1980). Parallel experiments with Thalassiosira rotula in outdoor plastic tanks. Development of dissolved free amino acids during an algae bloom. *Mar. chem.* (in press).

KATTNER, G., HAMMER, K.D., EBERLEIN, K. and BROCKMANN, U. (1980). An attempt to determine fluxes of nitrogen and phosphorus in special time periods during FLEX '76. "Meteor" Forsch. Ergebn. A, 22, 99-104.

KATTNER, G., HAMMER, K.D. and BROCKMANN, U. (1980). Development of organic compounds at the Central Station during FLEX '76 (same volume).

LARSSON, U. and HAGSTRÖM, A. (1979). Phytoplankton exudate release as an energy source for the growth of pelagic bacteria. *Mar. Biol.*, 52, 199-206.

ROTH, M. and HAMPAI, A. (1973). Column Chromatography of amino acids with fluorescence detection. *J. Chromat.*, 83, 353-356.

SHARP, J.H. (1977). Excretion of organic matter by marine phytoplankton: Do healthy cells do it? *Limnol. Oceanogr.*, 22, 381-399.

SOETJE, K.C. and HUBER, K. (1980). A compilation of data on the thermal stratification at the central station in the northern North Sea during FLEX '76. "Meteor" Forsch. Ergebn. A, 22, 69-77.

SMITH, O.S., JR., BARBER, R.T. and HUNTSMAN, S.A. (1977). Primary production off the coast of northwest Africa: Excretion of dissolved organic matter and its heterotrophic uptake. *Deep Sea Res.*, 24, 35-47.

SOROKIN, Y.J. (1977). The heterotrophic phase of plankton succession in the Japan Sea. *Mar. Biol.*, 41, 107-117.

WHEELER, P.A., NORTH, B.B., LITTLER, M. and STEPHENS, G.C. (1977). Uptake of Glycine by natural phytoplankton communities. *Limnol. Oceanogr.*, 22, 900-910.

Zooplankton distribution pattern in the FLEX box (May 1976)

Measurements with the Dalhousie electronic plankton counter and comparisons with CPR, UOR and HSLE sampling systems*

David L. MACKAS**

Abstract

Four independent sampling systems were used during May 1976 to describe the horizontal distribution of zooplankton abundance within the FLEX box. The purpose of this paper is to present the distribution data obtained by one of these sampling systems (the Boyd/Mackas electronic plankton counter) and to compare data from this system with the patterns obtained by the other three zooplankton sampling methods.

Methods

Data presented here were collected during two cruises aboard the FRV *Explorer* (11-24 May and 26 May - 4 June 1976). During each of these cruises *Explorer* surveyed two full grid patterns within the FLEX box plus 1 or 2 "mini-grids" (see the draft FLEX Atlas for grid coverage and dates). A variety of parameters including near-surface temperature, salinity, nitrate, and chlorophyll fluorescence were measured (Steele and Henderson, 1979) in addition to the four estimates of zooplankton concentration. However only the zooplankton methods and results will be discussed in detail here.

Two of the zooplankton samplers (the "Continuous Plankton Recorder" = CPR, and the "Undulating Oceanographic Recorder" = UOR) were operated by IMER and are derived from the Hardy Recorder (Hardy, 1936). In both of these, organisms entering the sampler are first trapped on and then sandwiched

---

* This is JONSDAP '76 contribution n° 53.

** Institute of Ocean Sciences, P.O. Box 6000, Sidney, B.C., Canada V8L 4B2.

between two moving gauze strips. The rate of movement of the gauze is mechanically matched to the towing speed such that a standard volume of water (3 m^3) is filtered onto each segment of the gauze. (Williams, pers. comm.) During FLEX, the CPR sampled at a fixed depth of 10 m, while the UOR traced a sawtooth pattern of wavelength 2.5 km between 10 and 70 m depth. Plankton on the gauze strips were analyzed into coded abundance categories following standard IMER procedures (Colebrook, 1960).

The third system (the "High Speed Loch Ewe net" = HSLE, designed and operated by DAFS) is a relatively conventional metered plankton net adapted for towing at 5-6 kts. The standard sample unit during FLEX was a double oblique haul from surface to near-bottom and back to the surface. Abundance (species counts) and dry weight of "macrozooplankton" (see Table 1 for definitions) were normalized to a standard filtered volume of 100 m^3 (Adams, pers. comm.).

Table 1

Characteristics of FLEX zooplankton samplers

Device	Depth Sampled	Size selectivity	Horizontal Resolution (km)	Average Abundance (#/liter) 12-20 May	26 May-3 June
DAL	~ 3 m	Particles 0.35-3mm diameter	~ 0.2	4.8	11.7
HSLE	0-bottom (~ 0-120 m)	Zooplankton retained by:	~ 5 (dryweight)		
		250 µ mesh (="macro")	~ 15 (species)	0.51	1.0
		68 µ mesh (-"micro")			
CPR	~ 10	Zooplankton retained by 280 µ mesh	~ 16	0.64	0.5
UOR	10-70	Zooplankton retained by 280 µ mesh	~ 5	0.10	0.15

The fourth system (the "Boyd/Mackas plankton counter" = DAL) is less conventional. It is an electronic particle counter designed to automatically enumerate organisms in the 0.5-3 mm size range (Mackas and Boyd, 1979) and was supplied during FLEX with water from a pump intake at ~ 3 m depth. This sampler is not specific for zooplankton except on

the basis of size thresholds; however only a very small fraction (0-5%) of particles in this size range are detrital or phytoplankton. Most were copepods of the genera Calanus, Pseudocalanus, and Oithona. Characteristics of the samplers are summarized in Table 1.

Probably the most important difference between the various samplers is their depth coverage (3 m for DAL, 10 m for CPR, 0-150 m for HSLE, and 10-70 m for UO). This resulted in varying overlap with the vertical distribution of the zooplankton. In general, both DAL and CPR data are subject to severe contamination due to diel vertical migration (to compensate for this, the DAL sampler was operated only at night). The HSLE data (surface to bottom) should be almost immune to artifacts of the vertical distribution, while the UOR data will be contaminated if any significant fraction of the zooplankton population resides for some portion of the day either above or below the 10-70 m sampled interval.

Results and discussion

1.- HORIZONTAL DISTRIBUTION PATTERN AS MEASURED BY THE DAL SAMPLER

Because the DAL sampler was operated only at night (typically 2300-0400 hrs GMT), coverage of the FLEX box was incomplete on any single survey. Figures 1 and 2 show plots of zooplankton abundance from the four large-scale grid surveys (corresponding to CPR/UOR and HSLE surveys within each of the two *Explorer* cruises). Both temporal and spatial variability is apparent in the figures.

The zooplankton abundance showed a major increase over the 22 day span (fig. 3). Taking 4 May as an arbitrary starting time for an equation fitting the logarithm of estimated abundance vs. time in days, I obtain a regression significant at the P = 0.1 level. Figure 3 also shows an apparent U-shaped temporal variation within each of the two cruises. This is an artifact resulting from interaction between spatial pattern and sampling schedule. All four samplers found higher transect-averaged plankton abundance in the west half of the grid, and this side was sampled at the start and finish of each cruise.

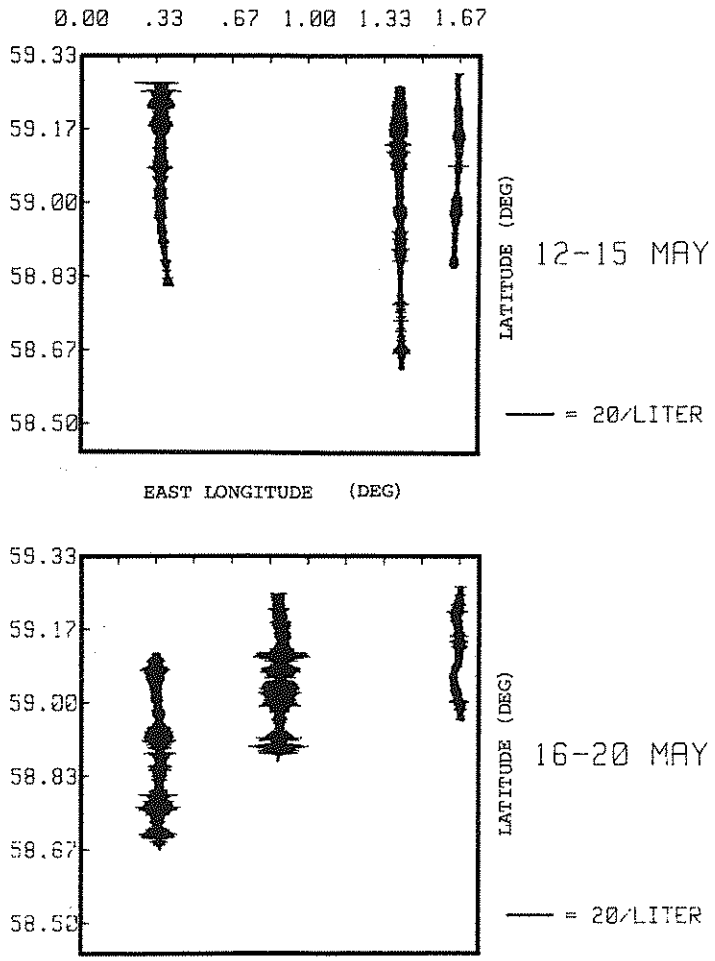

fig. 1.

Zooplankton abundance measured by the DAL sampler during the first *Explorer* cruise. Local abundance is proportional to the width of the shaded zone, which is centered on the sampling track. Upper panel (12-15 May) is concurrent with UOR and CPR, lower panel (16-20 May) is concurrent with HSLE.

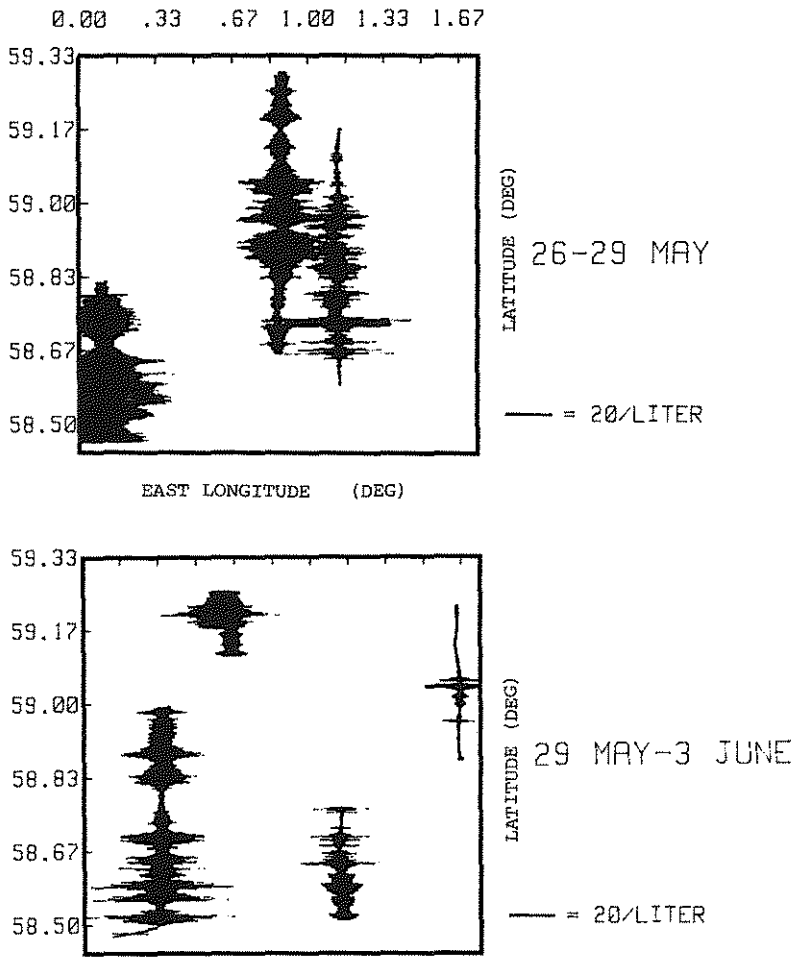

fig. 2.

Zooplankton abundance measured by the DAL sampler during the second *Explorer* cruise. Upper panel (26-29 May) is concurrent with UOR/CPR, lower panel (29 May - 3 June) is concurrent with HSLE.

The most unique feature of the zooplankton spatial pattern revealed by the DAL sampler is the intense 0.5-10 km scale variability in abundance (Mackas and Boyd, 1979). This variability was more-or-less integrated by the CPR, UOR and HSLE samplers, and hence only marginally detectable

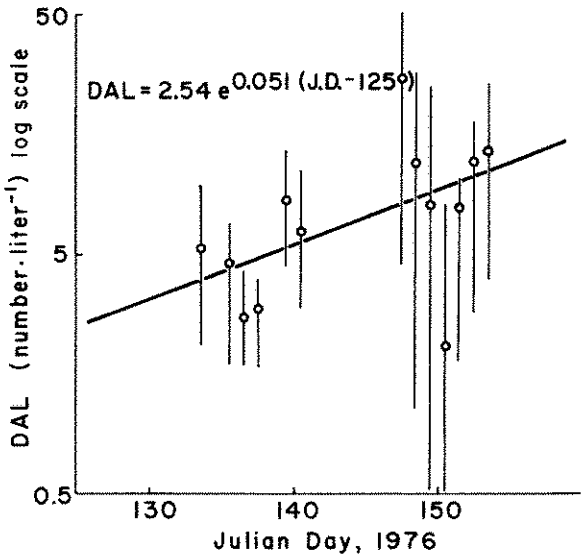

fig. 3.

Zooplankton abundance versus time for the DAL data. Circles are nightly transect average, vertical lines show the range of averages over 5 km segments within that night's transect.

by them. However, despite this intense small-scale variability, the major features of the large-scale pattern are apparent on inspection of the DAL data. As mentioned previously, the zooplankton abundance was generally higher in the west half of the box. The northeast corner of the box had consistently low abundance; this was particularly evident during the second cruise. Both DAL (Mackas, 1977) and DAFS (Steele, 1978; Steele and Henderson, 1979) measurements of chlorophyll fluorescence showed the development and subsequent decline of a late May phytoplankton bloom (peak concentration ~ 4 mg m^{-3} chl a) in the same region. Quite high zooplankton abundance (5 km average ~ 25 $liter^{-1}$) occurred in a band along the southwest margin of this phytoplankton bloom, roughly running 59° 20'N - 00° 20'E to 58° 40'N - 01° 40'E. The only region showing higher zooplankton concentrations (5 km average 20-50 $liter^{-1}$) was the extreme southwest corner of the FLEX box.

2.- COMPARISONS WITH HSLE, CPR AND UOR

I have averaged the DAL data over sets of navigational intervals corresponding to the intervals sampled by the HSLE, UOR, and CPR samplers. (USLE data were provided by J.A. Adams of DAFS; CPR and UOR data were provided by R. Williams of IMER). All data were log-transformed (the DAL data *after* the spatial averaging), and log-log regression equations were calculated between:

1. DAL (counts liter^{-1}) vs HSLE (total copepods liter^{-1})
2. DAL (counts liter^{-1}) vs HSLE (mg m^{-3} dryweight)
3. DAL (counts liter^{-1}) vs CPR (total copepods liter^{-1})

The data were significantly correlated for the first three pairings (HSLE dryweight was marginal) but showed no significant relationship between DAL and UOR abundance estimates. Plots of the data and calculated "predictive" and "GM" regressions (*sensu* Ricker, 1972) are shown in figs. 4 and 5. To some extent, the correlation between DAL and CPR and UOR is reduced by the coarse quantization of the IMER samplers. The "GM" regression compensates for the decrease in regression slope caused by low correlation and provides the best estimate of the true functional relationship between the variates, as opposed to the smallest mean square error of prediction of the dependent variate given a known value of the independent variate. It should be noted that the strength of the correlations depended on joint detection of the large-scale spatial and temporal patterns, and that, for both HSLE and CPR, the GM regression predicts zooplankton concentrations roughly 10 - 15 % of the corresponding DAL estimates. Direct calibration of the DAL electronic count rate against visually analyzed replicates from the sampling pump discharge gave essentially a 1:1 relationship (Mackas and Boyd, 1979), so these abundance differences appear to be real. The UOR estimates of plankton concentration were even smaller than CPR and USLE; typically ~ 20 % of the simultaneous CPR estimates (see e.g. data reported by Williams in the draft FLEX Atlas and cruise averages in Table 1).

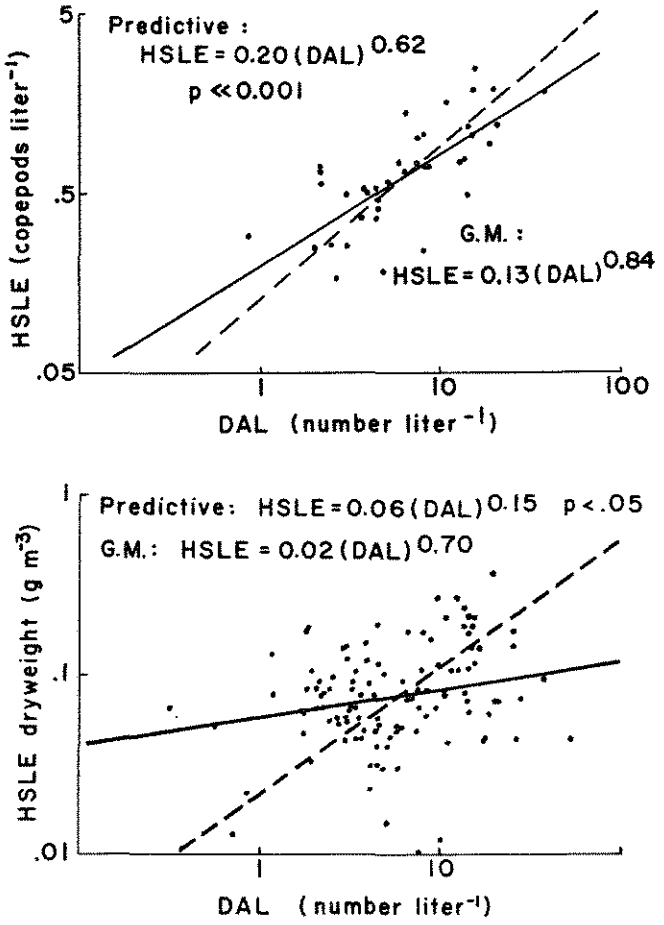

fig. 4.

(Upper) HSLE copepod abundance (* liter^{-1}) and (lower) HSLE dryweight (g m^{-3}) versus DAL abundance estimate (* liter^{-1}). Roughly every third tow was analyzed for species; the sampling interval for the upper panel is therefore ~ 15 km. The dryweight sampling interval, the sample length and the DAL averaging window are all ~ 5 km. Predictive regressions are solid lines, GM (= functional) regressions are dashed lines. The abundance regression is significant at the $p = 0.001$ level and the dryweight regression is significant at the $p = 0.05$ level.

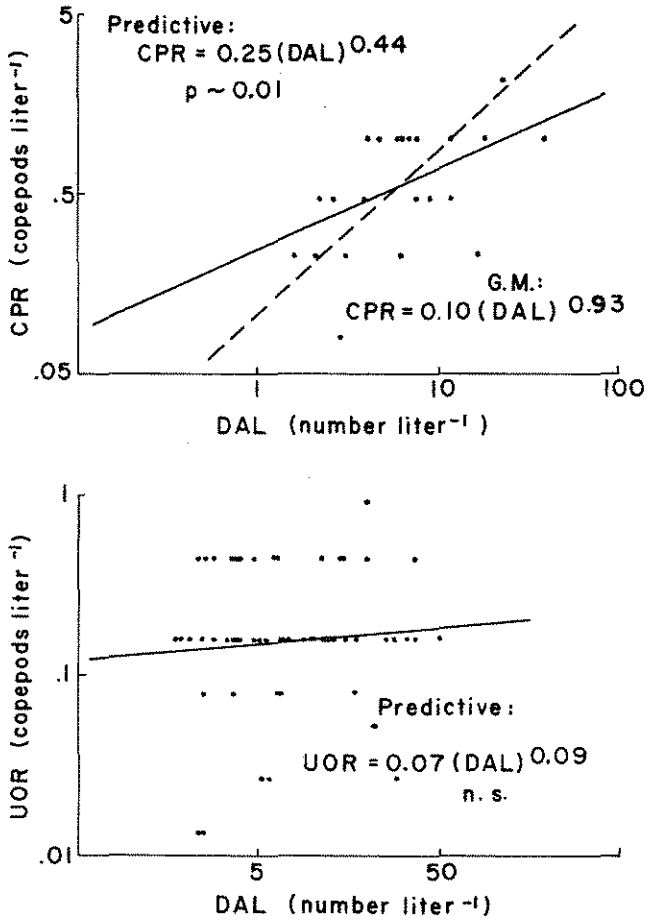

fig. 5.

(Upper) CPR abundance (* liter^{-1}) and (lower) UOR abundance (* liter^{-1}) versus DAL abundance (* liter^{-1}). Sampling and averaging windows are ~ 16 km (upper) and ~ 5 km (lower). Predictive regressions are solid lines, GM regression (shown only for the CPR data) is dashed line. The CPR regression is significant at the $p = 0.01$ level; the UOR regression is not significant at the $p = 0.25$ level.

3.- EFFECTS OF VERTICAL DISTRIBUTION OF ZOOPLANKTON

Expressing the abundance of zooplankton at depth z as N_z (applicable to the fixed-depth DAL and CPR samplers) and the average over a depth interval z_1 to z_2 as

$$\frac{1}{z_2 - z_1} \int_z^z N_z \, dz$$

(applicable to the vertically-integrating HSLE and UOR samplers), I can summarize the average night-time vertical distribution of copepods as follows :

$$\frac{1}{60} \int_{10}^{70} N_z \, dz \ll \frac{1}{120} \int_0^{120} N_z \, dz \sim N_z = 10 \ll N_z = 3 \qquad (1)$$

(UOR) (HSLE) (CPR) (DAL)

The data are inadequate to determine the precise functional relationship between N_z and z. However, it is clear that N_z must be large near the surface and must rapidly approach a small asymptotic value for the above inequalities to be consistent. Lacking more sophisticated information, I have assumed a mathematically simple two-layer model in which a thin (order 5 m) wave-mixed surface layer with uniform zooplankton concentration overlies a sub-surface region where the decrease of plankton abundance with depth follows a negative exponential relationship, thus:

$$N_z = N_0 \qquad \text{for} \quad z \leq 5 \text{ m} \qquad (2)$$

$$N_z = N_0 \, e^{-k(z-5)} \qquad \text{for} \quad z > 5 \text{ m} \qquad (3)$$

I have substituted these relationships, along with the between-sampler ratios of average zooplankton abundance (from Table 1) into the inequalities from (1), and have solved for the only free variable in this model, the exponential efficient k. The range of this estimate is wide; 0.08 (CPR vs UOR) to 0.75 (HSLE vs CPR). However, the remaining estimates were clustered near the mean value (± standard error of the mean) of 0.35 ± 0.10. The abundance profile predicted from the model is shown in figure 6.
The most important feature is that, even with a minimal estimate for the rate of abundance decrease with depth ($k \sim 0.2$), more than 80 % of the animals were above 10 m. For the mean estimate ($k = 0.35$) the abundance gradient is even

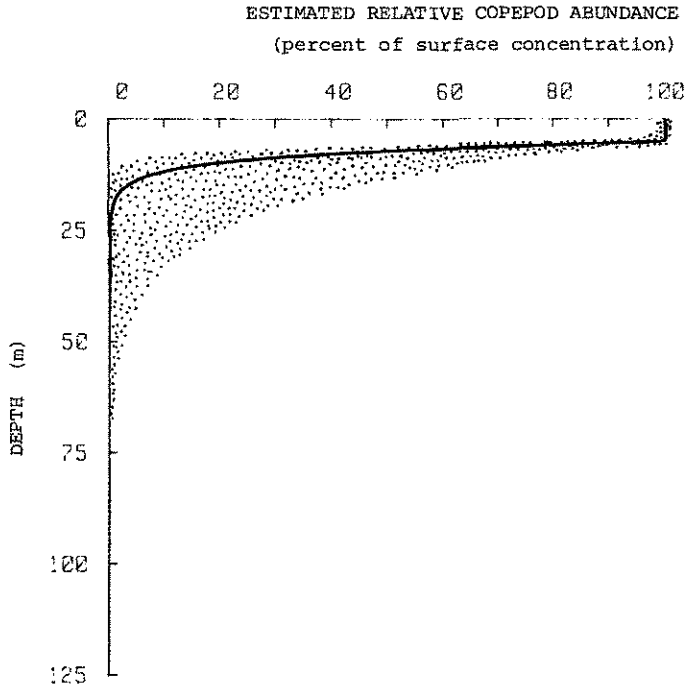

fig. 6.

Copepod abundance versus depth as estimated from catch ratios of fixed-depth and oblique (vertically integrating) samplers. Solid line is the mean estimate of a negative exponential coefficient; stippled area encloses the range of estimates from six comparisons.

sharper, with roughly 94 % of the population above 10 m depth. A qualitatively similar but less intense vertical distribution of zooplankton biomass during FLEX has been discussed by Longhurst and Williams (1979) and Williams and Lindley (in press). They show, using Longhurst-Hardy Plankton Recorder data, that roughly 75% of the night copepod biomass occurred in the upper 25 - 30 m. Since most of the zooplankton in the surface layer were small (stage 2-4 copepodites of *Calanus finmarchicus*, late copepodites and adults of *Pseudocalanus* and *Oithona*), this difference between abundance and biomass gradients was expected.

On the basis of the above information, I conclude that the best (least biased) estimate of large-scale zooplankton pattern during FLEX was provided by the HSLE. The UOR probably gave a consistent estimate of relative abundance at smaller scales (i.e. comparable to the resolution for HSLE dry-weights) but severely under-sampled the very large fraction of the population occurring above 10 m depth. Assuming that horizontal abundance variations in the surface layer penetrated downward to 10 m depth, it is probable that the CPR gave a reasonable "average" abundance estimate; however it had poor spatial resolution, and may have included some artifacts due to spatial variations in vertical distribution. The DAL sampler gave good estimates of relative small-scale (0.2-5 km) pattern but showed severe biasing of absolute abundance (high at night, low in daylight). Given the intense small-scale horizontal patchiness (some of which may have resulted from vertical displacement of the region of strong vertical abundance gradient), it is not surprising that the observed correlations between the DAL, HSLE and UOR samplers were based primarily on large-scale spatial and temporal trends. The small-scale patchiness observed by the DAL sampler would have been aliased by the undulation patterns of HSLE and UOR, and would thus appear almost entirely as random scatter about the functional regression line.

Acknowledgements

I wish to thank C.M. Boyd of Dalhousie University, J. Adams, J. Steele and I. Baird of DAFS, R. Williams and A. Hiby of IMER for their invaluable advice and assistance. The data for this report were collected while Mackas was supported by a National Research Council of Canada Post-Graduate Fellowship.

References

COLEBROOK, J.M. (1960). Continuous Plankton Records : methods of analysis, 1950-1959. *Bull. Mar. Ecol.*, 5, 51-64.

HARDY, A.C. (1936). The continuous plankton recorder. *Discovery Reports*, 11, 457-510.

LONGHURST, A. and WILLIAMS, R. (1979). Materials for plankton modelling : vertical distribution of Atlantic zooplankton in summer. *J. Plankton Res.*, 1, 1-28.

MACKAS, D.L. (1977). *Spatial variability and covariability of marine plankton*, Ph. D. Thesis, Dalhousie University, 228 pp.

—— and BOYD, C.M. (1979). Spectral analysis of zooplankton spatial heterogeneity, *Science*, 204, 62–64.

STEELE, J.H. (1978). *Some comments on plankton patches*, in *Spatial Pattern Plankton Communities* (J.H. Steele, ed.), pp. 1–20, NATO Conference Series, IV, 3, Plenum Press.

STEELE, J.H. and HENDERSON, E.W. (1979). Spatial patterns in North Sea plankton, *Deep Sea Res.*, 26, 955–963.

WILLIAMS, R. and LINDLEY, J. (in press). Plankton of the Fladen Ground during FLEX 76 III. Vertical distribution, population dynamics and production of *Calanus finmarchicus* (Gunnerus) (Crustacea : Copepoda). To appear in *Mar. Biol.*

Computation of secondary production of *Calanus finmarchicus* using a multiple regression method*

H.G. FRANSZ**

Abstract

A method is described to estimate development and mortality rates from time series of densities of development classes. The growth rate or P/B ratio can be derived from the development rate and the weight increment between stages. The method is applied to estimate the production of *Calanus finmarchicus* during the diatom spring bloom in the FLEX box, April-May 1976, in the northern North Sea. Two sets of data could be used. The total production of *Calanus finmarchicus* is estimated to be at most 50 mg C $.m^{-2}.d^{-1}$ during the peak of the diatom bloom. Although the growth rates derived are of the same order of magnitude as those estimated from growth characteristics by Fransz and van Arkel (1980), there is evidence that growth and development was considerably lower in the largest copepodid stages.

Introduction

The Fladen Ground Experiment 1976 has produced nice time series of copepodid stage densities of the calanoid copepod *Calanus finmarchicus* (Gunn.) during the spring bloom in the northern North Sea. Such data sets are obtained for the central station (Krause, 1980) and for more scattered locations in the FLEX box (Williams, 1977). Time series of densities in different development classes provide the necessary information about the actual in situ growth and mortality of the population. Estimates of growth and development can be used to estimate production.

---

* This is JONSDAP '76 contribution n° 59.

** Netherlands Institute for Sea Research, Texel, The Netherlands.

A relatively short generation time, a long reproduction period and variable growth rate make cohorts and generations indistinguishable in natural copepod populations. Therefore, rather complicated methods are used to estimate the population parameters, often based on rigid assumptions about the way, the increment rate of age classes changes with time (e.g. Parslow *et al.*, 1979). Fransz (1976) used a method based on multiple linear regression to estimate levels of growth rate, production and mortality of developmental copepod stages for a particular time period. This method is not complicated, requires no special techniques, and can be applied under most conditions. This method is used to estimate production and mortality of *Calanus* copepodids from the data sets. The results are compared with indirect production estimates, based on growth characteristics of the species (Fransz and van Arkel, 1980).

Material and method

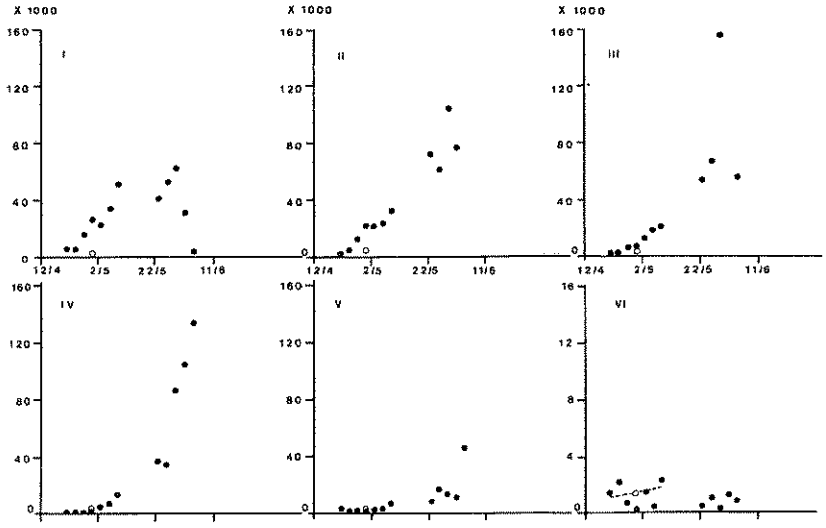

fig. 1.

Average number per m^2 of Calanus finmarchicus copepodids in three-day periods at the Central Station in the FLEX box according to Krause. Open circles indicate own observations.

During the *Meteor* expeditions, the zooplankton was sampled twice a day at the Central Station with a 5 ℓ water sampler at different depths. For *Calanus finmarchicus*, numbers per m^2 of the six copepodid stages were provided {M. Krause, personal communication (1980)} . Averages of consecutive three day periods are plotted against time in Fig. 1. Numbers per m^2, derived from catches by a Longhurst Hardy Plankton Recorder (Williams, 1977) are plotted in Fig. 2. Own determinations at the central station (Fransz and van Arkel, 1980) are also indicated in these figures.

The density levels of the three independent determinations correspond rather well, only the youngest copepodids reach an exceptionally high level in the Meteor data. A more or less exponential increase can be observed during the period before May 22, the period of the phytoplankton spring bloom. Thereafter, the density pattern is much more irregular and the numbers tend to decline.

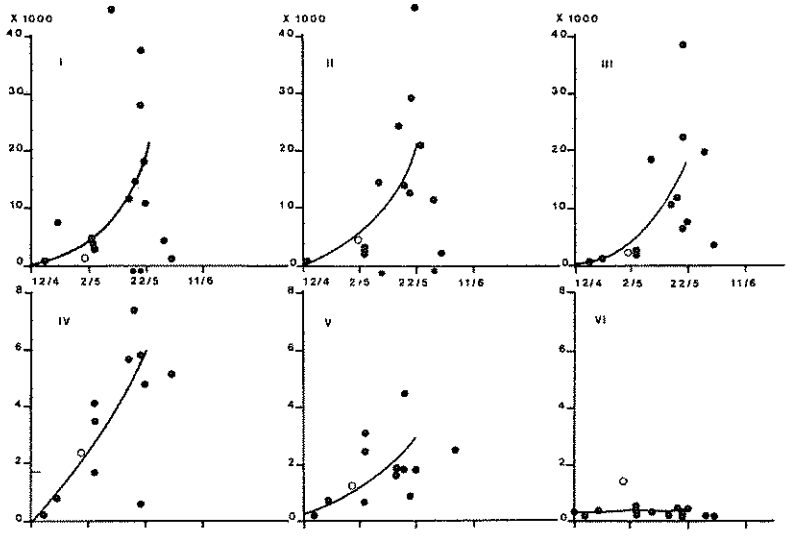

fig. 2.

Number per m^2 of Calanus finmarchicus copepodids from different locations in the FLEX box according to Williams, plotted against time. Lines are drawn by eye to obtain a smooth data set. Open circles indicate own observations.

Presumably, the population parameters were more or less constant during the period from April 12 to May 10, the period of the diatom spring bloom with a chlorophyll peak at April 28 - May 7. Data points after May 10 are discarded in the computations to reduce the estimate variance and to obtain an unbiassed estimate of *Calanus* productivity during the spring bloom, to evaluate the role of *Calanus* in terminating this bloom.

To time series of estimated densities D_i of development stages i and arbitrary time intervals t, the following equation applies for each pair of consecutive observations:

$$\frac{D_{i_t} - D_{i_o}}{t} = d_{i-1} \frac{D_{i-1_t} + D_{i-1_o}}{2} - (d_i + m_i) \frac{D_{i_t} + D_{i_o}}{2} + \bar{e}$$

where d_i is the individual development rate, m_i the individual mortality rate of stage i and $\bar{e}$ is a residual error term. This equation states that the rate of change of D_i during t equals the rate of development of the preceding stage minus the rate of development to the next stage and the rate of mortality. The only condition is that the D_i's change approximately linearly during t, hence the observation intervals must be reasonably short (one week or shorter). Migration will influence $\bar{e}$ and m_i mainly, usually it is not typically proportional to the density of the preceding stage. Extensive migration by advective or diffusive transport, however, biasses the estimated population parameters and should be accounted for by independent determinations.

For two observations in time the above rate equation can not be solved. For n+1 observations with n time intervals (n>2) the equation can be used as a linear regression model $Y = aX_1 - bX_2$ to estimate d_{i-1} (a) and $d_i + m_i$ (b). This model represents a plane through the origin in three-dimensional space with the least sum of squares of deviations perpendicular to the X_1, X_2 plane. Expectation and variance estimates of the regression coefficients can be derived (e.g. Draper and Smith, 1967). The computation of these values is given in the appendix.

In this way d_i is estimated for each stage as a level in the period between the first and the last observation. Of course, d_i is not a constant, it depends on the age composition of the development stage. But since we are interested in the productivity during a particular period, the d_i's estimated in this way represent suitable "mean" values of development rate.

The variance estimates can be used to evaluate the confidence of the expectation values. Fór this purpose the square root of the variance is multiplied with the value of Students t distribution at n-2 degrees of freedom and desired confidence level, where n is the number of time intervals. To find the confidence interval this value is added to and subtracted from the expectation value. Because m_i is found by subtracting d_i from $d_i + m_i$, the variance of m_i equals the sum of the variances of the latter estimates. In estimation methods like this it is very important to understand the relativity of the results.

Growth is usually expressed as production per unit of time and biomass (P/B). If the stages i have a constant dry weight W_i, the growth rate $(P/B)_i$ can be defined by:

$$(P/B)_i = d_i(W_{i+1} - W_i)/W_i$$

and the production per time unit by growth of stage i is simply :

$$P_i = (P/B)_i D_i W_i$$

Results

The regression method was applied to Krauses and Williams' data. To reduce the excessive variance in Williams' data set, smooth curves were fitted by eye (see Fig. 2) and the computation was repeated for data points on the lines at corresponding sampling times. Table 1 gives the resulting growth and mortality rates and growth rates indirectly estimated by Fransz and van Arkel (1980). Upper confidence limits are also given. The lower limits are usually negative and senseless. Reliable estimates are indicated by a small difference between expectation value and upper confidence limit.

The P/B values for copepodid I and II according to Krauses data and according to Fransz and van Arkel for the other stages were used to estimate optimistically the production during the peak of the diatom bloom, about April 29. The necessary information and the results are given in Table 2. To consider the whole *Calanus* population, information about naupliar stage densities (J. Trahms, personal communication (1980), Fransz

Table 1

Growth rate (P/B) and mortality rate (m) estimates in d^{-1} with upper 95% confidence limit between brackets per copepodid stage of *Calanus finmarchicus* during the spring diatom bloom in the FLEX box. In italics: growth rates used to estimate production.

Stage	Origin			Fransz indirectly estimated
	Krause	Williams	Williams smoothed	
P/B				
I	*.21* (.84)	.38 (.94)	.06 (.13)	.25
II	*.15* (.76)	-2.78 (0.00)	.25 (.81)	.24
III	- .06 (.15)	- .13 (.23)	- .02 (.01	*.17*
IV	.76 (1.65)	- .37 (1.10)	- .31 (0.00)	*.18*
V	.00 (.01)	- .01 (.03)	- .00 (0.00)	*.14*
m				
I	- .29 (.34)	- .30 (.38)	- .07 (0.00)	
II	.10 (.90)	1.43 (2.52)	- .10 (.13)	
III	.06 (.49)	-1.54 (.00)	.09 (.35)	
IV	- .59 (0.00)	- .02 (.67)	.02 (.13)	
V	.36 (1.01)	- .41 (1.24)	- .29 (0.00)	
VI	- .02 (0.00)	- .14 (.41)	- .01 (0.00)	

and van Arkel (1980)} and nauplius growth and egg production (Fransz and van Arkel, 1980) is used to estimate the production in naupliar stages and adults.

Table 2

Estimation of secondary production (P) of *Calanus finmarchicus* in the FLEX box during the peak of the diatom bloom, about April 29, 1976. In italics: densities used.

Copepodid	Number per m^2			W (µg)	B $mg.m^{-2}$	P/B d^{-1}	P $mg.m^{-2}.d^{-1}$
	Krause	Williams smoothed	Fransz				
I	*26260*	4000	920	2.7	70.9	.21	14.9
II	*21900*	6000	4760	5.7	124.8	.15	18.7
III	*6370*	4000	2800	20.1	128.0	.17	21.8
IV	*2405*	2200	2360	40.2	96.5	.18	17.4
V	435	1100	*1240*	145.2	180.0	.14	25.2
VI	1163	300	*1400*	191.6	268.2	.03	8.0
Total					868.4		106.0
Nauplius stage	Trahms	Fransz					
I	*7880*	5840		.24	1.7	-	-
II	395	*23080*		.23	5.3	.2	1.1
III	2775	*22160*		.41	9.1	.2	1.8
IV	*3691*	8400		.54	4.7	.2	.9
V	*12991*	2640		.65	8.4	.2	1.7
VI	*10157*	3840		.77	7.8	.2	1.6
Total					37.0		7.1

The highest density estimates are used consequently, to arrive at a maximum production estimate. The copepodid dry weights are those used by the zooplankton working group of FLEX, the nauplius dry weights are adopted from Fransz and van Arkel (1980). The *Calanus* production during the peak of the diatom bloom was at most 113 $mg.m^{-2}.d^{-r}$ dry weight, which is about 50 $mgC.m^{-2}.d^{-1}$.

Because the mortality estimates given in Table 1 are rather poor due to the high variance, mortality during the diatom peak (April 29) was also estimated in a different way. Starting from the probable (P/B) values and known dry weights the corresponding development rates d were calculated. The daily increase of the densities D as expected from development alone can be derived from the values of D and d. The real increase at April 29 can be measured from the density - time plots (Figs. 1 and 2). The difference is an estimate of mortality. The results of this calculation are given in Table 3.

Table 3

Estimation of mortality rate (d^{-1}) of *Calanus finmarchicus* copepodids during the peak of the diatom bloom in the FLEX box.

Stage	D	P/B	W	d	Daily increase		mortality rate
					Expected	Observed	
Nauplius VI	10157	.20	.8	.07			
Copepodid I	26260	.21	2.7	.19	- .16	.15	- .31
II	21900	.15	5.7	.06	.17	.23	- .06
III	6370	.17	20.1	.17	.04	.20	- .16
IV	2400	.18	40.2	.07	.38	.17	.21
V	1240	.14	145.2	.44	.30	.05	.25
VI	1400	.03	191.6	-	.39	.02	.37

Discussion and conclusions

Although in the period observed the densities increase very regularly, particularly in Krauses data, the regression plane does not fit quite well for most development stages. Apart from sources of variance such as spatial differences and migration, probably an unequal accuracy of the methods

used to measure the density of the different stages has played a role. However, the results indicate that the growth rates were of the same order of magnitude as those estimated by Fransz and van Arkel (1980). There is evidence, that the growth rate of the largest copepodid stages (with the largest share in biomass) was considerably lower and stage V hesitated to become adult. Possibly the low temperature (about $7^{o}C$) kept the animals in a hibernation state. Growth rates as given by Fransz and van Arkel must be compensated by a high mortality in the largest copepodids (Table 3) to explain the low daily increase in number. Probably the P/B ratios of the oldest stages and the *Calanus* production of 50 $mgC.m^{-2}.d^{-1}$ are overestimated.

Fransz and van Arkel (1980) estimated the production of *Calanus* during the diatom peak as 20 $mgC.m^{-2}.d^{-1}$. This is lower than the estimate presented here, because they determined a lower density of the first three copepodid stages and also a lower dry weight of stage V. The dry weights adopted by the FLEX working group yield in combination with a regular set of P/B ratios an unrealistically alternating set of corresponding development rates for the copepodid stages (see Table III). The dry weights of the different stages must be reconsidered.

Even if *Calanus* produced 50 $mgC.m^{-2}.d^{-1}$, the corresponding consumption of about 250 $mgC.m^{-2}.d^{-1}$ can not explain the phytoplankton decline following the chlorophyll peak, when the primary production was about 1700 $mg\,C.m^{-2}.d^{-1}$ (Gieskes and Kraay, 1980).

Appendix

Estimation of expectation values and variances of the coefficients in the regression model $Y = a X_1 - b X_2$ with n datapoints.

Let :

$$P = \Sigma X_1^2 \; \Sigma X_2^2 - (\Sigma X_1 X_2)^2 ,$$

then

$$\varepsilon a = \frac{\Sigma X_1 Y \; \Sigma X_2^2 - \Sigma X_2 Y \; \Sigma X_1 X_2}{P}$$

$$\varepsilon b = \frac{\varepsilon a \; \Sigma X_1^2 - \Sigma X_1 Y}{\Sigma X_1 X_2}$$

Let :

$$Q = \frac{\Sigma Y^2 - \varepsilon a \Sigma X_1 Y + \varepsilon b \Sigma X_2 Y}{P(n - 2)} ,$$

then :

$$\text{var (a)} = Q \Sigma X_2^2 \qquad \text{and} \qquad \text{var (b)} = Q \Sigma X_1^2 .$$

If Y and X are one and two column matrices with n rows, the sums in the above equations are found as elements of the matrices $Y'X$, $Y'Y$ and $X'X$.

References

DRAPER, N.R. and SMITH, H. (1967). *Applied regression analysis*, Wiley, New York, 407 pp.

FRANSZ, H.G. (1976). The spring development of calanoid populations in the Dutch coastal waters as related to primary production. *Proc. 10th E.M.B.S.*, Ostend, Belgium, Sept. 17-23, 2, 247-269.

FRANSZ, H.G. and van ARKEL, W.G. (1980). Zooplankton activity during and after the phytoplankton spring bloom at the Central Station in the FLEX box, northern North Sea, with special reference to the calanoid copepod *Calanus finmarchicus* (Gunn.), "Meteor" Forsch.-Ergebn. A, n° 22.

GIESKES, W.W.C. and KRAAY, G.W. (1980). Primary productivity and phytoplankton pigment measurements in the northern North Sea during FLEX '76, "Meteor" Forsch.-Ergebn. A, n° 22.

KRAUSE, M. (1980). On the vertical distribution of fecal pellets in relation to the standing stock of *Calanus finmarchicus* (this volume).

PARSLOW, J., SONNTAG, N.C. and MATTHEWS, J.B.L. (1979). Technique of systems identification applied to estimating copepod population parameters, *Journal of Plankton Research*, 1 (2), 137-151.

WILLIAMS, R. (1977). Vertical profiles of zooplankton, *Draft FLEX Atlas*, 7.1.3, 1-23.

FLEX 1976 nutrient intercalibration*

K. EBERLEIN**, R. JOHNSTON*** and K.O. HAMMER**

Introduction

Since the main objectives of the Fladen Ground Experiment (FLEX) 1976 were an investigation of the dynamics of the mixed layer and the development of the spring plankton bloom, the obtainment of comparable nutrient results from all participating ships was of particular importance. During the whole period of FLEX, nutrient measurements at a Central Station (58°55'N, 0°32'E) were carried out in regular time intervals (all 6 h) alternately and at times simultaneously on board the research vessels *Meteor* and *Anton Dohrn*. The cruises of the other participating ships, carrying out survey programs like grids, mini-grids and horizontal sections in the FLEX Box around the Central Station, had the main objectives to describe the horizontal variability and to indicate hydrodynamic influences on the development at the Central Station. In order to evaluate the comparability of nutrient data obtained on board different ships and to match values from one ship with those of others, intercalibration experiments were carried out during FLEX.

---

* This is JONSDAP '76 contribution n° 60.

** Institut für Organische Chemie und Biochemie, Universität Hamburg, F.R.G.

*** Marine Laboratory, Department of Agriculture and Fisheries for Scotland, Aberdeen, Scotland.

Methods

In general nutrients were measured on board the ships immediately after sampling according to the methods described in the New Baltic Manual (Carlberg, 1972). Measurements were carried out by means of autoanalyzer instruments, but orthophosphate was determined manually on board *Anton Dohrn*. On board this research vessel nitrate and silicate samples were fast frozen, they were analyzed later in the laboratory.

The general plan for inter-ship calibration experiments was that all ships present in the FLEX Box would meet simultaneously at the Central Station in around two week-intervals. Each of the samples taken for intercalibration at ten different depths by the central ship was supposed to be divided up among all participating ships within one hour.

In practice a sample exchange in the planned extent never could be realized. Very often bad weather conditions prevented the transfer of samples from one ship to the other. In this case parallel samples were taken at the same time and from the same depths by the participating ships. Because of organizational reasons at no time more than two ships met for carrying out an intercalibration experiment. In the later evaluation it was revealed that the results of some of the ships were unsatisfactory so that they were withdrawn by the originators.

Data of twelve intercalibration stations were obtained for final evaluation, seven ships participating, *Meteor* being involved on all occasions. For the comparison of measurements from different ships regression equations and standard errors about the regression were computed. Data of several intercalibration stations between two same ships were combined for one computation.

From intercalibration stations without sample exchange only those sample depths were referred to for the computations which did not lie in the region of a thermocline with higher nutrient variability. On April 2nd, 1976, when the first intercalibration station was carried out between *Meteor* and *Argos*, nutrient data showed no vertical variations at all, since the

phytoplankton had not yet started to grow. In this case only mean values and standard deviations were computed from the whole depth profiles.

In order to evaluate the comparability of nutrient results obtained at the Central Station from the research vessels *Meteor* and *Anton Dohrn* additionally the routine measurements of both ships were used for a comparison. Mean values and standard deviations were calculated for each leg from the sum of all values which were obtained for the depth range of 90 m to the bottom. After the concentration of particulate matter began to increase in the deep water on May 5th, 1976 (Eberlein et al., 1980) the onset of remineralization in this layer must be taken into account for the following part of the experiment. For that reason only those values were used for comparison which were obtained from samples taken before this date.

Results and discussion

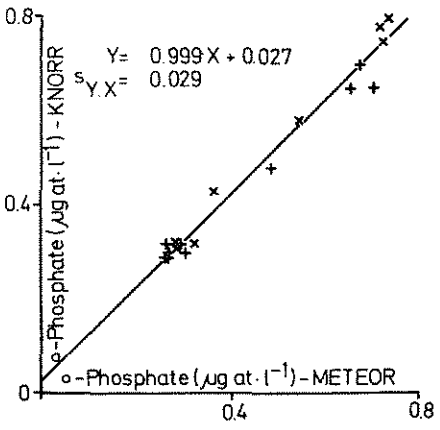

fig. 1.
Phosphate intercalibration between Meteor (x) and Knorr (Y) measurements on 16-5-1976. Meteor samples : + ; Knorr samples : x .

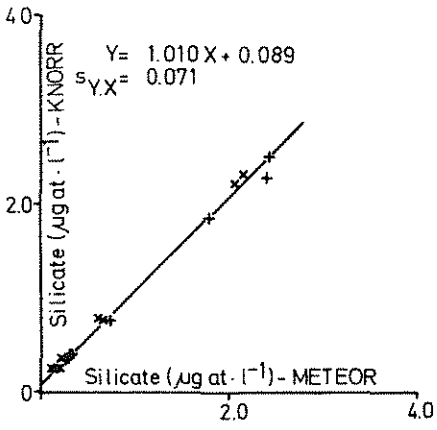

fig. 2.
Silicate intercalibration between Meteor (x) and Knorr (Y) measurements on 16-5-1976. Meteor samples : + ; Knorr samples : x .

All nutrient intercalibration data are given in the Appendix of this representation. Figs. 1 - 6 show the results of the regression analyses.

In figs. 1 and 2 nutrient data from *R.V. Knorr* are plotted against those from *R.V. Meteor*. The comparison is based on two sets of data obtained from two intercalibration stations, carried out on the same day (May 16th, 1976). Linear regressions were obtained, the standard errors about the regressions - $S_{Y,X}$ - are within acceptable limits of precision. The gradients of the regression curves are very near to 1, small but significant systematic differences of 0.03 µmol phosphate·ℓ^{-1} and of 0.09 µmol silicate·ℓ^{-1} were found.

Fig. 3 shows the regression analysis between nitrate measurements from *R.V. Meteor* and *R.V. Explorer*, based on two different intercalibration stations, which were carried out on May 23rd and June 3rd, 1976. A linear regression was found with a small standard error about the regression and a small systematic error of -0.13 µmol nitrate·ℓ^{-1}.

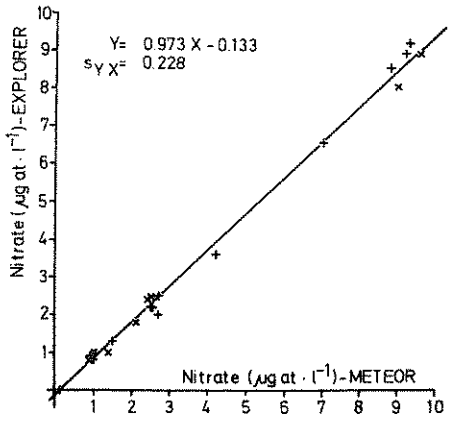

fig. 3.

Nitrate intercalibration between Meteor (X) and Explorer (Y) measurements on 23-5 and 3-6-1976. (Meteor samples : + ; Explorer samples : x).

Figs. 4 - 6 show the regression analyses between *Meteor* and *Anton Dohrn* data. For all three parameters the majority of values lies very near the regression lines although the analysis is based on three intercalibration stations, carried out at different points of time (April 12th, April 27th and May 5th, 1976).

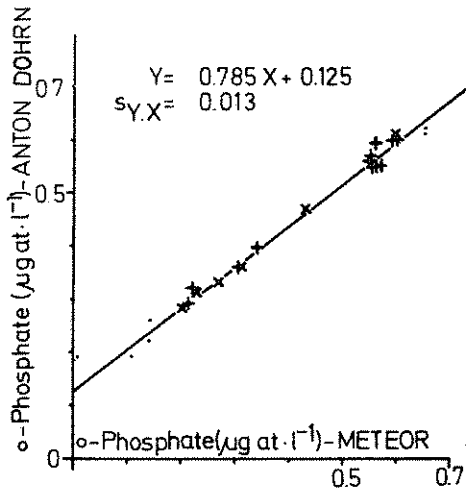

fig. 4.

Phosphate intercalibration between Meteor (X) and Anton Dohrn (Y) measurements on 12-4, 27-4 and 4-5-1976 (Meteor samples : + ; Anton Dohrn samples : x ; parallel measurements without exchange of samples : .)

All phosphate values (fig. 4) lie very near the computed linear regression line, the standard error about the regression is very low, but the gradient (m = + 0.79) strongly differs from 1. This means that only the relative high values between both measurements are in good accordance. The differences become greater the smaller the measured values are. This might be due to the different methods used on board of *Anton Dohrn* and *Meteor;* measurements were carried out manually and by means of an autoanalyzer, respectively.

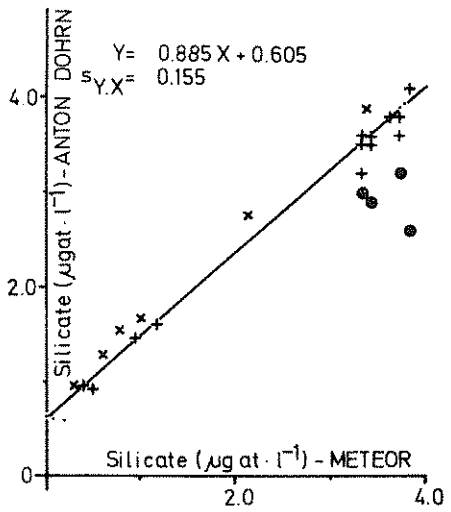

fig. 5.

Silicate intercalibration between Meteor (X) and Anton Dohrn (Y) measurements on 12-4, 27-4 and 4-5-1976 (Meteor samples : + ; Anton Dohrn samples : x ; parallel measurements without exchange of samples : .)

In figs. 5 and 6 not all values lie near the linear regression lines. There are some *Anton Dohrn* measurements from *Meteor* samples (not from *Anton Dohrn* samples) which give much too low values. These are marked by encircling, they were not used for computations of regressions. These much too low values may be explained by the fact that *Anton Dohrn* measurements of nitrate and silicate - unlike the phosphate measurements - were not carried out on board the ship, but later in the laboratory from deep frozen samples. Support for this hypothesis is given by fig. 7, showing measurements on board *Meteor* plotted against laboratory measurements of frozen samples, which were carried out by *Meteor* scientists some months after sampling. The samples for both measurements were identical. After analysis on board *Meteor*, the remaining part of the sample was frozen for laboratory analysis. Most laboratory results were close to the measurements on board, but some were much lower.

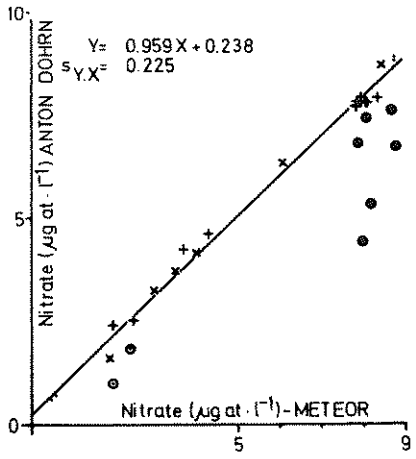

fig. 6.

Nitrate intercalibration between Meteor (X) and Anton Dohrn (Y) measurements. Explanation of symbols : see fig. 4.

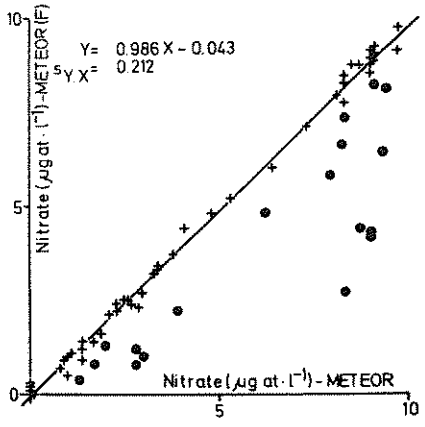

fig. 7.

Comparison of Meteor nitrate measurements between on board (X) and laboratory (Y) analyses from frozen (F) samples.

The lower values may be explained by the fact that *Meteor* samples on board *Anton Dohrn* (for later analyses) as well as on board *Meteor* (for additional analyses) were frozen after a delay of about two hours caused by sample transfer and by autoanalyzer analysis, respectively. On the contrary, *Anton Dohrn* samples for later analyses were routinely fast frozen within a few minutes. Since the low *Anton Dohrn* values of nitrate and silicate measurements were not from *Anton Dohrn* samples, omission of those (figs. 5 and 6) seems admissible.

An important result of the freezing experiments is that for exact nitrate and silicate measurements samples can be fast frozen and stored for some months. But the freezing has to be done within a few minutes after sampling. This result is also proved by the comparison of *Meteor* and *Anton Dohrn* measurements in fig. 8.

Without regard to the omitted values in fig. 6 the regression analysis of nitrate measurements from *Meteor* and *Anton Dohrn* shows that the gradient of the linear regression line is

very near to 1 and that a systematic error of + 0.24 µ mol nitrate·ℓ^{-1} is recognizable. The gradient of the linear regression line computed for silicate (fig. 5) differs from 1, the intercept on the y-axis (+0.61) is relatively high. But it should be emphasized that the standard error about the regression is low for all *Meteor* - *Anton Dohrn* comparisons: ± 0.23 µ mol nitrate·ℓ^{-1}, ± 0.16 µ mol silicate·ℓ^{-1} and ± 0.01 µ mol phosphate·ℓ^{-1}. This means that data conversion with help of regression equations permits the fitting of values from *Anton Dohrn* to those of *Meteor* and vice versa.

These results throw no light on the reasons for the systematic errors which in most cases are small but significant. There is also no basis for determining absolute values and absolute errors. On board *Meteor* measurements were checked by comparison with internationally recommended CSK standards (Sugawara, 1969), available from Sagami Chemical Research Center (Sagamihara, Japan). But these calibrations encountered problems because of the different media of samples, standards and baseline references; e.g. CSK phosphate standards could not be measured exactly by means of an autoanalyzer against synthetic seawater according to Strickland and Parsons (1968).

Had it been possible for all the ships to meet and exchange samples at the one time, more exact intercalibrations would have been achieved. On the other hand such a condition is not mandatory for the practical evaluation of the FLEX data. The essential result of the intercalibration experiments is that sufficient and reliable data were obtained from the research vessels *Anton Dohrn*, *Explorer*, *Knorr*, and *Meteor* and that subsequent corrections with help of regression equations permit the elimination of systematic errors and the fitting of values from one ship to those of others, since the standard errors about the regressions are small for all calculated regressions.

Reliable nutrient data were also obtained for the intercalibration station *Argos* - *Meteor* (table 1), but no regression analysis could be carried out because vertical variation was absent. The standard deviations in table 1 are small. Between

Table 1

Argos-Meteor intercalibration station : mean values and standard deviations computed from depth profiles (μ mol.ℓ^{-1})

	nitrate + nitrite	o-phosphate	silicate
Argos	8.29 $\pm$ 0.05	0.62 $\pm$ 0.05	3.45 $\pm$ 0.15
Meteor	8.83 $\pm$ 0.08	0.62 $\pm$ 0.003	3.60 $\pm$ 0.24

Argos and *Meteor* measurements systematic differences of 0.54 μ mol nitrate$\cdot\ell^{-1}$ and of 0.15 μ mol silicate$\cdot\ell^{-1}$ were found. No difference was found for the ortho-phosphate measurements, but *Argos* values show more scattering.

From the research vessels *F. Heincke* and *J. Murray* not sufficient intercalibration data were obtained to carry out any regression analyses.

Fig. 8 gives a survey of all nutrient data measured at the Central Station in the depth range of 90 m to bottom and in the time period of March 25th - May 4th, 1976. During this part of the experiment there was no obvious temporal trend in the deeper water. No important differences between *Meteor* and *Anton Dohrn* measurements could be detected, this is also shown by comparison of the computed mean values and standard deviations in table 2. Hence it does not appear necessary to include correction terms when comparing nutrient results of the two ships in the deep water concentration range. Also for the period of April 27th - May 5th no essential differences between *Meteor* and *Anton Dohrn* data could be detected although *Anton Dohrn* samples were not taken at the Central Station but at various stations within the FLEX Box.

In spite of the good accordance between *Meteor* and *Anton Dohrn* measurements small but significant short term fluctuations could be found in the results of both vessels (fig. 8). They were especially high during the first *Meteor* leg (March 25th - April 12th, 1976) and were possibly caused by hydrodynamic

Table 2

Comparison of the Central Station nutrient data at depths between 90 m and the bottom. Mean values ± standard deviations in µmoles.ℓ^{-1} (N = number of samples) obtained from *Meteor* and *Anton Dohrn* measurements.

Nutrient	Name of ship	March 25th - April 7th	April 8th-12th	April 13-23rd	April 24th - May 4th
Nitrate + nitrite	*Meteor*	8.63 ± 0.26 (N=106)	8.36 ± 0.27 (N=55)	-	8.66 ± 0.19 (N=79)
	Anton Dohrn	-	8.38 ± 0.64 (N=21)	8.68 ± 0.29 (N=93)	8.60 ± 0.32 (N=93)
Silicate	*Meteor*	3.69 ± 0.24 (N=111)	3.77 ± 0.16 (N=55)	-	3.66 ± 0.15 (N=77)
	Anton Dohrn	-	3.49 ± 0.18 (N=23)	3.81 ± 0.15 (N=89)	3.82 ± 0.27 (N=92)
o-phospate	*Meteor*	0.60 ± 0.02 (N=102)	0.60 ± 0.02 (N=45)	-	0.63 ± 0.02 (N=68)
	Anton Dohrn	-	0.59 ± 0.02 (N=33)	0.59 ± 0.01 (N=99)	0.60 ± 0.01 (N=93)

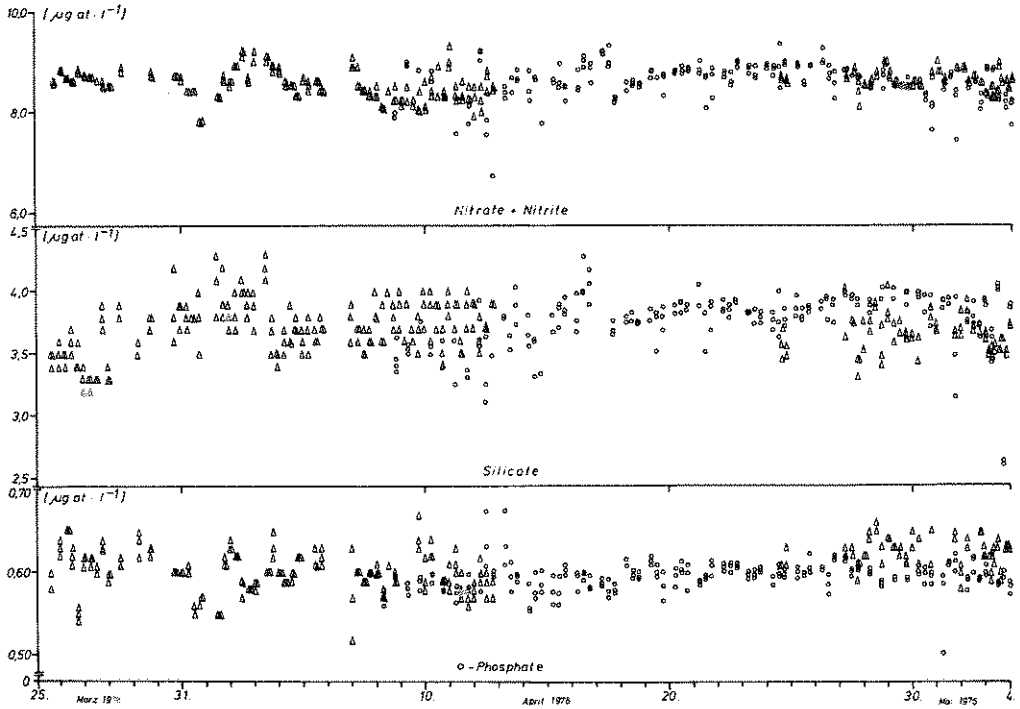

fig. 8.

Comparison of nutrient measurements at the Central FLEX Station
in the depth range of 90 m to the bottom.
(△ : Meteor; o : Anton Dohrn measurements).

disturbances, since during this period the weather conditions were worse than during the later part of FLEX.

During the period April 27th - May 4th, 1976, *Anton Dohrn* samples were not taken at the Central Station but in different distances to it. In spite of this *Anton Dohrn* phosphate samples show a small standard deviation, indicating that hydrodynamic disturbances during this period are small in deeper layers of the FLEX Box.

Conclusions

Reliable nutrient data were obtained from measurements on board the research vessels *Argos, Anton Dohrn, Explorer, Knorr* and *Meteor*. These data only show relatively small differences caused by systematic differences; it is not possible to assess the absolute values and errors of these data sets. The fitting of regression equations permits the merging of data from different ships.

A comparison of standard deviations and standard errors about the regressions with those of the ICES intercalibration exercise (Koroleff et al., 1977) and of the Baltic Intercalibration Workshop 1977 in Kiel (Grasshoff, 1977) shows that the FLEX results must be regarded as satisfactory perhaps laudable in the circumstances. Many analyses had to be performed on water samples from the upper layers having very low nutrient concentrations. Also the analyses were carried out on board different research vessels lacking the stability and convenience of a large shore laboratory.

For further ventures like FLEX these studies emphasize the necessity for planned intercalibration exercises including, if at all possible, one session when all the ships exchange samples from one area simultaneously. Should bad weather be encountered it may be possible to arrange sample exchanges or if need be an intercalibration exercise in less exposed waters.

Appendix – FLEX 1976 nutrient intercalibration data

1. Intercalibration experiments with exchange of samples

1.1. METEOR - ANTON DOHRN

12.4.76,12.30GMT	nitrate + nitrite		o-phosphate		silicate	
Analysis by	METEOR	A.DOHRN	METEOR	A.DOHRN	METEOR	A.DOHRN
Samples	M1f	M2fF	M1f	M2f	M1f	M2fF
Depth (m)						
4	7.9	6.8	0.56	0.55	3.4	2.9
10	7.9	7.7	0.55	0.55	3.4	3.5
20	8.0	7.7	0.57	0.55	3.3	3.6
30	7.9	7.8	0.55	0.56	3.3	3.5
40	8.0	7.9	0.56	0.55	3.4	3.6
50	8.0	4.4	0.56	0.55	3.3	3.0
60	8.1	7.8	0.55	0.55	3.6	3.8
70	8.1	7.8	0.55	0.57	3.8	4.1
80	8.2	5.3	0.56	0.59	3.8	2.6
90	8.4	7.9	0.57	–	3.7	3.8
100	8.7	7.6	0.59	0.60	3.7	3.6
143	8.8	6.7	0.60	0.60	3.7	3.2

27.4.76,18.30GMT												
Analysis by	METEOR		A.DOHRN		METEOR		A.DOHRN		METEOR		A.DOHRN	
Samples	M1u	AD2u	M2uF	AD1uF	M1u	AD2u	M2u	AD1u	M1u	AD2u	M2uF	AD1uF
10	2.0	1.9	2.4	1.6	0.21	0.20	0.29	0.28	0.39	0.31	0.95	0.85
20	2.5	3.0	2.5	3.2	0.22	0.23	0.32	0.31	0.50	0.59	0.92	1.27
30	–	3.5	–	3.7	–	0.27	–	0.33	–	0.77	–	1.53
40	3.7	4.0	4.2	4.1	0.31	0.31	0.36	0.36	0.96	1.00	1.45	1.67
50	4.3	6.1	4.6	6.3	0.34	0.43	0.40	0.47	1.18	2.12	1.60	2.75
100	8.1	8.5	7.4	8.7	0.59	0.60	0.60	0.61	3.31	3.34	3.20	3.88

1.2. METEOR - EXPLORER

23.5.76,6.00GMT	nitrate + nitrite			
Analysis by	METEOR		EXPLORER	
Samples	M1f	E2u	M2f	E1u
Depth (m)				
3	0.9	0.9	0.9	0.8
10	0.9	1.0	0.8	1.0
20	1.0	1.4	0.8	1.0
30	1.5	2.1	1.3	1.8
40	2.6	2.5	2.2	2.5
50	2.5	2.4	2.2	2.4
60	2.7	–	2.5	–
80	8.8	9.0	8.6	8.1
100	9.3	9.6	9.3	9.0

3.6.76,7.00GMT				
	M1f	E2u	M2f	E1u
3	0	0	0	0
10	0	0	0	0
20	0	0	0	0.6
30	0.1	1.0	0	2.0
40	2.7	3.1	2.0	3.6
50	4.2	2.9	3.6	3.9
60	7.0	4.9	6.6	6.0
80	9.2	9.2	9.0	9.3
100	9.3	9.4	9.3	9.4

Sample code

A, M etc. – Name of ship doing the sampling
1, 2 – Duplicate sets of samples, where taken
u – unfiltered samples
f – Whatman GF/C filtered
F – Deep frozen samples analysed at a later date

1.3. METEOR - KNORR

16.5.76,5.30GMT Analysis by Samples	o-phosphate METEOR K2	o-phosphate KNORR K1	silicate METEOR K4	silicate KNORR K3
Depth (m)				
3	0.28	0.31	0.20	0.24
10	0.32	0.32	0.19	0.25
20	0.28	0.32	0.16	0.25
30	0.32	0.32	0.12	0.26
40	0.36	0.43	0.22	0.38
50	0.54	0.58	0.66	0.77
60	0.54	0.58	0.61	0.81
80	0.73	0.80	2.03	2.23
100	0.72	0.75	2.12	2.33
135	0.71	0.78	2.13	2.33
16.5.76,8.00GMT	M1u	M2u	M1u	M2u
3	0.26	0.29	0.32	0.39
10	0.27	0.29	0.32	0.39
20	0.26	0.32	0.31	0.39
30	0.30	0.30	0.30	0.36
40	0.27	0.30	0.29	0.36
50	0.29	0.32	0.28	0.36
60	0.48	0.48	0.73	0.77
80	0.65	0.65	1.78	1.86
100	0.70	0.65	2.38	2.28
135	0.67	0.70	2.39	2.49

1.4. METEOR - JOHN MURRAY

12.4.76,12.00GMT Analysis by Samples	nitrate + nitrite METEOR JM2u	nitrate + nitrite J.MURRARY JM1u	o-phosphate METEOR JM2u	o-phosphate J.MURRAY JM1u	silicate METEOR JM2u	silicate J.MURRAY JM1u
Depth (m)						
4	7.9	8.8	0.63	1.47	3.3	5.2
10	7.9	8.6	0.58	1.50	3.3	5.4
30	7.9	9.0	0.57	1.45	3.3	5.2

2. Intercalibration experiments without exchange of samples

2.1. METEOR - ANTON DOHRN

3.5.76,24.00GMT Analysis by Samples	nitrate + nitrite METEOR M1f	nitrate + nitrite A.DOHRN AD1uF	o-phosphate METEOR M1f	o-phosphate A.DOHRN AD1u	silicate METEOR M1f	silicate A.DOHRN AD1uF
Depth (m)						
3	0.7	0.1	0.03	0.15	0	0.93
10	1.5	0.2	0.08	0.14	0.05	0.91
20	1.8	0.5	0.10	0.22	-	1.33
30	1.7	0.9	0.11	0.24	0.10	1.58
40	1.7	4.0	0.15	0.40	0.10	2.46
50	3.8	6.5	0.29	0.55	0.83	3.51
60	7.0	7.3	0.49	0.56	2.13	3.76
70	8.5	7.2	0.60	0.56	3.15	3.79
80	8.6	7.3	0.62	0.57	3.51	3.82
100	8.7	8.2	0.63	0.59	3.71	3.88

4.5.76,6.30GMT	nitrate + nitrite		o-phosphate		silicate	
Analysis by	METEOR	A.DOHRN	METEOR	A.DOHRN	METEOR	A.DOHRN
Samples	M1f	AD1uF	M1f	AD1u	M1f	AD1uF
Depth (m)						
3	0.6	0.7	0.08	0.19	0.08	0.59
10	0.5	0.6	0.11	0.19	0.01	0.62
20	2.0	1.0	0.14	0.22	0.09	0.59
30	2.4	1.8	0.14	0.26	0.20	0.57
40	2.4	2.0	0.12	0.28	0.20	0.62
50	5.2	4.1	0.31	0.39	1.35	1.16
60	8.1	6.1	0.58	0.51	2.91	2.01
70	8.8	8.5	0.65	0.60	3.64	3.45
80	8.8	8.8	0.63	0.61	3.69	3.91
100	8.8	8.9	0.63	0.62	3.75	3.96

2.2. METEOR - ARGOS

2.4.76,6.00GMT	nitrate + nitrite		o-phosphate		silicate	
Analysis by	METEOR	ARGOS	METEOR	ARGOS	METEOR	ARGOS
Samples	M1F	A1u	M1f	A1u	M1f	A1u
Depth (m)						
10	8.8	8.2	0.62	0.60	3.4	3.5
20	8.7	8.2	0.62	0.62	3.4	3.5
30	8.7	8.3	0.62	0.57	3.3	3.5
40	8.9	8.3	0.62	0.61	3.3	3.5
50	8.9	8.3	0.62	0.59	3.4	3.5
60	8.8	8.3	0.62	0.63	3.8	3.5
70	8.8	8.3	0.62	0.62	3.7	3.5
80	8.8	8.3	0.63	0.76	3.8	3.5
90	8.9	8.3	0.62	0.61	4.0	3.0
100	8.9	8.3	0.62	0.61	3.7	3.5
140	8.9	8.4	0.62	0.63	3.8	3.5

	ammonia	
	M1f	A1u
10	0	0.2
20	0.1	0.1
30	0.2	0.1
40	0.1	0.2
50	0	0.1
60	0.4	0.1
70	0.5	0.1
80	0.4	0.1
90	0.4	0
100	0.5	0.1
140	0.4	0.2

2.3. METEOR - EXPLORER

16.5.76,12.00GMT	nitrate + nitrite	
Analysis by	METEOR	EXPLORER
Samples	M1u	E1u
Depth (m)		
3	1.2	2.1
10	1.2	1.9
20	1.2	1.8
30	1.2	2.3
40	1.2	2.3
50	1.2	2.3
60	1.2	5.7
80	5.8	8.2
100	9.1	8.3
130	-	8.3
142	9.1	-

2.4 METEOR - FRIEDRICH HEINCKE

15.5.76,0.30GMT Analysis by Samples	ammonia METEOR M1f	ammonia HEINCKE FH1u	o-phosphate METEOR M1f	o-phosphate HEINCKE FH1u
Depth (m)				
30	1.50	0.83	0.27	0.22
40	1.41	1.51	0.28	0.33
50	1.38	1.59	0.29	0.26
60	1.41	1.49	0.50	0.28
70	1.78	1.71	0.59	0.49

Acknowledgements

Thanks are due to all who to all who contributed FLEX nutrient intercalibration data, in particular to E.J. Hamilton, G. Kattner, P. Mangelsdorf, D.W. Spencer, A. Svansson and G. Weichart.

This work was supported by the Deutsche Forschungsgemeinschaft through the Sonderforschungsbereich 94 — Meeresforschung — Hamburg.

References

CARLBERG, S.R. (1972). New Baltic Manual. ICES Coop. Res. Report A 29, 145 pp.

EBERLEIN, K., KATTNER, G., BROCKMANN, U. and HAMMER, K.D. (1980). Nitrogen and phosphorus in different water layers at the central station during FLEX '76. "Meteor" Forsch. Ergebn. A, 22, 87-98.

GRASSHOFF, K. (1977). *Report of the Baltic Intercalibration Workshop Kiel*, 7.-19. March 1977, 156 pp.

KOROLEFF, F., PALMORK, K.H., ULLTANG, O. and GIESKES, J.M. (1977). The International Intercalibration Exercise for Nutrient Methods, ICES Working Group on Chemical Analysis of Sea Water. ICES Coop. Res. Report 67

STRICKLAND, J.D.H. and PARSONS, T.R. (1968). A practical Handbook of Seawater Analysis, *Fish. Res. Bd. Can. Bull.*, 167.

SUGAWARA, K. (1969). On the preparation of CSK standards for marine nutrient analysis. Scientific Committee on Oceanic Research, ICSU, IOC, UNESCO, Chemistry Working Group, Sub-Committee for CSK, National Committee on Oceanic Research, Science Council of Japan, 56 pp.

The estimation of the photosynthetic activity of chlorophyll in phytoplankton*

J. AIKEN**

Abstract

It is suggested that the fluorescence measurements of chlorophyll *in vivo* detect only that fraction of the pigment not active in the photosynthetic raction. Active chlorophyll *a* can be computed by subtraction of the inactive concentration from the total value, measured by a fluorescence measurement at night or by solvent extraction of a filtered sea water sample. Active chlorophyll *a* should be the parameter used in primary production modelling. Computed production should be a function only of active chlorophyll *a* and incident radiant energy, and should be absolutely related to the quantum yield of photosynthesis in an invariant relationship.

Introduction

Chlorophyll *a*, the major photosynthetic pigment in the marine environment, and incident solar radiant energy, are the fundamental parameters of all models of primary production in the pelagic ecosystem. (For review see Platt *et al.*, 1977.) Measurements of the amount of chlorophyll *a* do not necessarily provide a sound basis for estimating photosynthetic production since, even in conditions of ample nutrients, the available chlorophyll may not be fully utilised because of the wide range of incident radiant energy due to the variability of cloud cover and sea-state. It is important, therefore, to investigate the photosynthetic activity of chlorophyll under these variable conditions and determine the concentration of active chlorophyll *a* at any time.

---

* This is JONSDAP '76 contribution n° 57.

** Institute for Marine Environmental Research, Plymouth, England.

Interpretation of *in vivo* fluorescence measurements of chlorophyll *a*

The measurement of chlorophyll *in vivo* in the marine environment, by fluorescence (Lorenzen, 1966) has been regarded as a standard technique for many years. Calibration of fluorometers must be repeated frequently for different phytoplankton assemblages and different physiological states of the phytoplankton (Strickland, 1968; Kiefer, 1973).

Slovacek and Hannan (1977) found that, in the presence of the herbicide DCMU [3 - (3,4 - Dichlorophenyl) - 1,1 - dimethylurea], electron transport photosynthesis is inhibited and "the *in vivo* fluorescence yield becomes maximal and a constant function of cellular chlorophyll *a*, regardless of growth conditions and of the species examined". By inference, therefore, natural chlorophyll *a* fluoresces only if it is in its ground state condition, and not engaged in photosynthesis; photosynthesis and fluorescence-emission are separate and competing photo-reactions, and any chlorophyll molecules active in photosynthesis will not be available for fluorescence excitation. Thus, fluorescence measurements, *in vivo*, provide a measurement of total chlorophyll at night only, when photosynthesis is not occuring. An estimation of the concentration of chlorophyll *a* active in photosynthesis C_a can be obtained by subtraction of the daylight *in vivo* fluorescence measurement C_{fl} from an estimate of total chlorophyll *a*, obtained by solvent extraction or from nocturnal fluorescence C_{tot} , as expressed in equation (1) :

$$C_a = C_{tot} - C_{fl} \qquad (1)$$

Any errors arising in the fluorescence measurements due to the presence of other chlorophylls or phaeophytins fluorescing in the same wavelengths, will be minimised, though not completely eliminated, in this subtraction.

Absolute calibration of the fluorometer can be performed in two ways : firstly, by injecting cultures of natural samples with DCMU in laboratory calibrations, so that all the chlorophyll present fluoresces, for accurate comparison with the measurements by extraction (Richards with Thompson, 1952; Strickland and Parsons, 1972); secondly, by using only night-time measurements in the field when no photosynthesis is occurring, to establish the calibration between the fluorometer and the extracted samples; with this latter technique, back calibration of previously obtained field data can be used to evaluate the concentration of chlorophyll engaged in photosynthesis.

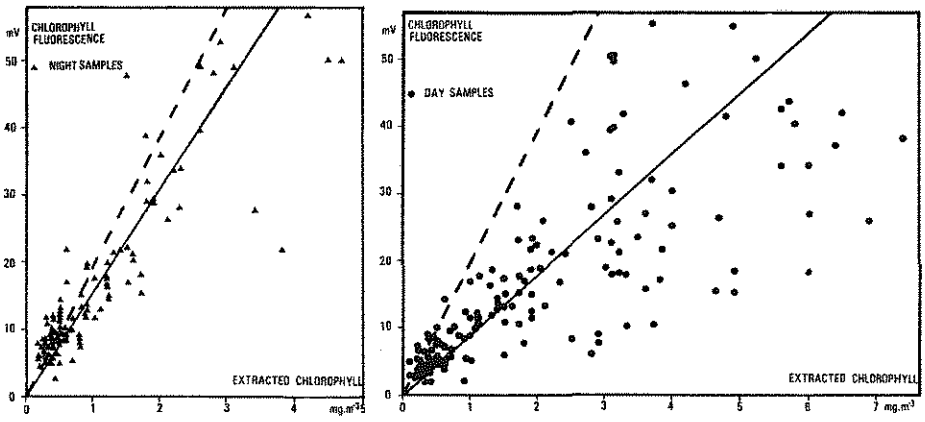

fig. 1.

Chlorophyll sensor fluorescence yield *in vivo*, plotted against chlorophyll concentration ($mg.m^{-3}$), for 274 pairs of samples : left 109 night stations (slope = 15.51, r = 0.89); right 165 day stations (slope = 9.14, r = 0.81). The broken lines correspond to laboratory measurements of unialgal cultures injected with DCMU.

Fig. 1 shows the fluorescence yield *in vivo*, as measured by a sensor developed in this laboratory, plotted against extracted chlorophyll concentration for 274 pairs of samples obtained in a cruise in the Bristol Channel and Celtic Sea in May 1977, covering a wide range of phytoplankton assemblages and physiological conditions; on the right, 165 day stations (slope = 9.14; r = 0.81) and on the left, 109 night stations (slope = 15.51; r = 0.89). The *in vivo* fluorescence yield per unit chlorophyll concentration was greater at night and the data are less scattered and better correlated. These results support the suggestions of Slovacek and Hannan (1977) as interpreted in this paper, that only those chlorophyll molecules not active in photosynthesis are available for fluorescence; the proportion of inactive chlorophyll (fluorescing) is variable by day and generally constant by night. The broken line in fig. 1 are approximate back-calibration curves for the fluorescence sensor from laboratory measurements of samples of unialgal cultures injected with the herbicide DCMU ; the comparison was obtained by cross-reference of the measurements of standard fluorescing samples recorded on each occasion. The calibration by this method gives a relationship not unlike that obtained from night samples only.

Primary Production Modelling

In conditions of nutrient and trace element luxury, solar radiant energy I is the forcing function of any simple model of primary production, and chlorophyll *a* concentration $Chla$ is a major state variable as expressed in equation (2) :

$$P = \phi_m . I . Chla \qquad (2)$$

where ϕ_m is the quantum yield of photosynthesis in weak light (Bannister, 1974). This most basic of all models is rarely successful; photosynthesis per unit chlorophyll biomass P^B [in units of $mg\,C.(mg\,Chla)^{-}.h^{-}$] reaches saturation, P_m^B, at relatively low levels of radiant energy and photoinhibition occurs. The models of Steele (1962), Vollenweider (1965) and Fee (1969) all compute P_m^B, which represents the largest fraction of production in the water column. These models are applicable only to specific locations and all break down after running for only part of the duration of the spring bloom.

Platt and Jassby (1976) examined the proposition of Bannister (1974) using data from a series of 188 experiments, spread over three years, on natural assemblages of phytoplankton in Nova Scotian waters. They found that α (the slope of the P^B to I curve, which is directly related to ϕ_m) showed a five-fold variation throughout the year, the highest values (approaching the theoretical maximum) occurring in the summer and early autumn with a secondary peak sometimes in January and February.

The breakdown of simple production models (and for the variation of α as measured by Platt and Jassby) has been explained as a species variation of the ability of different cells to capture light. All the methods use solvent extraction of a sea water sample, but chlorophyll *a* may be in surplus for substantial parts of the day at certain seasons of the year; the computed values of P^B, α and ϕ_m may therefore be an overestimate.

Since the concentration of active chlorophyll *a*, derived by the methods described above should be a direct measure of that quantity of chlorophyll *a* participating in the photosynthetic reaction, the value should be an exact parameter for the computation of primary production, regardless of growth conditions or phytoplankton species composition, even when photoinhibition occurs, a smaller fraction of the total chlorophyll concentration is active.

References

BANNISTER, T.T. (1974). Production equations in terms of chlorophyll concentration, quantum yield, and upper limit to production, *Limnol. Oceanogr.*, 19, 1-12.

FEE, E.J. (1969). A numerical model for the estimation of photosynthetic production, integrated over time and depth in natural waters, *Limnol. Oceanogr.*, 14, 906-911.

KIEFER, D.A. (1973). Fluorescence properties of natural phytoplankton populations, *Mar. Biol.*, 22, 263-269.

LORENZEN, C.J. (1966). A method for the continuous measurement of *in vivo* chlorophyll concentration, *Deep-Sea Res.*, 13, 223-227.

PLATT, T. and JASSBY, A.D. (1976). The relationship between photosynthesis and light for natural assemblages of coastal marine phytoplankton, *J. Phycol.*, 12, 421-430.

PLATT, T., DENMAN, K.L. and JASSBY, A.D. (1977). Modelling the productivity of phytoplankton, in *The Sea : Ideas and Observations on Progress in the Study of the Seas*, vol. VI, E.D. Goldberg (Editor), John Wiley, New York, pp. 807-856.

RICHARDS, F.A., with THOMPSON, T.G. (1952). The estimation and characterization of plankton populations by pigment analyses, II : A spectrophotometric method for the estimation of plankton pigments, *J. Mar. Res.*, 11, 156-172.

SLOVACEK, R.E. and HANNAN, P.J. (1977). *In vivo* fluorescence determinations of phytoplankton chlorophyll *a*, *Limnol. Oceanogr.*, 22, 919-925.

STEELE, J.H. (1962). Environmental control of photosynthesis in the sea, *Limnol. Oceanogr.*, 7, 137-150.

STRICKLAND, J.D.H. (1968). Continuous measurement of *in vivo* chlorophyll; a precautionary note, *Deep-Sea Res.*, 15, 225-227.

STRICKLAND, J.D.H. and PARSONS, T.R. (1972). A practical handbook of seawater analysis, 2nd ed., *Bull. Fish. Res. Bd. Can.*, 167, 1-311.

VOLLENWEIDER, R.A. (1965). Calculation models of photosynthesis-depth curves and some implications regarding day rate estimates in primary production measurement, in *Primary Productivity in Aquatic Environments*, C.R. Goldman (Editor), University of California Press, Berkeley, pp. 425-457.

Variation in the composition of phytoplankton populations during FLEX '76*

Karin WANDSCHNEIDER**

Abstract

Fixed samples from the Fladen Ground Experiment (FLEX '76) were analysed by counting and identifying the phytoplankton as far as possible. Though cell volume of the Dinophyceae and the flagellates were relatively high, a detailed investigation of succession had to be restricted to diatoms. The results expressed as cell volume reveal a dominance of *Corethron hystrix*, *Coscinodiscus* spec., *Porosira glacialis* and *Thalassiosira* spec. during the first cruise of *F.S. Meteor*. These species decreased during the second cruise while *Nitzschia delicatissima* (group) and *Skeletonema costatum* were abundant during all cruises, but reached a maximum during the second one. The dominant genus during the second cruise of the *F.S. Meteor* was *Chaetoceros* followed by a bloom of small species of *Minidiscus* and *Thalassiosira*. Some factors of the pelagic ecosystem possibly influencing the change in composition of species are discussed.

Introduction

A special feature of the pelagic ecosystem is the continuously changing species composition of phytoplankton in the course of the year. Coming to a better understanding of the dynamics and laws of succession will lead to a qualitative and quantitative analysis of phytoplankton (Smetacek, 1975).

Therefore the enumeration and taxonomic identification of samples from the Fladen Ground was directed towards gaining further knowledge on the importance of ecological factors influencing the composition of phytoplankton populations.

---

* This is JONSDAP '76 contribution nº 69.

** Institut für Allgemeine Botanik der Universität Hamburg, Hamburg, Germany (F.R.G.).

Methods

Samples were taken from two different depths once a day. Results were calculated as the mean value of these two samples. During the first cruise of *F.S. Meteor* (26-3 to 12-4-76) the sampling stations were between the positions 58°54' N 0°31' E and 58°57' N 0°34' E. During the second and the third cruise (27-4 to 16-5-76 and 22-5 to 3-6-76) sampling took place on the Central FLEX Station at the position 58°55' N 0°32' E. Further details of sampling and phytoplankton analysis have been published in Wandschneider (1980).

Photographs of living cells were obtained with a *Zeiss* Photomicroscope, the methods used for preparation of specimens observed in a Scanning Electron Microscope (*Leitz*) were given by Hasle and Fryxell (1970).

Calculating cell volume is done in part from the values of Smetacek (1975).

Results and discussion

In general a diatom community was followed by a population of flagellates (fig. 1), but a detailed investigation of species succession had to be restricted to diatoms because of the following reasons. Most of the small flagellates including the Chrysophyceae, Cryptophyceae and Haptophyceae are lacking morphological features facilitating identification by light microscopy. Although the total cell volume of the Dinophyceae was quite high (fig. 1) on account of the largeness of the cells, the total number of Dinophyceae cells was too small to contribute a significant variation in the composition of species (*cf.* Wandschneider, 1980). The fluctuation of cell volume results mainly from an unequal distribution of large particles with low number as well as from migration and zooplankton grazing. In the beginning of the phytoplankton bloom a great variety of phytoplankton species were found. The presence of bottom-living forms in the samples like *Bacillaria paxilifer, Licmophora* spec., *Paralia sulcata, Raphoneis surinella* and *Triceratium reticulatum*

Plate 1

Lightmicrographs of living cells, ca. 500 × : isolated cultures from FLEX '76.
1.- *Chaetoceros pelagicus*, heavy grazing of bacteria on one half of the chain.
2.- *Chaetoceros pelagicus*, intact chain.
3.- *Chaetoceros diadema.*
4.- *Chaetoceros furcellatus.*
5.- *Porosira glacialis.*
6.- *Nitzschia delicatissima* group.

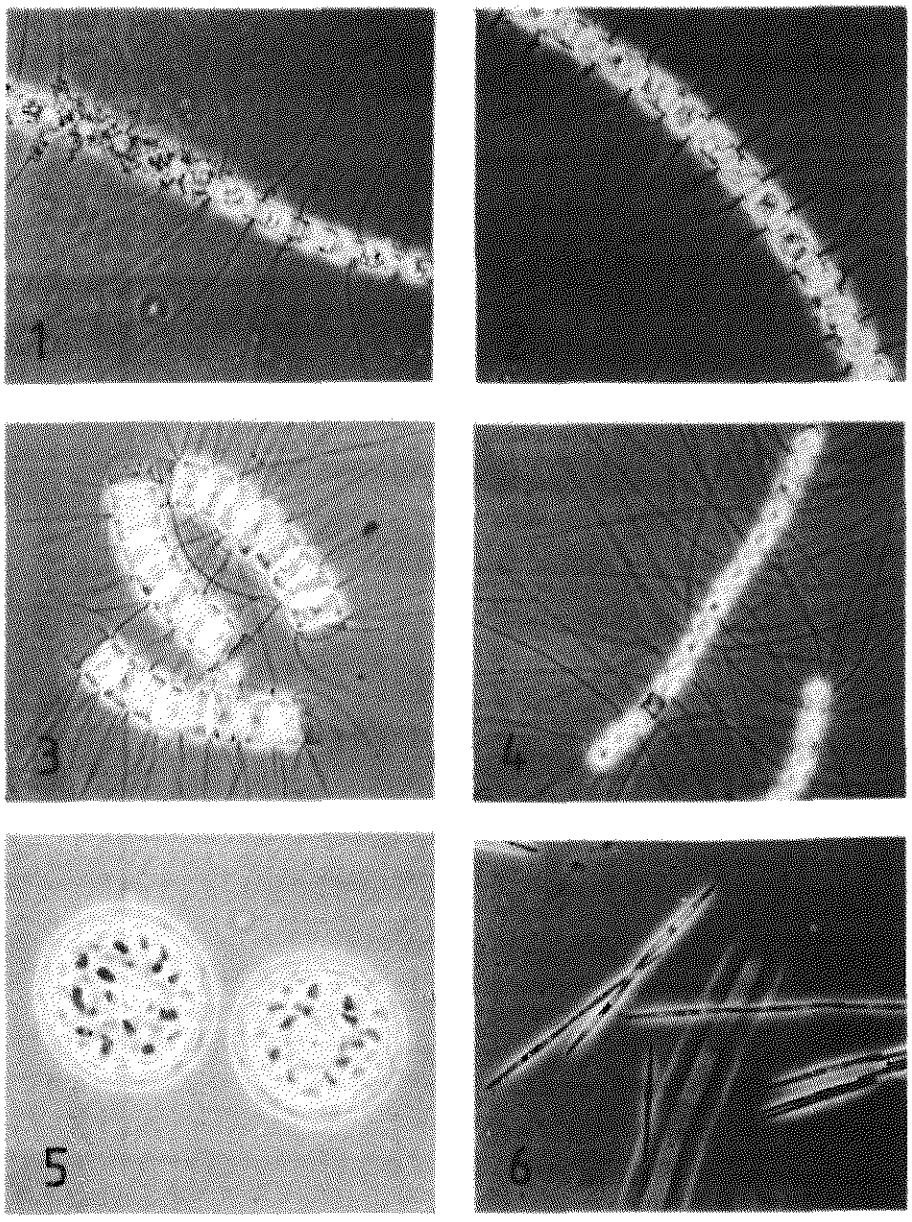

Plate 1

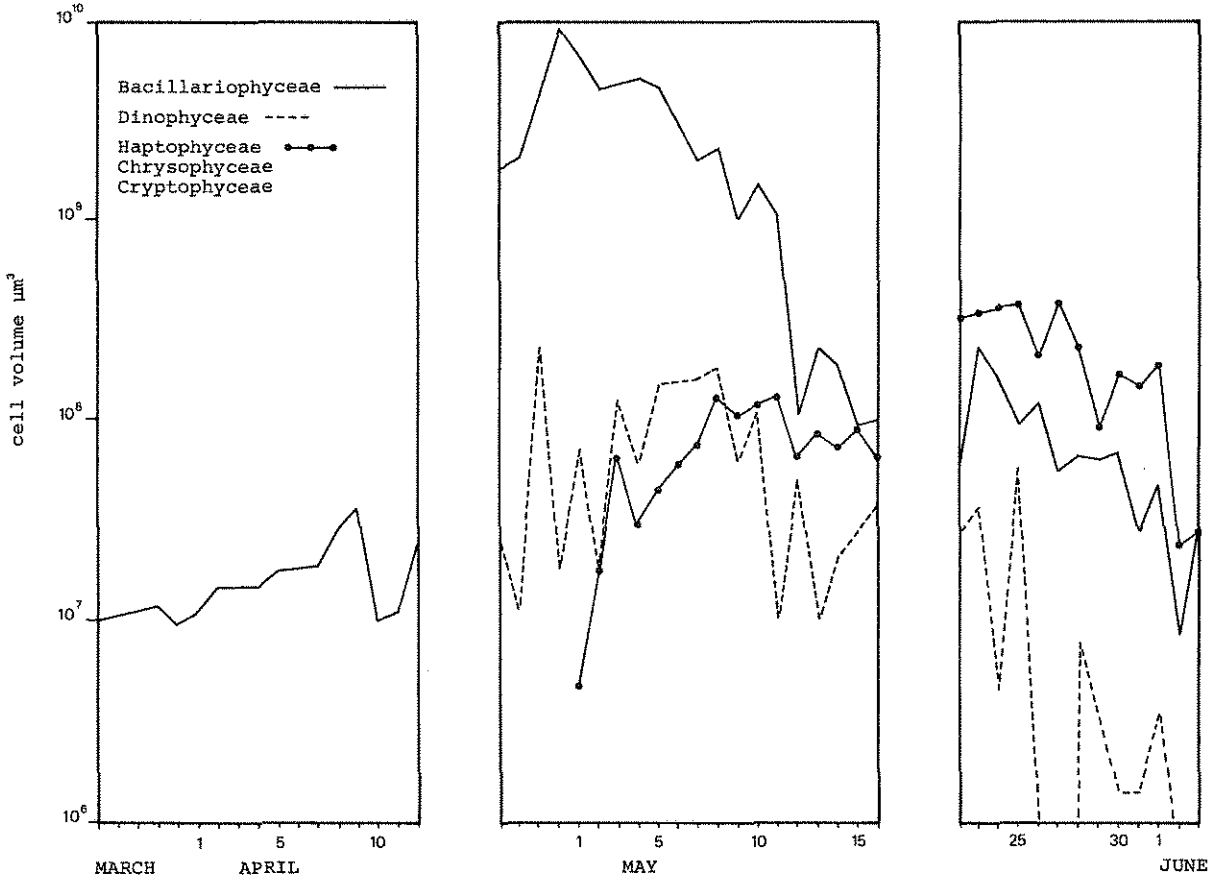

fig. 1.

Abundance of diatoms, Dinophyceae and flagellates including Chrysophyceae, Cryptophyceae, Haptophyceae during the three cruises of *F.S. Meteor* in the Fladen Ground in spring 1976.

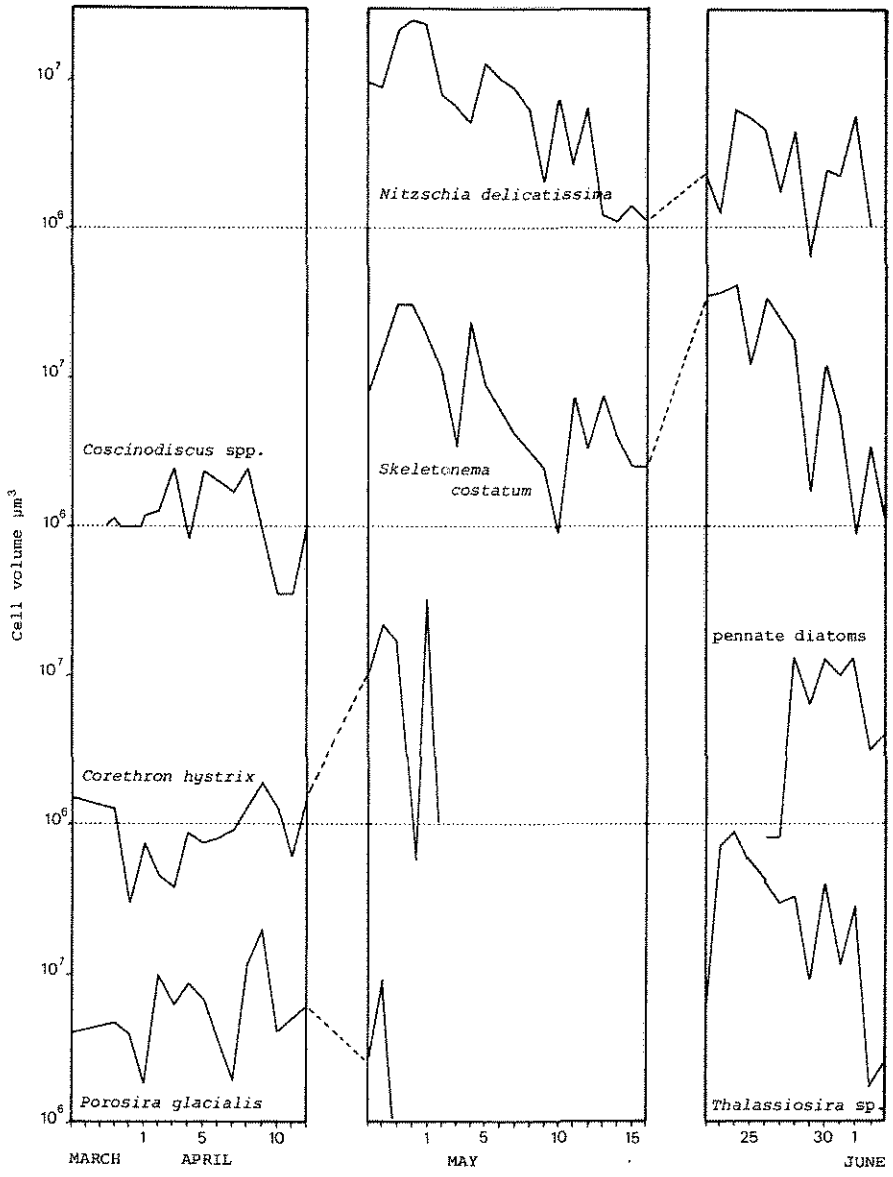

fig. 2.

Abundance of dominant species apart from *Chaetoceros* and *Thalassiosira* spp. during the three cruises of *F.S. Meteor* in the Fladen Ground in spring 1976.

in the planktonic community indicated strong water turbulence. The number of bottom-living cells decreased as the number of dividing cells of planktonic species like *Porosira glacialis* (Plate 1, n° 5), *Corethron hystrix, Coscinodiscus* spec., *Nitzschia delicatissima* (group), *Skeletonema costatum* and *Thalassiosira* and *Chaetoceros* species increased (fig. 2).

In the beginning of the second cruise there was also a great quantity of cells but then a sudden decrease in the number of *Porosira glacialis, Corethron hystrix, Coscinodiscus* spec. could be observed. *Nitzschia delicatissima* (group) (Plate 1, n° 6) and *Skeletonema costatum* on the contrary were still abundant in greater numbers at the end of the second cruise and the beginning of the third cruise, too. The third cruise of *F.S. Meteor* was mainly characterised by a population of *Minidiscus* and *Thalassiosira* species 4 - 5 µm in diameter (Plate 2, n° 2,4) and a population of small pennate diatoms not identified as yet.

Small diatoms have a higher growth rate than large ones and on the account of the higher ratio of surface to cell volume the smaller species are better able to grow and exist at low nutrient levels.

During the second cruise of *F.S. Meteor* the cell volume of *Thalassiosira* (only a part is shown in Plate 2) had increased on the whole compared with the first cruise but varied considerably from day to day (fig. 3).

Chaetoceros was the dominant genus during the second cruise and was the most important species during the phytoplankton bloom between the 29-4 and the 1-5-76 (*cf.* Wandschneider, 1980). Some of the dominant species are shown in Plate 1, n° 2-4.

Selective grazing of herbivorous zooplankton on species like *Porosira glacialis, Thalassiosira* spp. and others compared to *Chaetoceros* may be an explanation for this phenomenon (Hargrave and Geen, 1970; Schnack, 1979), so that *Chaetoceros* species considering their relative short generation time have a double advantage compared to other species.

Plate 2

Scanning Electron Micrographs : isolated cultures from FLEX '76.
1.- *Porosira glacialis* in comparison with "nanoplanktonic" *Thalassiosira* species.
2.- *Thalassiosira delicatula.*
3.- *Thalassiosira conferta.*
4.- *Minidiscus* spec.
5.- *Thalassiosira exigua.*
6.- *Thalassiosira* spec. (unidentified).
7-10.- *Thalassiosira conferta.*

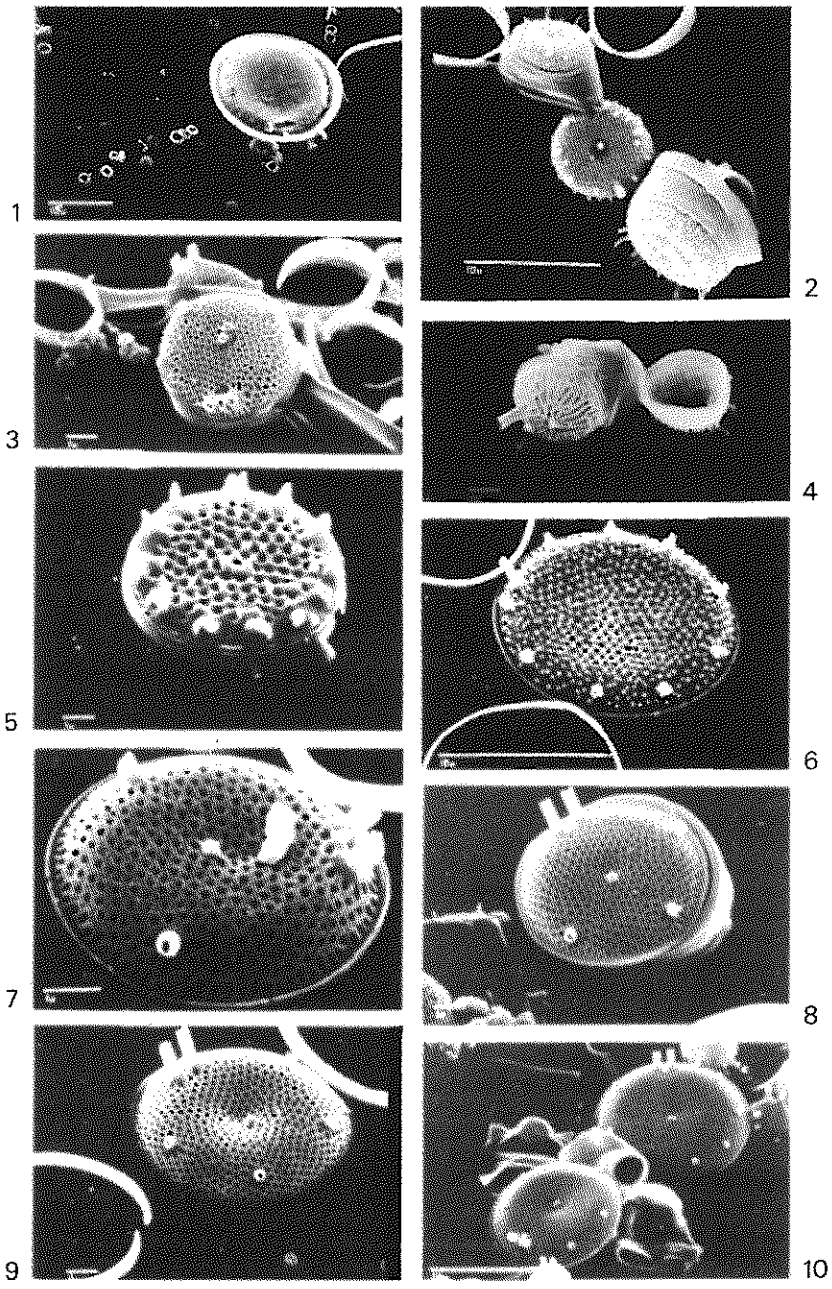

Plate 2

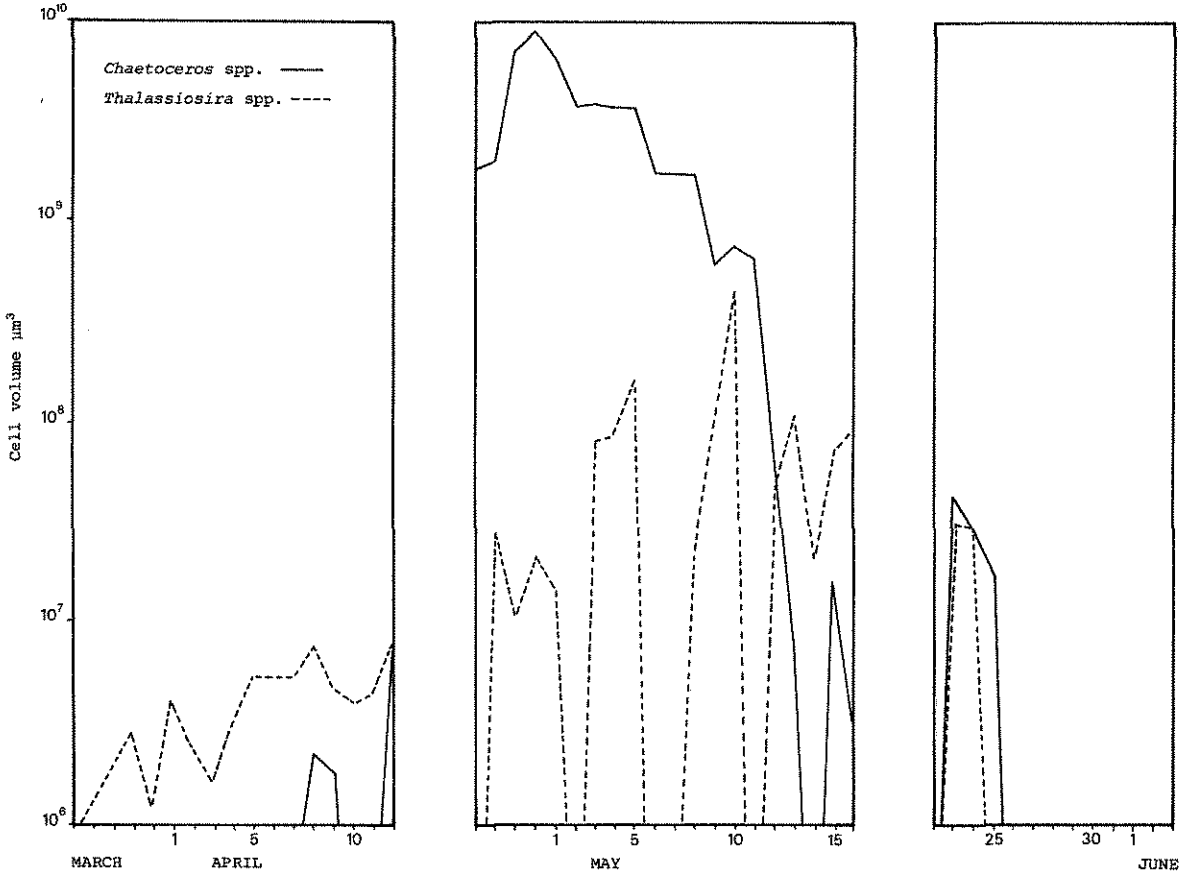

fig. 3.

Abundance of *Chaetoceros* spp. and *Thalassiosira* spp. during the three cruises of *F.S. Meteor* in the Fladen Ground in spring 1976.

As well as the zooplankton there also exists a grazing effect of bacteria on phytoplankton (Plate 1, n° 1). This is a biological factor influencing succession which may have greater importance than supposed hitherto (Delucca and Mc Cracken, 1977). Further investigations have to be carried out in the future.

The results of counting and identification are in good agreement with the data from Gillbricht (unpublished) and Williams and Lindley (1980) although Gamble (1978) showed a sudden change in the zooplankton population shortly after the peak of the phytoplankton bloom.

Acknowledgements

I wish to thank Prof. G.R. Hasle and Mr. E.E. Syvertsen, University of Oslo, for help in identification. Thanks are also due to Mrs. H. Halliger, BAH List/Sylt, for technical assistance for taking the Scanning Micrographs and to Dr. C. Roden, Shellfish Res. Laboratory — Ireland, for correcting the English manuscript. This work was supported by the Sonderforschungsbereich (SFB) 94, Hamburg, of the Deutsche Forschungsgemeinschaft.

References

DELUCCA, R. and Mc CRACKEN, M.D. (1977). Observations on interactions between naturally-collected bacteria and several species of algae, *Hydrobiologia*, 55, 71-75.

GAMBLE, J.C. (1978). Copepod grazing during a declining spring phytoplankton bloom in the northern North Sea, *Mar. Biol.*, 49, 303-315.

HARGRAVE, B.T. and GEEN, G.H. (1970). Effects of copepod grazing on two natural phytoplankton populations, *J. Fish. Res. Board Canada*, 27, 1395-1403.

HASLE, R.H. and FRYXELL, G.A. (1970). Diatoms : Cleaning and mounting for light and electron microscopy, *Trans. Amer. Microsc. Soc.*, 89 (4), 469-474.

SCHNACK, S.B. (1979). Feeding of *Calanus helgolandicus* on phytoplankton mixtures, *Mar. Ecol. Prog. Ser.*, 1, 41-47.

SMETACEK, V. (1975). *Die Sukzession des Phytoplanktons in der westlichen Kieler Bucht*, Dissertation, Universität Kiel.

WANDSCHNEIDER, K. (1980). Die Artensukzession des Phytoplanktons während der Frühjahrsblüte 1976 im Flandengrundgebiet (nördliche Nordsee), *Mitt. Inst. Allgem. Bot. Hamburg*, 17.

WILLIAMS, R. and LINDLEY, J.A. (1980). Plankton of the Fladen Ground during JONSDAP '76, I.- Spring development of the plankton community, *Mar. Biol.* (in press).

Some features in the North Sea temperature data March-June 1976*

Artur SVANSSON**

1.- JONSDAP '76 data

JONSDAP '76 (J76) was a large interdisciplinary programme including physics, chemistry and biology of the North Sea. Temperature and salinity were among those parameters which were determined in largest quantities. In this short article the various types of temperature (T) and some salinity (S) data are briefly examined without any attempt to produce the final summary.

Let us discriminate between J76 data and Non-J76 data, starting with the latter ones.

2.- Non-J76 data

This data material, which was collected independantly of J76 and which usually is of permanent long-term character, consists of lightvessel data, moving vessel data, etc. Much of its outcome is being used in ICES annual publication *Annales biologiques.*

2.1.- THE DATA MATERIAL PER COUNTRY

2.1.1.- *Denmark*

The Danish Meteorological Institute is publishing annually *Oceanographical observations from Danish light-vessels and coastal stations.* The lightvessel (L/V) *Horns Rev* is positioned in the North Sea proper, whereas *Skagens*

---

* This is JONSDAP '76 contribution n° 63.

** National Board of Fisheries, Institute of Hydrographic Research, Göteborg, Sweden.

Rev and *Anholt* are to be found in the Skagerrak-Kattegat area. The "Anholt" time series of T and S are especially valuable, being practically unbroken from 1880, whereas the series of the other L/Vs have the usual war breaks. All the Danish L/Vs have been moved slightly once or twice. It is not clear how much the time series are effected by the changed position but it has been tested that for the "Horns Rev" series starting 1975 the "Vyl" series 1946-1974 cannot be used as reference without correction. Table 1 below therefore does not contain "Horns Rev" deviations.

The Danish L/Vs are observing temperature and salinity down to about 30 m depth once a day.

2.1.2.- *Federal Republic of Germany*

The German Hydrographic Institute in Hamburg is publishing annually data from 5 L/Vs in the North Sea, viz. *Borkumriff, TW/Ems, Deutsche Bucht, Weser* and *Elbe 1*. Temperature and salinity are measured about 3 times a day at the sea surface (*Elbe 1* also at subsurface depths). Below the decade of 1961-1970 is used as reference, but unfortunately time series at the two most off-shore L/Vs, *TW/Ems* and *Deutsche Bucht* are too short to allow the computation of 1961-1970 mean values. In *Annales biologiques* also surface data from "Helgoland Reede" is printed, a position which is visited by boat when weather permits. As the reference period here is 1965-1975 these deviations were not included in table 1.

The German Hydrographic Institute is also distributing weekly Sea Surface Temperature (SST) maps. SST maps for the J76 period have been included in the Draft FLEX Atlas and will hopefully be part of a Final J76 Atlas.

2.1.3.- *Netherlands*

The Meteorological Institute in De Bilt is conducting daily surface measurements of T and S at two L/Vs, viz. *Noord Hinder* and *Texel*. Monthly as well as 1961-1970 means are being published in *Annales biologiques*.

2.1.4.- *United Kingdom*

The Institute for Marine Environmental Research in Plymouth during its Continuous Plankton Recorder Surveys is recording temperature as well. Average temperatures at 10 m depth in standard areas of the North Sea are being published in *Annales biologiques*.

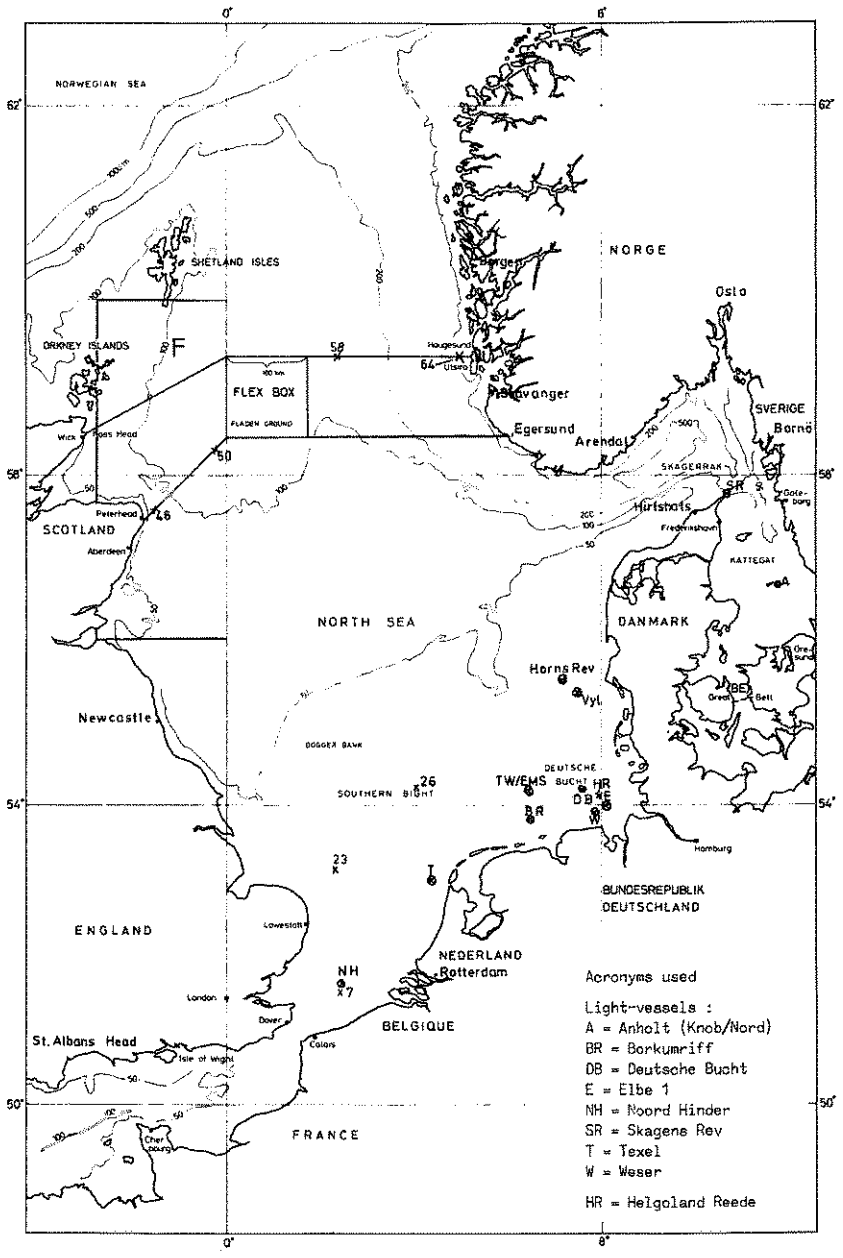
NORWEGIAN SEA
SHETLAND ISLES
ORKNEY ISLANDS
FLEX BOX
FLADEN GROUND
NORGE
Bergen
Stavanger
Egersund
Arendal
Oslo
SVERIGE
Borrö
SKAGERRAK
Hirtshals
Göteborg
KATTEGAT
DANMARK
SCOTLAND
Peterhead
Aberdeen
NORTH SEA
Horns Rev
Newcastle
DOGGER BANK
SOUTHERN BIGHT
DEUTSCHE BUCHT
TW/EMS
HR
DB
E
BR
W
Hamburg
BUNDESREPUBLIK DEUTSCHLAND
ENGLAND
Lowestoft
NEDERLAND
Rotterdam
NH
London
Dover
BELGIQUE
Calais
St. Albans Head
Isle of Wight
FRANCE
Cherbourg
Acronyms used
Light-vessels :
A = Anholt (Knob/Nord)
BR = Borkumriff
DB = Deutsche Bucht
E = Elbe 1
NH = Noord Hinder
SR = Skagens Rev
T = Texel
W = Weser
HR = Helgoland Reede

fig. 1.

2.1.5.- *Norway*

The Institute of Marine Research in Bergen is conducting T and S surface measurements at the ship routes (4-8 times a month) Bergen-Newcastle, Oslo-Newcastle and Stavanger-Rotterdam (Saetre, 1979). These data have so far not been used to describe 1976 conditions.

Some sections *e.g.* Arendal-Hirtshals in the Skagerrak are being surveyed regularly by research vessels.

2.1.6.- *Sweden*

The National Board of Fisheries in Göteborg is conducting daily T and S measurements down to 30 m depth at Bornö Station in the Gullmar Fiord. The measurements started 1933.

Some sections in the Skagerrak and the Kattegat are being surveyed regularly some 4 times a year.

2.2.- CHARACTERIZATION OF 1976 BY MEANS OF NON-J76 TEMPERATURE DATA

Table 1 summarizes temperature deviations during March-June 1976, in the upper part for coastal surface water and the lower part in off-shore or deeper water.

Table 1

Temperature deviations 1976

	March	April	May	June
L/V Skagens Rev, 0 m				
Ref: 1961-1970	- 0.2	+ 0.6	- 0.5	- 0.8
L/V Borkumriff, 0 m				
Ref: 1961-1970	- 0.3	- 0.3	- 0.8	+ 0.2
L/V Texel, 0 m				
Ref: 1961-1970	- 0.1	+ 0.1	- 0.4	+ 0.5
L/V Noordhinder, 0 m				
Ref: 1961-1970	- 0.1	+ 0.2	- 0.4	+ 0.3
Area F, 0 m				
Ref: 1876-1915	+ 0.7	+ 0.7	+ 0.8	+ 0.7
L/V Skagens Rev, 30 m				
Ref: 1881-1930	+ 0.8	- 0.2	+ 0.3	+ 1.3
1931-1960	+ 0.6	- 0.3	+ 0.4	+ 0.9

In the coastal waters the deviations are rather small, March and May negative, whereas April and June are mostly positive.

The lower part deviations show that the reference period for area F (N 56° - N 60° and W 0° - W 3°) is 1876-1915. A rough inspection of a 19 year sliding means smoothed "Anholt" series and also a study of *e.g.* Becker and Kohnke (1978) shows that there has been only small long term changes of temperature in March and April, a slight increase in May, whereas the June series has a minimum in the 10-20ies. We may therefore draw the very rough conclusion that the northern North Sea water was in March, May and June slightly warmer than normal.

Cold winter give rise to renewal of deep Skagerrak water (Ljöen and Svansson, 1972). Some Swedish data (see *Annales biologigues*) indicated such an event also 1976, but a study of the deep temperatures (600 m) shows that after a large renewal 1970 the temperature rose slowly to its normal value and did not get cooled again until the winter of 1978.

It should be notified that the original German SST maps (see 2.1.1.) also contain a short summary (in German) of the general situation. A careful investigation of the North Sea temperatures during J76 should include a study of these notes as well as the SST results 1968-1978 presented by Becker (1978).

Some non-J76 data is used below together with J76 data.

2.3.- J76 DATA

JONSDAP '76 consisted of FLEX with activities in a 100 × 100 km large area in the central North Sea during March 25th - June 15th 1976, and INOUT covering the whole North Sea but only during 40 days March 15th - April 25th. The main FLEX period, however, did not start until the middle of April when the primary production turned into spring bloom. Thereby the overlap between INOUT and the main FLEX is very short and it is difficult to extrapolate knowledge from one period to the next. Below is presented a few examples of temperature series recorded at buoy stations. When this paper was planned it was hoped that also German data series could be included, because many German series are much longer than the INOUT period. Unfortunately the German data has not been processed in this respect as yet.

Figures 2-4 are kind of extrapolation examples. Comparisons between data from *Noord Hinder* and Station 7 (fig. 2) as well as between *Texel* and Station 23 (fig. 3) show similar temperatures (Dutch data was kindly sent by Martin

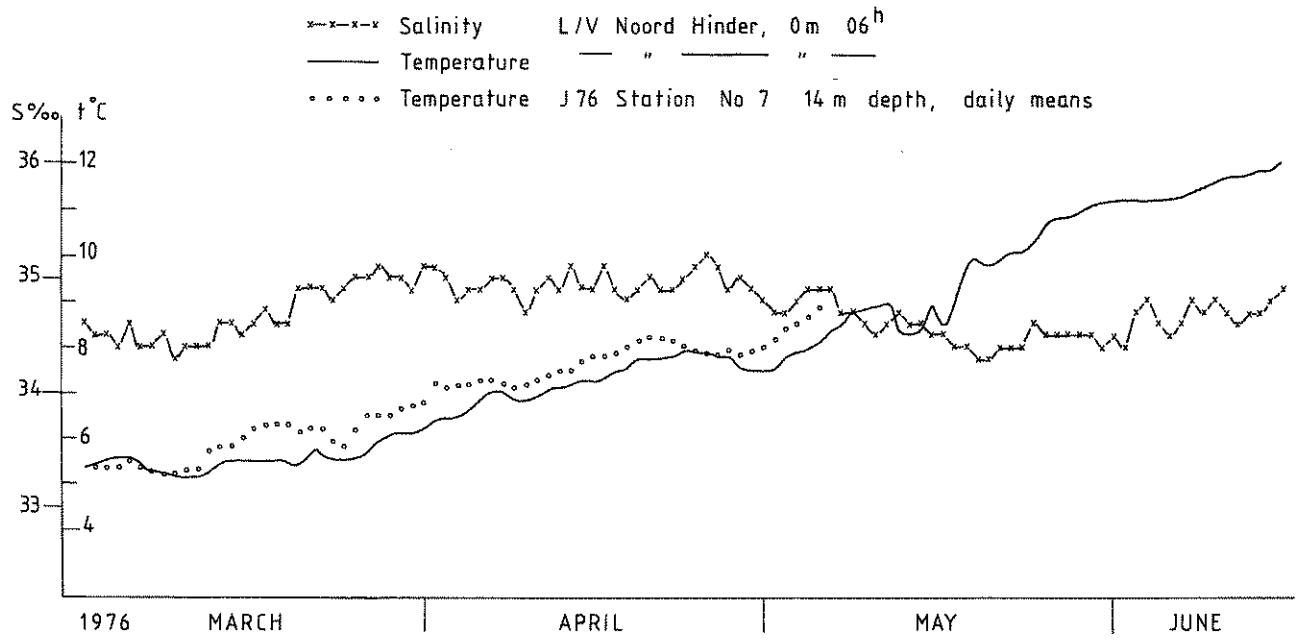
Salinity L/V Noord Hinder, 0 m 06h
Temperature " "
Temperature J 76 Station No 7 14 m depth, daily means
S‰ t°C
36
35
34
33
12
10
8
6
4
1976
MARCH
APRIL
MAY
JUNE

fig. 2.

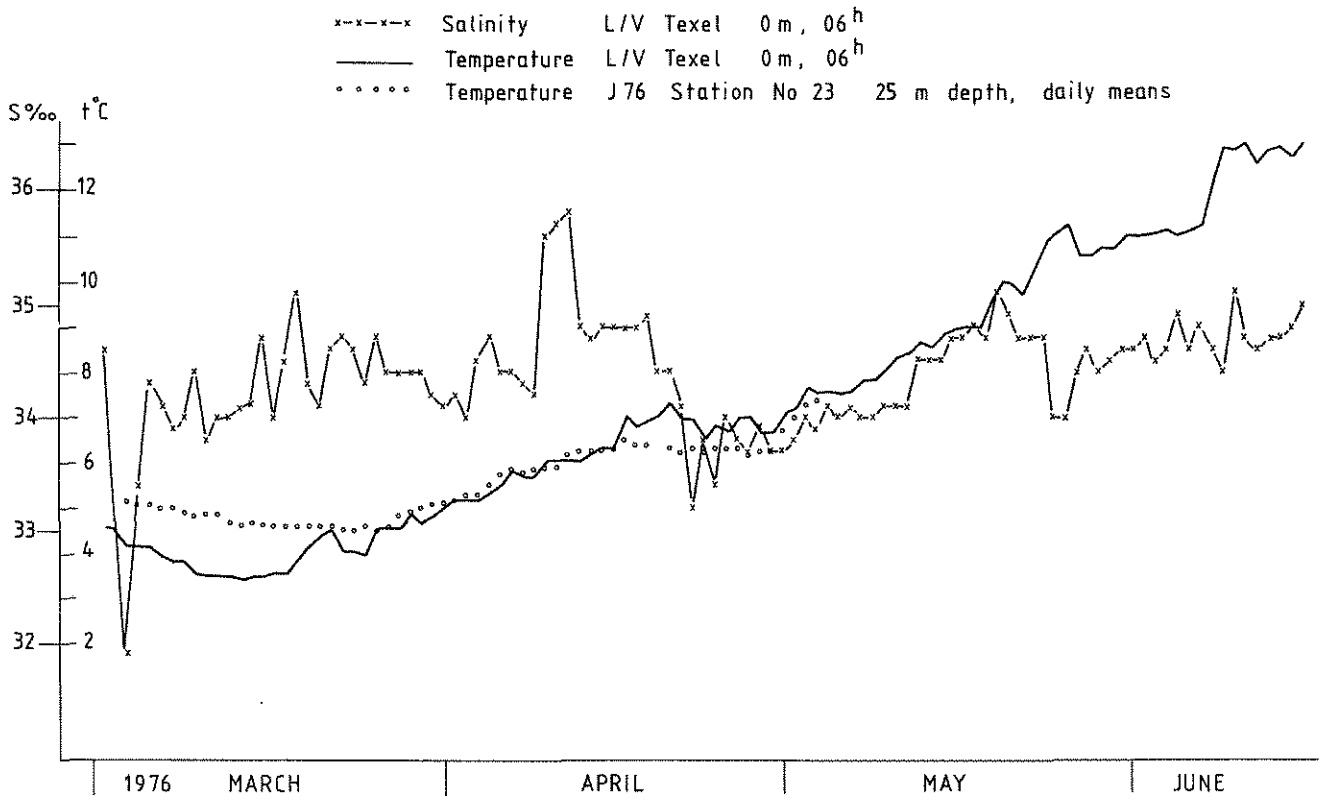
Salinity L/V Texel 0 m, 06 h
Temperature L/V Texel 0 m, 06 h
Temperature J 76 Station No 23 25 m depth, daily means
S‰
t°C
36
35
34
33
32
12
10
8
6
4
2
1976
MARCH
APRIL
MAY
JUNE

fig. 3.

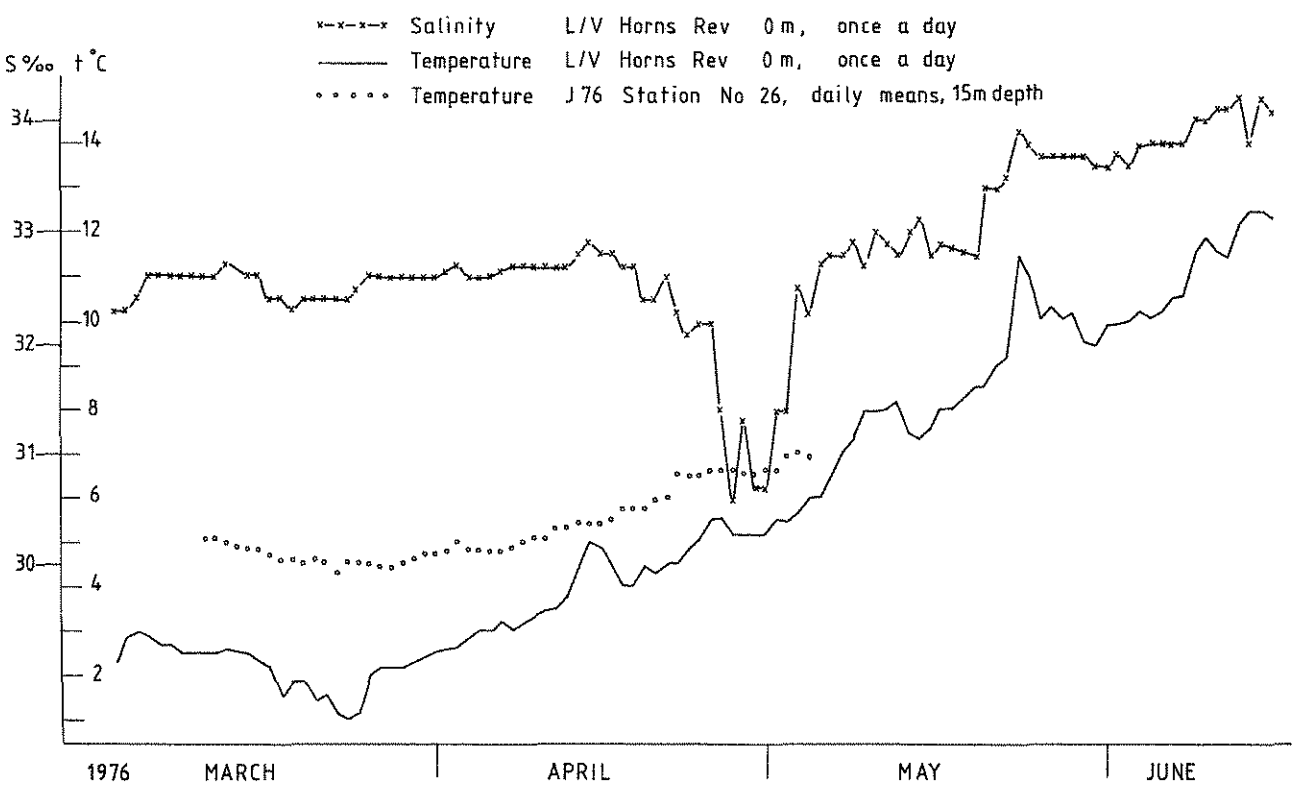
Salinity L/V Horns Rev 0 m, once a day
Temperature L/V Horns Rev 0 m, once a day
Temperature J 76 Station No 26, daily means, 15m depth
S ‰
t °C
34
33
32
31
30
14
12
10
8
6
4
2
1976
MARCH
APRIL
MAY
JUNE

fig. 4.

Visser). The temperatures of *Horns Rev* and the nearest station, n° 26 (fig. 4) are quite different, however. In this area the horizontal gradients of T and S are very large (*e.g.* Becker, 1978).

Figures 5-7 from the northern North Sea contain only INOUT data. Fig. 5 shows a difference 0.5 °C between the near-coast station n° 46 and the farther out situated one, n° 50. This is also in accordance with *Argos* measurements (Svansson, 1980). Fig. 6 shows measurements recorded at the western part of the Norwegian Rinne. Fig. 7, finally, demonstrates the quite different conditions along Norway.

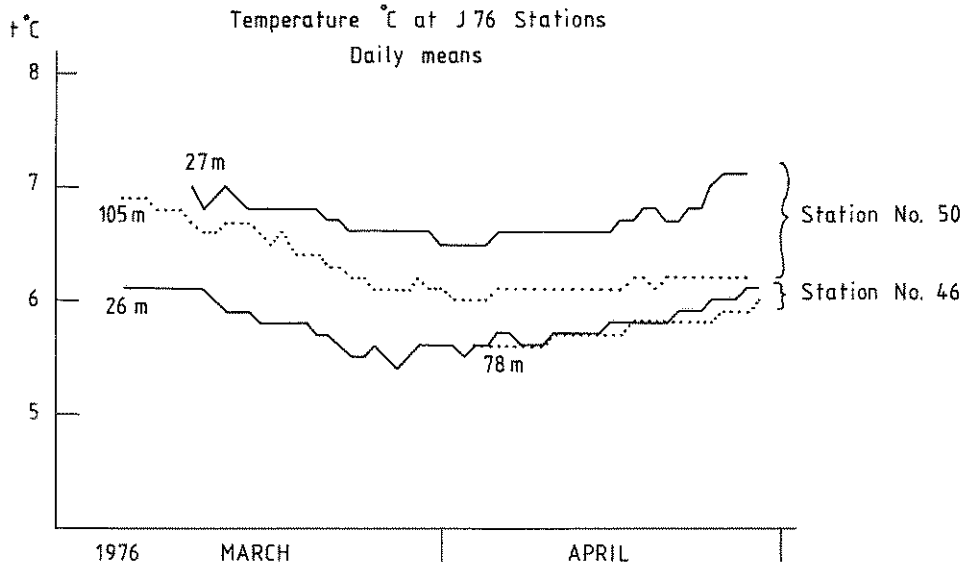

fig. 5.

The Draft FLEX Atlas contains 3 *Argos* sections, Peterhead-Egersund, made at the end of March and the beginning of April, and further 6 Norwegian sections, Wick-Haugesund (3 in March, 1 in April and 2 in May).

The vast material collected in the FLEX box has sofar been used by Soetje and Huber (1980, thermal stratification) and Steele and Henderson (1979, spatial patterns).

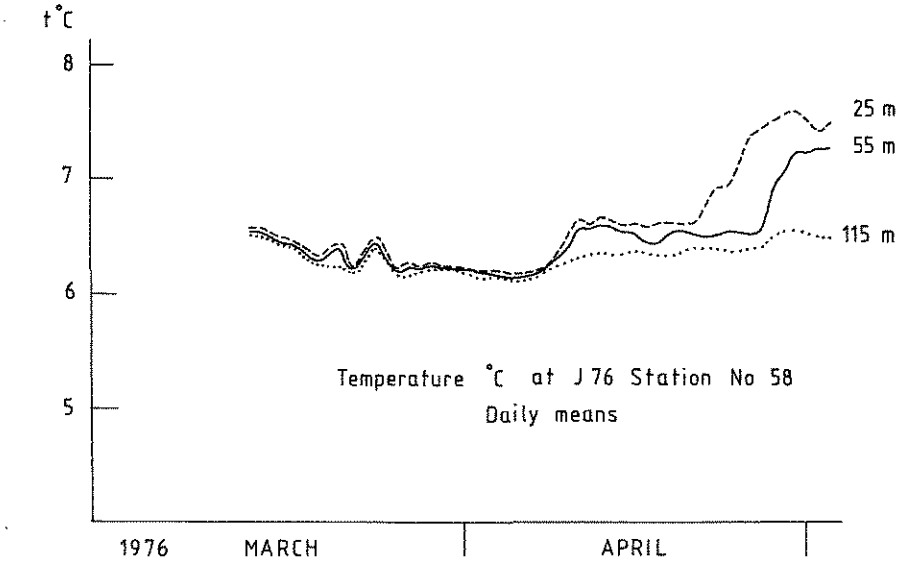

fig. 6.

3.- Conclusions

This paper dealing mainly with temperature conditions during JONSDAP '76, presents some compilations of data, and is not at all the final summary of the J76 temperature conditions. Such a summary awaits *e.g.* the German data, but it will also be necessary to look much more carefully into all the data and its reference periods before it can be stated if 1976 was a normal year or not. So far the rough conclusion is that the March-June period was rather normal in coastal areas and slightly warmer than normal in the open parts.

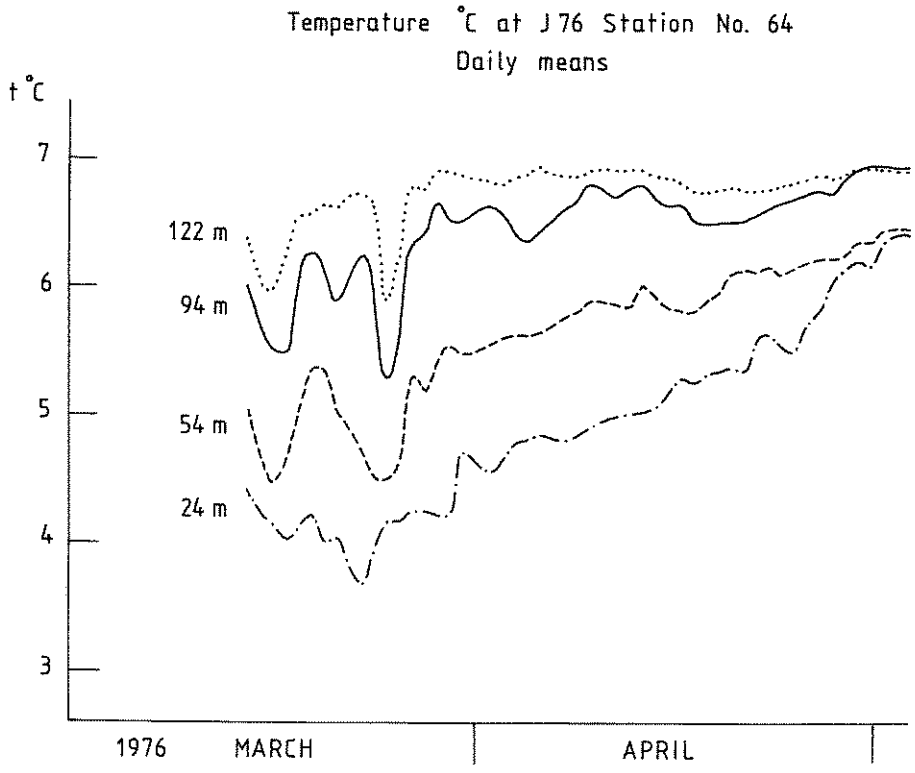

fig. 7.

References

BECKER, G.A. (1978). Statistical treatment of Synoptical SST maps of the North Sea (1968 to 1978), ICES C.M. 1978/C:36, 10 pp.

BECKER, G. and KOHNKE, D. (1978). Long-term variations of temperature and salinity in the inner German Bight, Rapp. P.-V. réun. (ICES), vol. 172, 335-344.

LJÖEN, R. and SVANSSON, A. (1972). Long-term variations of subsurface temperatures in the Skagerrak, *Deep-Sea Res.*, 19, 277-288.

SAETRE, R. (1979). Features of the mean annual surface salinity variations off southern Norway, The Norwegian Coastal Current Project Report 1/79, 15 pp.

SOETJE, K.C. and HUBER, K. (1980). A compilation of data on the thermal stratification at the Central Station in the northern North Sea during FLEX '76, Meteor Forschungsergebnisse JONSDAP '76 Volume (J76 n° 34), in press.

STEELE, J.H. and HENDERSON, E.W. (1979). Spatial pattern in North Sea plankton, *Deep-Sea Res.*, 26, 955-963.

SVANSSON, A. (1980). A hydrochemical section Norway-Scotland during March-April 1976, Meteor Forschungsergebnisse JONSDAP '76 Volume (J76 n° 33), in press.

Harmonic analysis of horizontal current data
The method and some new developments*

A. LOFFET**, Y. ADAM*** and A. POLLENTIER***

Introduction

The hydrodynamics of the North Sea and of adjacent marine areas is a problem of great practical importance. A valuable modelling effort has been devoted to it in the past, and it is still the subject of many current research works (3 dimensional models, residual circulation models).
On the other hand, much information has also been gathered in situ (sea elevation and horizontal current time series, for our purpose), and they are worth being examined in detail. Field data are important because they can provide the right boundary conditions to the numerical models, and also because they can be used to estimate the quality of the model and to detect its possible shortcomings. Finally, they are very interesting by themselves because they enrich our "naturalistic" knowledge of the area.

The tide is the leading hydrodynamic process in the North Sea basin. From a practical point of view, its most interesting feature is that the motion has components with well defined and accurately known periodicities.

It was thus interesting to perform the harmonic analysis of elevation and current data, in order to extract the harmonic components out of the

---

* This is JONSDAP '76 contribution n° 66.

** Aspirant F.N.R.S., Mécanique des fluides géophysiques, Université de Liège, Belgium.

*** Unité de Gestion du Modèle mathématique de la mer du Nord et de l'estuaire de l'Escaut.

records. Other effects which are not purely tidal (such as storm surges), are considered as noise in the present analysis and cannot be included in this framework. It is then evident that a description in terms of tidal components alone cannot be complete.

During JONSDAP 76, a valuable mooring effort has been performed, and in Belgium, current meters (and recently tide gauges) have been moored for several years in the Southern Bight of the North Sea. The analysis of the data set has not yet been completed, but we will summarize here the method we have developed so far to analyse sea elevation as well as currents, putting much stress on the determination of the maximum number of components, and on the estimation of the quality of the results.

1.- Tidal components

The cornerstone of all works on tides is the determination of the tide generating potential and of its harmonic development. This was performed originally by Doodson (1921), who showed that the tidal potential can be written as a sum of constituents

$$\Phi = \sum_r f_r R_r \cos(V_r + u_r) \qquad (1)$$

R_r is the amplitude of the constituent,

V_r is the argument of the constituent, i.e. an angle changing steadily at the mean speed of the constituent,

R_r and V_r depend on the location considered,

f_r and u_r are nodal modulation factors, taking into account the existence of several terms in one constituent. These terms have very close frequencies and cannot be separated in one year's analysis (the difference between their frequencies is less than $2.738\ 10^{-3}$ cycle/mean solar day).
f_r and u_r are determined from Doodson's original results (Godin,1972; Loffet, 1980 a), and depend on slowly varying astronomical arguments.

The tidal components can be gathered in groups and the groups in species. The average frequency difference is :

between groups of the same species : $\sim 3.66\ 10^{-2}$ cycle/mean solar day
between species : ~ 0.966 cycle/mean solar day.

A detailed list of the constituents and of all their features can be found in Loffet (1980 a).

The tidal potential is not found as such in nature, and only some effect of the periodic forcing introduced by the tidal potential can be found in the actual tidal records :

1) the relative magnitude of the different components can vary considerably from the results of the tidal potential;

2) the non linear interactions in the dynamic balance can introduce new terms, with new frequencies unknown in the development of the tidal potential. This is particularly the case in shallow water areas as the southern North Sea.

The tidal part of the data record will still be represented by an expression in some way similar to (1), i.e.

$$h = h_o + \sum_r f_r H_r \cos(V_r + u_r - K_r) \qquad (2)$$

(h denotes the elevation or one component of the current).

V_r, f_r, u_r have the same meaning as in the development of the tidal potential.

The amplitudes (h_o, H_r) and the phase lags K_r are the harmonic constants of the tidal component considered. They depend on the location.

The expression $(V_r + u_r) - K_r$ can advantageously be replaced by its equivalent $(V_r + u_r)_{Greenwich} - g_r$, where only the last argument g_r , the Greenwich phase lag depends on the location.

We have thus

$$h = h_o + \sum_r f_r H_r \cos[(V_r + u_r)_{Gr} - g_r] \qquad (3)$$

The harmonic constants for the elevation are H_r , g_r. For the horizontal current, rather than using the harmonic constants of the east and north components (i.e. H_{rx} , H_{ry} , g_{rx} , g_{ry}), it is advantageous to express the results in terms of the tidal ellipses elements, i.e. :

- the major semi-axis length M_r
- the minor semi-axis length m_r

• the ellipse orientation θ_r (geographical coordinates)

• the phase lag ϕ_r (or time lag ϕ_r/n_r , n_r being the speed of the constituent r) between culmination of the fictitious generating celestial body at Greenwich or at the local meridian, and the occurrence of the maximum velocity.

These are defined

$$M = \left\{\frac{1}{2}\left[H_x^2 + H_y^2 + \left[H_x^4 + H_y^4 + 2H_x^2 H_y^2 \cos 2(g_x - g_y)\right]^{\frac{1}{2}}\right]\right\}^{\frac{1}{2}}$$

$$m = \left\{\frac{1}{2}\left[H_x^2 + H_y^2 - \left[H_x^4 + H_y^4 + 2H_x^2 H_y^2 \cos 2(g_x - g_y)\right]^{\frac{1}{2}}\right]\right\}^{\frac{1}{2}}$$

$$\theta = \frac{\pi}{2} - \frac{1}{2}\{\arg(H_x \cos g_x + H_y \sin g_y \, , \, H_y \cos g_y - H_x \sin g_x)$$

$$+ \arg(H_x \cos g_x - H_y \sin g_y \, , \, H_y \cos g_y + H_x \sin g_x)\}$$

$$\phi = -\frac{1}{2}\{\arg(H_x \cos g_x + H_y \sin g_y \, , \, H_y \cos g_y - H_x \sin g_x)$$

$$- \arg(H_x \cos g_x - H_y \sin g_y \, , \, H_y \cos g_y + H_x \sin g_x)\}$$

The knowledge of all harmonic constants makes it possible to derive the tidal part of the sea elevation or currents. However, in practice several limitations will occur :

• we don't know which harmonics to consider, and we will have to restrict their number;

• it is not possible to derive all those which are wanted;

• the accuracy of the results is limited.

2.- Tidal constituents considered

The main constituents arising from the tidal potential will be searched for (Doodson, 1921; Godin, 1974).

Problems appear when trying to determine which shallow water constituents have to be added :

1°) the non linear interactions in the dynamic balance are known to generate harmonics. In order to determine them, the dynamic equations can be decomposed spectrally, and the harmonics appear in different terms of the

equations (Le Provost, 1974). Such developments are too far from our present purpose, and we will only consider harmonics obtained by linear combinations of the most important potential terms in species 1 and 2, i.e. :
species 1 : Q1 , O1 , P1 , J1 ,
species 2 : M2 , S2 , N2 , K2 , (ν2) , (μ2) , (L2).
Many constituents can be defined in this way, and in a first approach, we will finally restrict ourselves to the 93 components considered in the Table of Harmonic Constituents of the Tide of Monaco (Loffet, 1980 a).

2°) Many components, mainly in species 1 and 2, can have different origins (potential and/or different combinations between other components).
The component with frequency 1.864547227 cycle/mean solar day, e.g. finds its origin in the potential (μ2) but also in non linear combinations (2[M2] - [S2] (= 2MS2), [N2] + [ν2] - [M2] , a.s.o.). Depending on the point of view adopted, the definition of V_r , f_r and u_r is then not unique. In very special cases, methods can be developed to discriminate between separate origins (Le Provost, 1974). This will not be applied here, and every time a multiple interpretation is possible, the expression for the term which seems the most important has been chosen. If the interpretation seems too dubious, the nodal correction is only disregarded (Loffet, 1980 a).

3.- Limitations of the analysis

Two limitations occur concerning the number of components which can be analysed in a record :
a) the data are not recorded continuously, but only at predetermined time intervals, and this could limit the analysis at high frequencies;
b) the length of the data record is finite, and then all desired tidal components cannot be separated from each other.

3.1.- SAMPLING INTERVAL

It is well known that for a phenomenon sampled with a time interval Δt , the highest frequency which can be analysed is the Nyquist frequency $f_N = \frac{1}{2\Delta t}$.
If energy is present at higher frequencies, it will be projected on (o, f_N).
In tidal analysis, the highest interesting frequencies occur at species

12 or so [very seldom above, but often below (~ 8)] , so that with a Δt not exceeding one hour, the sampling interval does not introduce limitations. However, care must be taken to avoid aliasing during the recording of the data and the preparation of the time series.

3.2.- FINITE LENGTH OF THE RECORD

A signal of the form $f(t) = A \cos(2\pi nt + \phi)$ and defined for $t \in]-\infty, +\infty[$ has the Fourier transform $g(\lambda) = \frac{A}{2}[e^{j\phi}\delta(\lambda-n) + e^{-j\phi}\delta(\lambda+n)]$, where $\delta(\lambda)$ is Dirac's delta generalized function.

The same signal, but restricted to the finite time interval $[0,T]$, has the Fourier transform

$$\tilde{g}(\lambda) = \frac{AT}{2}\left\{e^{j\phi}e^{-j\pi(\lambda-n)T}\ \mathrm{sinc}\,[(\lambda-n)T] + e^{-j\phi}e^{-j\pi(\lambda+n)T}\ \mathrm{sinc}\,[(\lambda+n)T)]\right\}$$

where $\mathrm{sinc}(x) = \frac{\sin\pi x}{\pi x}$

The former spikes have now a finite width (the first zero crossing occurs at $\lambda = n \pm 1/T$), and as a consequence of this, it will be impossible to separate spikes occuring at two frequencies if they are too close.

The Rayleigh criterion considers that it becomes possible to separate two frequencies n_k and n_l if $|n_k - n_l|\ T \geqslant 1$, and that they are fully distinguishable if $|n_k - n_l|\ T \geqslant 2$.

Given a record of length T, if the Rayleigh criterion is applied, only a limited number of harmonic constants will be accessible, i.e. those for which $|n_k - n_l|\ T \geqslant 1$ holds. This will be restrictive in practice since the record lengths (for current data) seldom exceed two months.

This problem is directly related to the solution of the linear system of equations derived from the application of the least squares method to the estimation of the harmonic constants. The matrices to be inverted are

$$A_{kl} = \frac{1}{2}[S_N(n_k - n_l) + S_N(n_k + n_l)]$$

$k, l = 0, \ldots m;\ n_o = 0$; for the cosine terms,

$$B_{kl} = \frac{1}{2}[S_N(n_k - n_l) - S_N(n_k + n_l)]$$

$k, l = 1, \ldots m$, for the sine terms.

with $S_N(\lambda) = \frac{\sin(\pi N \lambda \Delta t)}{N \sin \pi \lambda \Delta t}$

If the Rayleigh criterion is satisfied, the matrices A and B have their main terms on the principal diagonal, and are thus well conditioned for inversion. The analysis of two close frequencies can lead to an ill conditioned system and computational problems.

However, even without computational problems, the consideration of two close frequencies can lead to a very poor estimation of the harmonic constants, as will be shown in the next paragraph.

The Rayleigh criterion has thus been used so far as a general guiding line when searching which components it is possible to analyse.

4.- Estimation of the accuracy of the results

The recorded sea elevations or currents are not due to the tide only, and it is customary to consider them as made of several contributions :

a) the components which are analysed;

b) the components which are not analysed, either because they cannot be separated from the ones which are analysed, or simply because they are not wanted;

c) other processes, called noise and which can be attributed to different causes :

- instrumental inaccuracies or failures, accidental errors occuring during the preparation of the time serie;
- physical processes which are not considered in the tidal analysis (storm surges, e.g.).

The presence of all these contributions has some effect on the quality of the estimation of the analysed components :

a) There is a systematic error introduced by the components which are not analysed. If the system is well conditioned, it can be shown to be of the order

$$\sim \gamma_{n.a.} \, S_N \, (n_a - n_{n.a.})$$

where $\gamma_{n.a.}$ is the amplitude of the non analysed component, n_a and $n_{n.a.}$ are the frequencies of the analysed and non analysed components, respectively.

The importance of this error increases with the relative magnitude of the non analysed component (with respect to the analysed one), and with the closeness of both frequencies

$$\left[S_N\ (n_a - n_{n.a.}) \sim 1 - \frac{[\pi(n_a - n_{n.a.})T]^2}{6} \qquad \text{for } (n_a - n_{n.a.})T \ll 1\right]$$

A new method is currently being developed to force separation in some way, but it is still too early to account for its results.

b) The noise introduces statistical variability in the estimation of the analysed components. This problem has been examined in details, and the results of the least squares theory have been applied to harmonic analysis (Hannan,1970; Rao,1973).

The noise was first assumed to be white, and the variances-covariances matrix of the estimators has been derived (Loffet, 1980 b). However, if the assumption of a white noise is reasonable for accidental failures and instrumental inaccuracies, it is far too restrictive if additional geophysical phenomena have to be included.

The least squares theory has then been developed in the case of a second order stationary noise process, and it makes use of its spectral properties (Loffet, 1980 b). The variances-covariances matrix of the estimators has been derived, as well as its asymptotic behaviour.

Using a particular application of the central limit theorem, it has become possible to derive statistical tests of hypotheses, and to build up confidence regions for the harmonic constants(Loffet, 1980 b). So far, the method has only been developed and applied when the system is well conditioned (the Rayleigh criterion is satisfied).

A detailed description of the method and of all the results involved is too lenghty to be described here. However, it is worth noting that if the system is well conditioned, the spectra sufficiently smooth, and the frequencies different from zero, one has :

$$\mathrm{cov}(a_i\ ,\ a_{i'}) \approx s(n_i)/T\ .\ \delta_{ii'}$$

$$\mathrm{cov}(b_i\ ,\ b_{i'}) \approx s(n_i)/T\ .\ \delta_{ii'}$$

$$\mathrm{cov}(a_i , b_{i'}) \approx 0$$

for the sea elevation, where a_i , b_i denote respectively the cosine and sine terms of the i^{th} component, $s(n_i)$ is the value of the noise spectrum at frequency n_i , and $\delta_{ii'}$ the Kronecker symbol.

One also has :

$$\mathrm{cov}(a_{ix} , a_{i'x}) \approx s_{xx}(n_i)/T \cdot \delta_{ii'}$$

$$\mathrm{cov}(b_{ix} , b_{i'x}) \approx s_{xx}(n_i)/T \cdot \delta_{ii'}$$

$$\mathrm{cov}(a_{ix} , b_{i'x}) \approx 0$$

$$\mathrm{cov}(a_{iy} , a_{i'y}) \approx s_{yy}(n_i)/T \cdot \delta_{ii'}$$

$$\mathrm{cov}(b_{iy} , b_{i'y}) \approx s_{yy}(n_i)/T \cdot \delta_{ii'}$$

$$\mathrm{cov}(a_{iy} , b_{i'y}) \approx 0$$

$$\mathrm{cov}(a_{ix} , a_{i'y}) \approx s_c(n_i)/T \cdot \delta_{ii'}$$

$$\mathrm{cov}(b_{ix} , b_{i'y}) \approx s_c(n_i)/T \cdot \delta_{ii'}$$

$$\mathrm{cov}(a_{ix} , b_{i'y}) \approx s_q(n_i)/T \cdot \delta_{ii'}$$

$$\mathrm{cov}(a_{iy} , b_{i'x}) \approx - s_q(n_i)/T \cdot \delta_{ii'}$$

for the horizontal current, where a_{ix} , b_{ix} , a_{iy} , b_{iy} denote the cosine and sine terms along East and North directions of the i^{th} component, $s_{xx}(n_i)$ and $s_{yy}(n_i)$ are the values at n_i of the noise spectrum of the East and North components, $s_c(n_i)$ and $s_q(n_i)$ are the values at n_i of the co- and quadrature spectra of the two-dimensional noise process.

To be applied, the method needs the knowledge of the noise spectrum. This one is not known a priori, but an estimate of it is obtained from the residuals (i.e. what remains after removing the analysed components from the original time serie). The estimate is obtained using standard FFT techniques (Jenkins and Watts, 1969; Otnes and Enochson, 1972; Bath, 1974) which will not be developed here.

If the Rayleigh criterion is not satisfied, it is still possible to derive the variances-covariances matrix of the estimators and to determine the order of magnitude of the statistical error affecting the estimation of the tidal components. This can be used to analyse more components than the criterion allows, if the level of the noise is sufficiently low so that the results are still meaningful. We have not yet used this technique, but we have concentrated our attention on the estimation of the quality of the results derived when the Rayleigh criterion is satisfied.

5.- Classification of the components considered

Applying the Rayleigh criterion, the determination of all constituents considered needs a record lasting at least one year.
The determination of one component in each group needs at least 27 days.
The species (1, 2, 3, 4, ...) are separated in one day.

The records we examined last from one week (when data were lost because of a failure in the instrument) to two months at most. Different record lengths are thus available, and the considerations above are rather crude, because they don't consider the detailed structure of the frequencies of the desired components, and because they don't take their relative importance into account. It is thus interesting to classify them in some way, taking into account the points mentioned above. This was performed as follows : every component is given a weight,and the time needed for the determination of all of them is computed, applying the Rayleigh criterion; the ones giving way to this record length are determined, and among them, the one having the smallest weight is then extracted; the process goes on with the remaining ones, and is stopped when all have been extracted.

In this way, a classification giving the components which can be analysed versus the record length is obtained. In theory, the weights are unknown a priori, and the aim of the harmonic analysis is to determine them. However, it is possible to run the classification using known results at a close location.

Table 1

This table lists the harmonic components which can be determined, versus the length of the record. 60 components; results for Oostende after data from Melchior *et al.* (1967).

Record length (days)	Components
0.5	M2,M4,2MS6
1.1	+ O1,MO3
9.6	+ MNS2
13.7	+ K1,MK3
14.8	+ S2,M6,MS4,2SM2,MSf,2SM6,SK3,SO1,S4
27.3	+ M3,M1
27.6	+ N2,2MN6,N4,Q1,2Q1
31.8	+ L2,2MS2,MSN2,MSN6,Mm,SN4,J1
182.6	+ K2,P1,MK4,2MK6,MKS2,OQ2,OP2,SO3,Mf,MSK6,MP1, SK4,KJ1,OO1
193.6	+ χ1
205.9	+ ν2,λ2,2N2,ρ1,σ1,θ1
365.2	+ Sa,Ssa,S1,ψ1,ϕ1,T2,R2,π1

In the present analysis, we took the sea elevation given at Oostende (Melchior *et al.*, 1967) and the mean sea elevation at three belgian coastal harbours (Hydrographische Dienst der Kust, private communication) as weights (60 components). The results are listed in table 1 and 2. They are very similar, and will be used as a guide in the Southern Bight of the North Sea.

Table 2

This table lists the harmonic components which can be determined, versus the length of the record. 60 components; mean for Nieuwpoort, Oostende and Zeebrugge. (Hydrographische Dienst der Kust, private communication.)

Record length (days)	Components
0.5	M2,M4,2MS6
1.1	+ O1,MK3
9.6	+ MNS2
13.7	+ K1,MO3,OO1
14.8	+ S2,M6,MS4,2SM2,MSf,2SM6,SK3,S4
27.3	+ M3,M1
27.6	+ N2,MN4,Q1,2MN6,2Q1,J1
31.8	+ 2MS2,L2,MSN2,Mm,MSN6,SN4
182.6	+ K2,P1,MK4,2MK6,OP2,Mf,SO3,MSK6,MKS2,KJ2,ϕ1, SK4,MP1,SO1
193.6	+ χ1
205.9	+ ν2,2N2,λ2,ρ1,σ1,θ1,
365.2	+ Sa,Ssa,S1,ψ1,T2,R2,π1

6.- Practical realization of the harmonic analysis

The harmonic analysis of the current data records is made of several steps we will develop here.

6.1.- PREPROCESSING OF THE DATA

The data are usually recorded with a time interval of the order of 5 to 10 minutes. As mentioned above, a time step of 0.5 to 1 hour is usually sufficient for the purpose of tidal analysis. However, in order to avoid any aliasing of high frequency noise, the original time serie is first low-pass filtered, and then decimated to the desired time interval. The filter we use is an autoregressive sine-Butterworth , modified to avoid any phase-shift at all frequencies.

6.2.- SPECTRAL ANALYSIS OF THE ORIGINAL DATA

The spectrum of the time serie is computed using standard FFT techniques, or the Blackman-Tukey method. This allows us to see at which frequencies variance can be found. In particular, it is possible to determine all species worth being considered. However, in order to achieve some statistical reliability for the estimate, it is necessary to consider relatively large bandwiths, and usually it is not possible to separate components or even groups within one species. This would be possible with longer records (one year).

6.3.- HARMONIC ANALYSIS

From 6.2. and the length of the tidal record, the components which are desired can be determined, and the harmonic analysis is performed.

6.4.- SPECTRAL ANALYSIS OF THE RESIDUALS

The residuals are computed and spectrally analysed as in 6.2.

6.5.- ESTIMATION OF THE QUALITY OF THE RESULTS

Confidence limits are determined for the harmonic constituents, and several tests can be applied. The consideration of the spectrum of the residuals makes it possible also to get some idea of the effectiveness of the analysis. The effect of the non analysed components is not considered sepa-

rately. They must appear in the residual spectrum, and thus enlarge the statistical variability of the current estimate.

If needed, a new analysis can be performed, and its results compared to the previous ones.

7.- Application

As an example, the method is applied to current data from a current meter moored off the belgian coast by the "Unité de Gestion du Modèle Mathématique de la Mer du Nord".

Characteristics

latitude : 51° 27' N ; longitude : 2° 59' 18" E
depth : 3 m vs bottom ; total depth : 15.6 m
start of analysis : 27 jan. 1977 at 21 h
length of the record : 61.4 days
time interval : 0.5 hours

a) The time serie was obtained after filtering and decimating the original data. The - 3dB cut off frequency was 0.8 cycle/hour.

b) Figures 1 and 2 show the spectrum of the total variance of the horizontal current $S(\lambda) = s_{xx}(\lambda) + s_{yy}(\lambda)$. As we are in a shallow water area, many high order species can be noticed (2, 4, 6, 8, 10, 12, 14, even 16).
However, the species higher than 8 carry a very small part of the variance and will be disregarded in the harmonic analysis.

c) 29 components have been searched for.
The results are listed in table 3.

d) Figure 2 shows the total residual spectrum.
It can be seen that most of the energy has been removed in species 2, 4, 6 and 8. As expected there is no change in the species 10 and higher. The low frequency end of the spectrum looks also very similar to its original shape. However, the "noise" level within each species is still much higher than between them. This is due to the non analysed components, and to interactions between tide and noise ("harmonic" constants is only a first approximation).
The hypothesis : $M = 0$, $m = 0$ for every component has been tested at 95 % global confidence level.

Table 3

Results of harmonic analysis

Constituent	Major semi-axis length (cm/sec)	Minor semi-axis length (cm/sec)	Major semi-axis direction (°, geog. coord.)	Lag related to culmination at Gwch (°)	
mean	2.78	-	109.	-	
MSf	1.54	0.65	229.	177.	*
Q1	0.62	- 0.05	236.	132.	*
O1	1.20	- 0.27	62.	39.	
K1	1.59	- 0.29	219.	17.	
MNS2	1.31	- 0.47	46.	129.	
2MS2	3.40	2.10	60.	120.	
N2	6.94	1.73	44.	24.	
M2	48.63	16.58	47.	37.	
L2	1.93	0.66	247.	1.	
S2	18.43	5.33	47.	96.	
MSN2	1.10	0.05	209.	91.	*
2SM2	1.53	0.34	226.	142.	
MO3	0.29	0.15	296.	151.	*
MK3	0.56	- 0.05	63.	175.	*
MN4	1.30	- 0.11	233.	120.	*
M4	4.80	0.25	240.	135.	
MS4	3.42	- 0.02	58.	21.	
S4	0.74	- 0.21	92.	125.	
2MN6	1.03	0.57	286.	54.	
M6	2.93	0.97	265.	79.	
MSN6	0.96	0.30	273.	93.	
2MS6	3.91	1.55	267.	135.	
2SM6	0.78	0.32	97.	28.	
S6	0.33	0.08	234.	61.	*
M8	0.73	0.19	207.	90.	*
3MS8	1.59	0.87	206.	146.	
2(MS)8	0.98	0.24	40.	29.	
3SM8	0.20	0.04	102.	74.	*
S8	0.11	0.01	40.	23.	*

A negative minor semi-axis indicates clockwize rotation.

The components with an asterisk in table 3 are those which cannot be considered as different from zero at this level of confidence.

Some interesting conclusions can be drawn from this simple example :

a) The high level of the noise due to non tidal phenomena at low frequency ($\lambda < 1d^{-1}$) makes it difficult or impossible to derive the low frequency components of the tide (MSf in our case) with any confidence.

b) In the other frequency ranges, the noise introduces a limitation to the number of components which can effectively be extracted. It seems reasonable

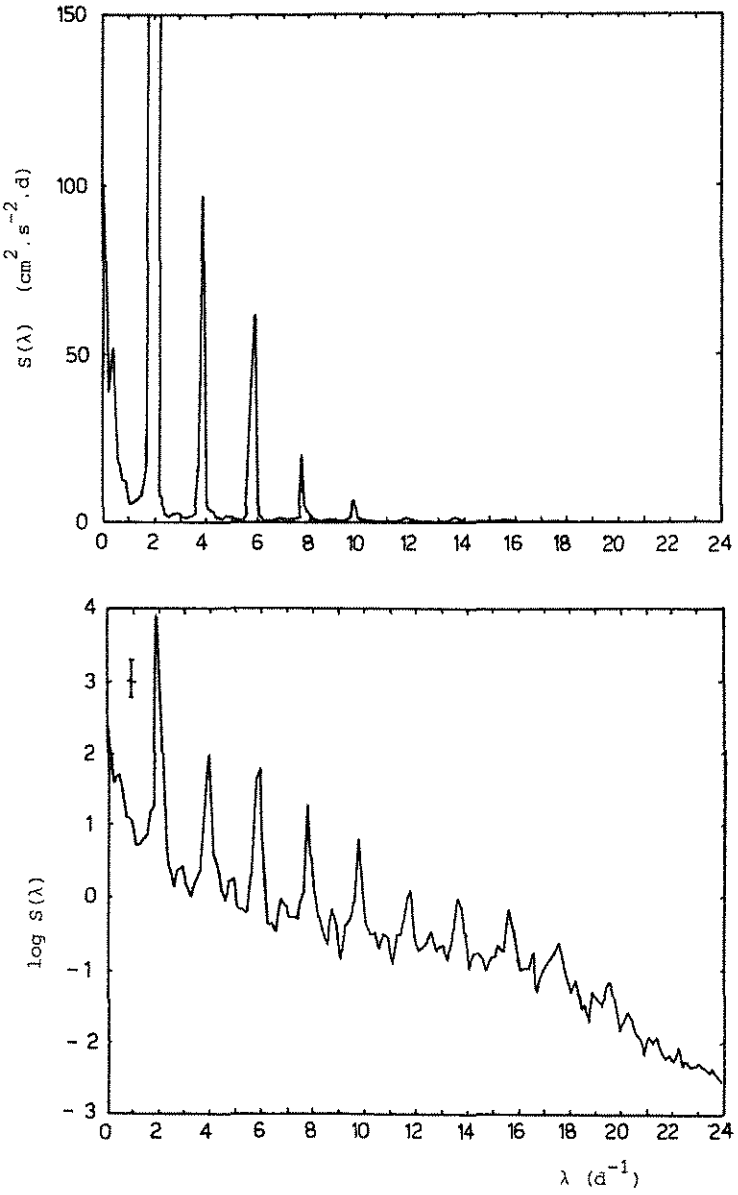

fig. 1.

Spectral representation of the variance of the horizontal current before harmonic analysis.

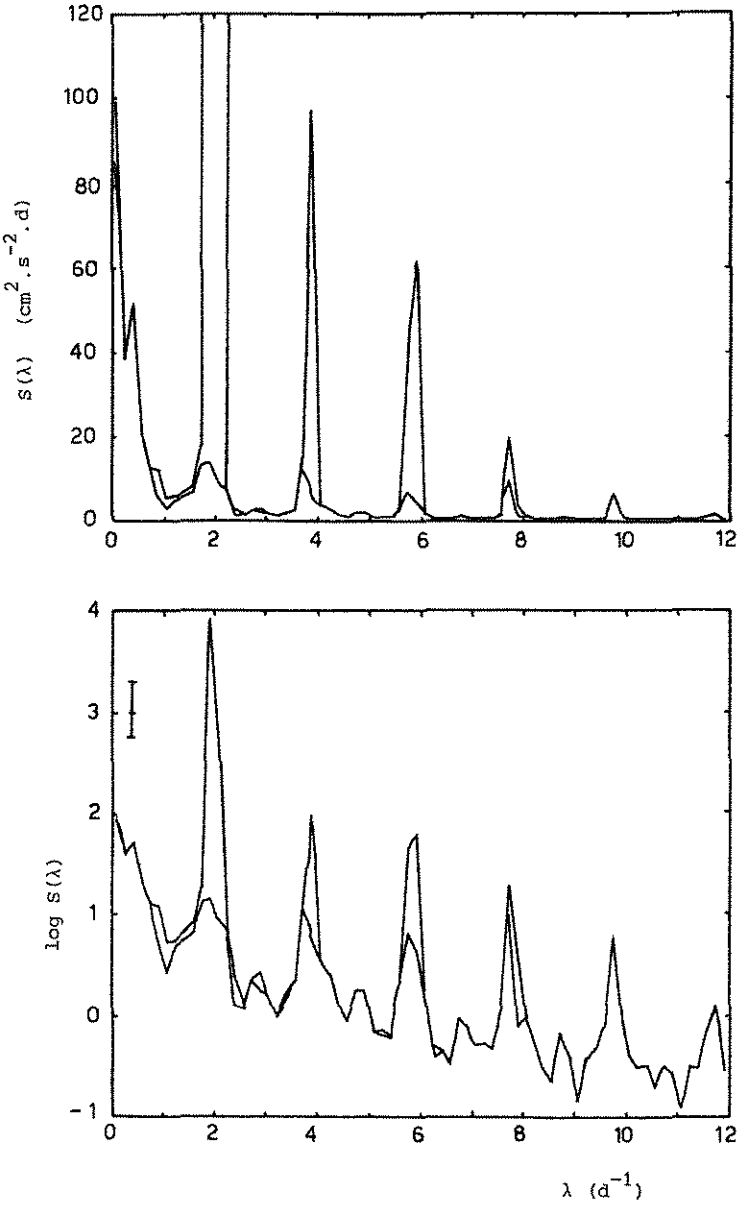

fig. 2.

Spectral representation of the variance of the horizontal current before (upper curve) and after (lower curve) harmonic analysis.

to discard those which are not significant (Q1, MSN2, MO3, MK3, MN4, S6, M8, 3SM8, S8, in our case). Other terms,even if they are significant, have large confidence regions, and it is difficult to use them directly for prediction purposes (O1, K1, ... in our case).

c) There is a need for longer records (6 months, one year or more), in order to separate all the tidal constituents and avoid some of the problems encountered with short records.

Conclusion

The method described above is applied to our current data set. In this way, we hope to derive the harmonic constituents in the area with some level of confidence.

New developments with the aim of enforcing separation but still keeping a sufficient confidence level for the estimates are under way.

References

BATH, M. (1974). *Spectral analysis in Geophysics*, Elsevier Scientific Company, Amsterdam, 564 pp.

DOOB, J.L. (1953). *Stochastic Processes*, John Wiley and Sons, New York, 654 pp.

DOODSON, A.R. and WARBURG, H.D. (1941). *Admiralty Manual of Tides*, Hydrographic Department of the Admiralty.

DOODSON, A.T. (1921). The Harmonic Development of the Tide-generating Potential. *Proc. Roy. Soc. (London)*, Ser. A 100, 305-329.

GODIN, G. (1972). *The analysis of tides*, Liverpool University Press, Liverpool, 264 pp.

HANNAN, E.J. (1970). *Multiple Time Series*, John Wiley and Sons, New York, 536 pp.

JENKINS, G.M. and WATTS, D.G. (1968). *Spectral analysis and its applications*, Holden-Day, San Francisco, 526 pp.

LE PROVOST, C. (1974). *Contribution à l'étude des marées dans les mers littorales, Application à la Manche*, PhD thesis, University of Grenoble, 228 pp.

LOFFET, A.M. (1980). *Determination of the tidal constituents to consider in the harmonic analysis*, Progress report, 1980, 1.

LOFFET, A.M. (1980). *Determination of the accuracy of the results of the harmonic analysis*, Progress report, 1980, 2.

MELCHIOR, P. , PAQUET, P. and VAN CAUWENBERGHE, C. (1967). *Analyse harmonique de 20 années d'enregistrements de marées océaniques à Ostende*, Koninklijke Academie van België, Klasse der Wetenschappen, 5de reeks, boek LIII, Brussels.

RAO, C.R. (1973). *Linear Statistical Inference and its Applications*, John Willey and Sons, New York, 625 pp.

VAN ETTE, A.B., and SCHOEMAKER, H.J. (1966). *Harmonic analysis of tides, essential features and disturbing influences*, The Netherlands Hydrographer, 33 pp.

Observed short-time temperature variations and tidal current constants in the North Sea south-east of the Doggerbank

(Comparison of two seasons)

H.W. RIEPMA*

Abstract

Observations are reported of variations in the thermal structure and of tidal current constants at various depths in the Bloden area south east of Doggerbank. Two seasons with measurements on the same position are compared. The first experiment took place during August 1975 in stratified waters. The second experiment took place during JONSDAP '76 in which stratification developed.

The subject of this contribution to the ICES/JONSIS workshop on JONSDAP '76 is also dealt with in a contribution submitted to the *Deutsche Hydrographische Zeitschrift*. The interested reader is directed to the appropriate volume.

* KNMI, Wilhelminalaan 10, 3730 AE De Bilt, The Netherlands.

Achevé d'imprimer le 11 septembre 1980
sur la presse offset d'é.t.a.b.é.t.y.p.
Quai de Longdoz, 72 — B-4020 LIEGE
Tél.: 041/42.59.21

D/1980/2750/3